

Development of an integrated in vitro model for the prediction of oral bioavailability of nanoparticles



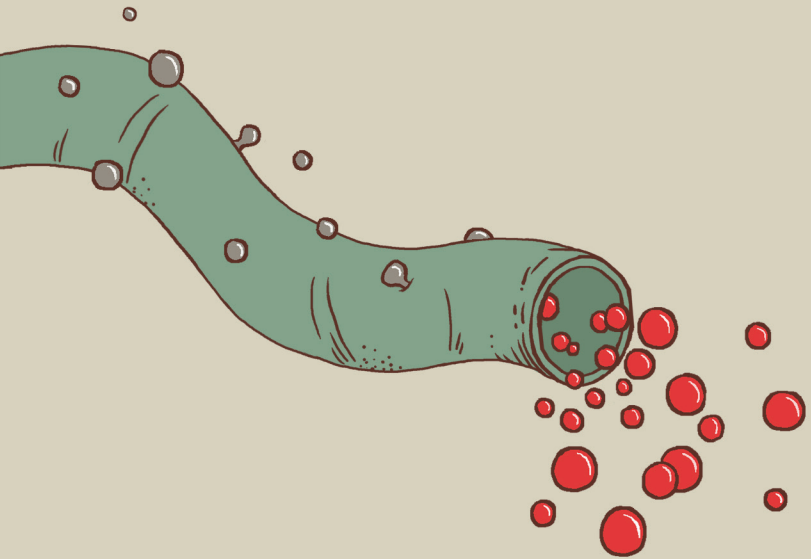
Agata Paulina Walczak

Development of an integrated in vitro model for the prediction of oral bioavailability of nanoparticles

Agata Paulina Walczak



2015



**Development of an integrated in vitro model
for the prediction of oral bioavailability
of nanoparticles**

Agata Paulina Walczak

Thesis committee

Promotor

Prof. Dr I.M.C.M. Rietjens
Professor of Toxicology
Wageningen University

Co-promotors

Dr H. Bouwmeester
Senior scientist, RIKILT- Wageningen UR
Wageningen UR

Dr P.J.M. Hendriksen
Senior scientist, RIKILT- Wageningen UR
Wageningen UR

Other members

Prof. Dr J.T. Zuillhof, Wageningen University
Prof. Dr F.R. Cassee, National Institute for Public Health and the Environment (RIVM),
Bilthoven and Utrecht University
Dr I. Lynch, University of Birmingham, United Kingdom
Prof. Dr A.H. Velders, Wageningen University

This research was conducted under the auspices of the Graduate School VLAG (Advanced studies in Food Technology, Agrobiotechnology, Nutrition and Health Sciences).

**Development of an integrated in vitro model
for the prediction of oral bioavailability
of nanoparticles**

Agata Paulina Walczak

Thesis

submitted in fulfilment of the requirements for the degree of doctor
at Wageningen University
by the authority of the Rector Magnificus
Prof. Dr M.J. Kropff,
in the presence of the
Thesis Committee appointed by the Academic Board
to be defended in public
on Monday 5 January 2015
at 11 a.m. in the Aula.

Agata Paulina Walczak

Development of an integrated in vitro model for the prediction
of oral bioavailability of nanoparticles

154 pages.

PhD thesis, Wageningen University, Wageningen, NL (2015)

With references, with summaries in Dutch and English

ISBN 978-94-6257-220-1

TABLE OF CONTENTS

Chapter 1	Introduction	7
Chapter 2	Behaviour of silver nanoparticles and silver ions in an in vitro human gastrointestinal digestion model	25
Chapter 3	Translocation of differently sized and charged polystyrene nanoparticles in in vitro intestinal cell models of increasing complexity	49
Chapter 4	In vitro gastrointestinal digestion increases the translocation of polystyrene nanoparticles in an in vitro intestinal co-culture model	71
Chapter 5	Bioavailability and biodistribution of differently charged polystyrene nanoparticles upon oral exposure in rats	93
Chapter 6	General discussion and future perspectives	113
Chapter 7	Summary	131
Chapter 8	Samenvatting	137
Appendix	Acknowledgements	145
	Curriculum Vitae	149
	List of publications	151
	Overview of completed training activities	153

1

Introduction

INTRODUCTION

Nanotechnology, applications of nanoparticles and potential risks

Nanotechnology is a relatively new field of science and technology, in which, amongst others, the development of nanomaterials (NMs) is increasing very rapidly. In this thesis the focus lies on the use of nanoparticles (NPs), which are NMs with sizes between ~1 and 100 nm in three dimensions. Because of their small size, resulting in a relatively large surface area compared to volume, NPs show unique physical and chemical properties that are not found in bulk counterparts of the same material, not even at the same mass (Chaudhry et al. 2008; Auffan et al. 2009; Allahverdiyev et al. 2011). Due to the high surface area to volume ratio NPs obtain higher reactivity. Because of these unique properties, NPs find many applications, including health care, pharmaceutical and food industries. While there are many benefits of using NP-containing products, the unique properties of NPs also give rise to safety concerns like adverse health effects upon exposure to and potential intake of NPs, intentional and unintentional (Oberdorster et al. 2005; Drake and Hazelwood 2005; Navarro et al. 2008; Sung et al. 2009).

There are many NP-containing products already on the market, and their number is expected to further increase in the near future (Duran and Marcato 2013). NPs are currently being used in consumer products, like electronics, clothing, textiles, wound dressings and cosmetics (e.g. sunscreens, lipsticks, skin creams, and toothpaste). In medicine, NPs are used for drug delivery, bio-imaging, regenerative medicine, and therapeutics. In food industry, they are used for processing and packaging (e.g. edible thin film packaging), but also as storage life sensors, food additives, and juice clarifiers (Bouwmeester et al. 2014). NPs can enter the gastrointestinal tract intentionally or unintentionally, mainly through food or cosmetics.

In food and food-related products a great variety of NPs are used. Silver, silica and titanium dioxide are the NPs that are used most commonly in the food sector, as a part of materials coming in contact with food during its processing and packaging, as well as a part of food itself.

1. Silver metal has been used by mankind for centuries, e.g. as coins, for utensils or in antimicrobial applications and as NPs in ancient glass, etc. (Wijnhoven et al. 2009). Since the introduction of engineered silver NPs (AgNPs) on the market, they gain a lot of attention for their properties resulting from nano-size, which are higher reactivity and ease of releasing Ag⁺ ions. AgNPs are increasingly being used in many industrial sectors for antimicrobial properties, e.g. in odor-resistant textiles and odor-killing and wound-dressing cosmetics (Nanoparticle Products Inventory, PEN; Wijnhoven et al. 2009). AgNPs constitute the majority of the NPs used in the food sector (Nanoparticle Products Inventory, PEN). They are used for their antimicrobial properties mainly in processing and packaging of food (e.g., kitchenware coated with AgNPs, or foils and containers with incorporated AgNPs), but they are also used in food products itself, for example, as health supplements and food additives (E174) (Nanoparticle Products Inventory, PEN; Chaudhry et al. 2008; Bouwmeester et al. 2009). Health supplements

in the form of aqueous dispersions of AgNPs for oral consumption are claimed to act as an antimicrobial and to augment the body's immune system. These suspensions are easily accessible from numerous sources (Nanoparticle Products Inventory, PEN). Therefore, the likelihood of oral human exposure to AgNPs is high. What makes AgNPs so attractive for industries is their dissociation of ions (Kittler et al. 2010; Liu and Hurt 2010; Maurer-Jones et al. 2013) and the release of Ag⁺ ions from AgNPs can reach up to 90% of their total mass, depending on the environmental conditions like pH and chemical composition of the medium and the temperature (Kittler et al. 2010; Maurer et al. 2014). Therefore, Ag⁺ ions are an inseparable element accompanying AgNPs in aqueous solutions and the behaviour of Ag⁺ ions should be considered in any biological study using AgNPs.

2. Another type of NP commonly used in the food industry is synthetic amorphous silica (SAS). In the EU it is registered as a food additive (E551), used as an anticaking agent and carrier of flavours (Dekkers et al. 2011). The highest concentrations of nano-sized silica are found in coffee creamers, instant soups, seasoning mixes and rubs (Dekkers et al. 2011).
3. Other types of NPs often used in the food industry include: titanium dioxide, zinc oxide, magnesium oxide, gold and platinum, alumina, copper, cerium oxide, calcium, selenium, iron oxides, cadmium telluride (Bouwmeester et al. 2009; Bouwmeester et al. 2014; Chaudhry et al. 2008; Frohlich and Roblegg 2012). Titanium dioxide is an authorized to be used as additive in food (E171) as a food colorant. The food-grade titanium dioxide has been shown to contain approximately 36% of the particles in size smaller than 100 nm (Weir et al. 2012). The highest content of titanium dioxide can be found in sweets, candies, and chewing gums (Weir et al. 2012; Peters et al. 2014).

Given the use of NPs in food and consumer products, consumers are very likely orally exposed to NPs. Presently, risk assessment of NPs relies mainly on *in vivo* studies (EFSA and Committee 2011). Given the enormous diversity of NPs, a high number of animals would be required to test all of them *in vivo*. For both scientific and societal reasons this is undesirable. Meanwhile, there is a strong societal demand to reduce animal studies for testing of chemicals (so also NPs). Reduction of animal studies could also potentially reduce costs and time needed for NP safety testing. In order to reduce *in vivo* testing, efficient alternative *in vitro* methods for prediction of toxicity and bioavailability of NPs would be of great value. The role of alternative *in vitro* methods is to reduce, refine and replace animal studies, three principles known as the “3Rs”. The search for alternative methods for testing chemicals is rapidly increasing due to special organisations and networks validating *in vitro* techniques to replace animal studies, like ECVAM, OECD and EUNETVAL. An approach for testing oral exposure to NPs was proposed by EFSA (European Food Safety Authority) in a guidance document on risk assessment of NPs in the food and feed chain (EFSA and Committee 2011). According to this document, testing NP behaviour and bioavailability upon oral ingestion should be a tiered approach, so it should encompass several steps.

These steps, relevant for the topic of the present thesis, are discussed in more detail in the next section.

***In vitro* models to assess NP behaviour upon oral ingestion and oral bioavailability**

As advised by EFSA, NPs should be tested in a series of *in vitro* assays, reflecting all steps that specifically occur after oral administration. The first step is the gastrointestinal digestion of NPs. The second step is the intestinal translocation of NPs across the intestinal barrier, resulting in systemic circulation of the NPs and thus their bioavailability. The currently existing *in vitro* models for human gastrointestinal digestion and for intestinal translocation are discussed below.

***In vitro* human gastrointestinal digestion model**

The first crucial step in studying the behaviour of NPs upon oral exposure would be testing their response to the dynamic conditions in the human gastrointestinal tract. Gastrointestinal digestion might influence the physicochemical properties of NPs due to multiple factors, such as an elevated temperature, variable pH, and variable concentrations of salts and proteins along the digestive tract. These parameters are known to affect the properties of NPs including their surface chemistry and agglomeration state (Chaudhry et al. 2008; Fabrega et al. 2009; El Badawy et al. 2010; Liu and Hurt 2010; Bihari et al. 2008; Greulich et al. 2009; Rogers et al. 2012), their interaction with biomolecules (Cedervall et al. 2007; Lundqvist et al. 2008; Lynch and Dawson 2008) and their dissolution rate, in case of dissolving NPs like zinc oxide and silver NPs (Liu and Hurt 2010).

Several *in vitro* digestion models are described in the literature that could be used to evaluate the behaviour of NPs during gastrointestinal digestion. The available models range in complexity and adequacy to recapitulate the whole human gastrointestinal digestion. Some simplified models simulate only gastric digestion, in which compounds are incubated in a salt buffer at low pH (Mahler et al. 2009; Mwilu et al. 2013). The Dynamic Gastric Model mimics changes in pH, enzyme addition, shearing, mixing and retention time of an adult human stomach (Vardakou et al. 2011). The Human Gastric Simulator in addition includes the continuous peristaltic movements of the stomach wall and dynamic gastric secretion, emptying systems and temperature control (Kong and Singh 2010). A model simulating the small intestinal conditions only is the pH-stat method, a simple *in vitro* lipolysis model which is used to characterize lipid digestion (Li and McClements 2010).

More complex models incorporate both the gastric and intestinal compartments. A static model that encompasses the majority of conditions relevant for oral exposure (*i.e.* the oral, gastric, and small intestinal conditions) was developed by Versantvoort et al. (Versantvoort et al. 2005) and was subsequently used in studies determining the bioaccessibility of orally ingested compounds like heavy metals (Oomen et al. 2003) and other contaminants (Versantvoort et al. 2005). This model mimics the human *in vivo* conditions, regarding pH values, salt and enzyme concentrations and incubation times. Other static digestion models are: the modified PBET method (Physiologically Based Extraction Test) operated by the BGS (United Kingdom), the German E DIN 19738, applied by the Ruhr-Universität Bochum

(Germany) and the SHIME (Simulator of the Human Intestinal Microbial Ecosystem) procedure used by LabMET (Ghent University, Belgium) (Van de Wiele et al. 2007). All these models differ slightly between one another, regarding composition and pH of digestive juices and incubation times. Furthermore, several dynamic digestion models have been developed, which are more sophisticated and computerized. They allow the simulation of the dynamics of digestion, with regulation of transit times, transport of the sample between digestive compartments and time-dependent regulation of pH values and enzyme concentrations. One of these models is the multi-compartmental digestion model, called TNO Intestinal Model 1 (TIM1), which simulates the physiological conditions of the human stomach and small intestine, including peristaltic mixing and transit and removal of the products of digestion (Minekus et al. 1999; Reis et al 2008; Helbig et al. 2013). Other examples of dynamic digestion models are the models of the English Institute of Food Research (Wickham et al. 2009; Wickham et al. 2012) and of the French INRA (Menard et al. 2014).

Even though dynamic models are more sophisticated and closer to a realistic digestion process, static models are used as well since they are simpler and suitable for more high throughput studies. In addition, static models provide the advantage that samples can be collected at each step of the digestion, gastric and intestinal, separately.

At the start of this project no studies were available using the digestion models for NPs.

***In vitro* human intestinal epithelium model**

After passing through the mouth and stomach, NPs reach the small intestine, which is the most prominent compartment for uptake of NPs into blood. The bioavailability of NPs, therefore, depends on the translocation efficiency of NPs through the small intestine influences their bioavailability. Following the already mentioned tiered approach, the intestinal translocation of NPs should be carefully evaluated to assess their bioavailability. *In vitro* translocation models, mimicking the small intestinal wall, are therefore the next step in line for the prediction of NP bioavailability after oral exposure *in vivo*. Mainly Caco-2 cells (human epithelial colorectal adenocarcinoma cells) have been used as an intestinal epithelial cell model, grown as a cell layer on semi-permeable membrane inserts which separate an apical from a basolateral chamber. *In vitro* intestinal cell models based on Caco-2 cells have a long history of use in the uptake screening of conventional chemicals (Hilgers et al. 1990; Prieto et al. 2010).

Caco-2 cells may be used as a mono-culture, which is the most commonly used intestinal barrier model (des Rieux et al. 2005; Mahler et al. 2009; Bhattacharjee et al. 2013a; Nkabinde et al. 2012; Natoli et al., 2012). Caco-2 cells lack mucus production, responsible for covering the cell layer with mucus, which has been shown to play an important role in affecting the permeability and resistance of the intestinal cell layer to hazardous compounds (Norris and Sinko 1997; Crater and Carrier 2010). Mucus presents a barrier to the absorption of NPs through the intestinal wall because of its thickness, high molecular weight and negative charge. It can entrap NPs or act repulsive (depending on the charge of NPs) (Crater and Carrier 2010) or simply pose a physical barrier due to density and thickness (Cone 2009). Mucus can also cause agglomeration of NPs (Ensign et al. 2012).

Therefore, Caco-2 cells are often used in co-culture with mucus producing HT29-MTX cells (human colon adenocarcinoma mucus secreting cells) (Mahler et al. 2009; Behrens et al. 2002; Scaldaferrri et al. 2012). Another cell type present in human intestinal epithelium is the human intestine microfold (M) cell. M cells are localized in the intestinal Peyer's patches, of which adult humans have about 30 and M cells in total compose less than 1 percent of the small intestine epithelial cell layer. M cells are responsible for the uptake and translocation of relatively larger particles (Kerneis et al. 1997; des Rieux et al. 2005; des Rieux et al. 2007; Bouwmeester et al. 2011b; Martinez-Argudo et al. 2007). Co-cultures of Caco-2 and M cells have been used for testing NP translocation (des Rieux et al. 2007; Bouwmeester et al. 2011b). The most complex model, employing all three cell types present in the human small intestinal epithelium, has been used (Bazes et al. 2011; Antunes et al. 2013), also for assessing translocation of polystyrene (PS)-NPs and demonstrated a role of M cells in translocation of larger (200 nm) NPs (Mahler et al. 2012).

A limited number of studies have used these *in vitro* models to test the translocation of NPs. These studies often use easily detectable NPs like fluorescently labelled PS-NPs as model NPs due to their stability and due to the availability of these NPs in various sizes and with different surface modifications resulting in different surface charges, steric hindrance, hydrophobicity properties, and fluorescent properties. All these properties make these NPs easy to use, reliable and suitable for testing biological effects in response to the surface characteristics (des Rieux et al. 2005; Lundqvist et al. 2008; Mahler et al. 2012). Using fluorescently labelled NPs facilitates detection in biological systems, enabling tracing and quantification. Taken together, PS-NPs are very suitable model NPs to apply in studies aiming to develop alternative *in vitro* models for NP testing. Table 1 gives an overview of the various human intestinal epithelium *in vitro* models for testing the translocation of different types of PS-NPs. For the study of translocation of NPs models with increasing complexity are used: mono-cultures, co- and tri- cultures, with and without a mucus layer. This overview demonstrates that the different intestinal cell models have been successfully used for studies on NP translocation. It is difficult, though, to draw any firm conclusion from these results, as the reported translocation values are highly variable between different studies. At the start of this PhD project, a systematic study comparing different cell models with use of different types of PS-NPs was still lacking.

At the start of this PhD project, a combination of *in vitro* digestion models with *in vitro* intestinal translocation models had never been used before to assess the fate and uptake of NPs. Such a combination had been applied only to test the bioavailability of conventional chemicals like iron from different foods (Mahler et al. 2009) or phenolic compounds from strawberries (Kosinska-Cagnazzo et al., 2014).

***In vivo* oral studies with PS-NPs**

Several *in vivo* oral studies have been performed before with differently sized and coated PS-NPs in rats. These studies have demonstrated the oral bioavailability of PS-NPs of 23% for 500 nm PS-NPs (Hussain et al. 1997) and ranging from 0.8 to 6.6% for PS-NPs in size of 1 μm to 50 nm (Jani et al. 1990). The results from these studies highlight the dependence

Table 1. Summary of human intestinal epithelium *in vitro* models used for testing the translocation of different types of PS-NPs.

NP type	Size	Concentration	Exposure		Translocation	Reference
			time	Cells		
PS-NPs, plain	460 nm	7.7x10 ⁸ NPs/ml	4 h	Caco-2	1%	(Martinez-Argudo et al. 2007)
				Caco-2 + M cells	11%	
PS-NPs -carboxylated -aminated -carboxylated	200 nm	4.5x10 ⁹ NPs/ml	1.5 h	Caco-2 cells	0%	(des Rieux et al. 2005)
				Caco-2 + M cells	~0.0007%	
				Caco-2 cells	~0%	
				Caco-2 + M cells	~0.002%	
PS-NPs, carboxylated	500 nm			Caco-2 cells	~0%	
				Caco-2 + M cells	~0%	
PS-NPs, carboxylated	200 nm	4.5x10 ⁹ NPs/ml	1 h	Caco-2 cells	2x10 ⁻⁵ %	(des Rieux et al. 2007)
				Caco-2 + M cells	8x10 ⁻⁴ %	
PS-NPs, carboxylated	50 nm	2x10 ¹¹ NPs/ml	45 min	Caco-2 + HT29-MTX	~2.3% *	(Mahler et al. 2012)
				Caco-2 + HT29-MTX + M cells	~3% *	
	200 nm	1.25x10 ¹⁰ NPs/ml			Caco-2 + HT29-MTX	~0.1% *
					Caco-2 + HT29-MTX + M cells	0.8% *
PS-NPs -aminated -carboxylated	50 nm	1 µg/ml	24 h	Caco-2	~35%	(Bhattacharjee et al. 2013c)
					~10%	
Latex NPs, plain	2 µm	5.68x10 ⁶ NPs	1.5 h	Caco-2	~0.006% *	(Moyes et al. 2007)
PS-NPs, plain	50 nm	100 µg/ml	2 h	Caco-2	5%	(Kulkarni and Feng 2013)
	100 nm				10%	

*Calculated from the numbers given in the manuscript

of absorption and accumulation of PS-NPs on several factors, including the size, surface charge and type of coating material (Jani et al. 1989; Hillery et al. 1994; Hussain et al. 1997; Hussain and Florence 1998). In general, smaller PS-NPs were taken up to a higher extent than the larger ones (Jani et al. 1990) and the non-ionized more than the carboxylated ones (Jani et al. 1989). The intestinal wall has been shown to be the main accumulation site for PS-NPs (Hussain et al. 1997). This could be related with the uptake of PS-NPs in lymphoid tissue associated with these organs, as shown in other studies (Seifert et al. 1996; Hillery et al. 1994; Florence et al. 1995). PS-NPs were distributed also to liver, spleen and kidney (Hussain et al. 1997; Jani et al. 1990).

Despite the results of the *in vivo* exposures, no data are available from studies that used the same PS-NPs *in vitro* and *in vivo*.

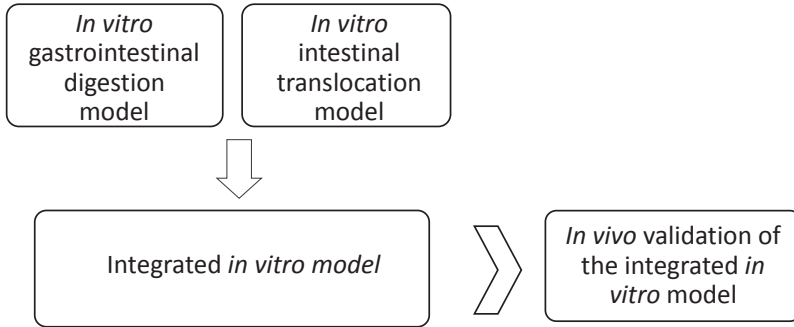


Figure 1. Schematic overview of the steps taken in the present thesis to develop an integrated *in vitro* model for the prediction of oral bioavailability of nanoparticles.

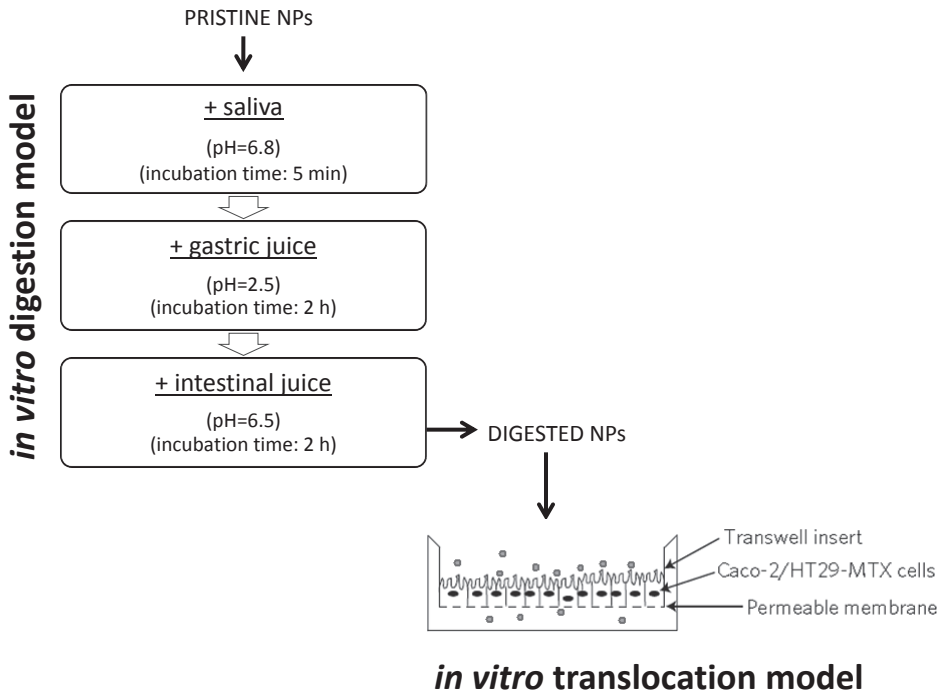


Figure 2. Schematic representation of the integrated *in vitro* model developed in the present thesis.

Physicochemical characterization of NPs

In discussions NPs are often considered as homogenous materials. This is reflected in assumptions that all NPs are alike and trigger similar biological responses. In practise this is by far not true, one might regard the group of NPs as diverse as chemicals (ranging from metals to complex organic compounds). Perhaps the most simple illustration is that a batch of a given NP contains NPs with different sizes (i.e., a size distribution, with a different number of particles per size), that in an ideal case follows a normal distribution. In attempts to describe this huge variability in NPs and to adequately characterize NPs, long lists of physicochemical parameters have been compiled by expert committees. No single metric is known that fully describes the relation between physicochemical properties and the biological effects, but the most important parameters that influence the properties of NPs are size, chemical composition, surface charge, chemical composition of the core, surface functionalization, dissolution into ions and shape (Oberdorster et al. 2005; Bouwmeester et al. 2009; Bouwmeester et al. 2011a). These factors influence NP kinetics at the cellular level and at the level of the whole body (uptake, distribution, and excretion), thereby affecting their possible toxicity (Oberdorster et al. 2005; Sager and Castranova 2009; Park et al. 2011; Bhattacharjee et al. 2013b). An additional degree of complexity in describing NPs arises from their high reactivity in different biological environments. Upon contact with any media, the size and surface charge of NPs can be modified, and the NPs might become coated with molecules present in the media. The resulting changes in physicochemical characteristics will in turn affect the biological effects exerted by NPs.

To understand the observed biological effects, a sound characterization of the NPs in the testing environment is required. Different analytical chemical methods are being used for this characterization. The size of NPs can be measured with several techniques. NPs can be visualized by electron microscopy techniques, like transmission electron microscopy (TEM) or scanning electron microscopy (SEM), enabling measurement of the diameter. Other techniques are dynamic light scattering (DLS) and nanoparticle tracking analysis (NTA), which measure the hydrodynamic diameters of NPs. DLS analyses the velocity distribution of particle movement by measuring dynamic fluctuations of light scattering intensity caused by the Brownian motion of the particle. The hydrodynamic diameter given by DLS is the diameter of the core of NPs together with a hydration layer surrounding the particle. Therefore, the size measured with DLS is slightly larger than the one given by electron microscopy techniques, which only measure the core NP without a hydration layer. Another technique for measuring the size of NPs is (single particle-) inductively coupled plasma-mass spectroscopy (SP-ICPMS). With this technique the masses of NPs are measured, which are further mathematically converted into sizes, using the assumption that all NPs have spherical shape. SP-ICPMS enables detection of AgNPs in relatively complex matrices and at very low concentrations.

The next important physicochemical parameter to measure is the chemical composition. The composition of the NP core is crucial for the function, but the whole range of physicochemical properties of NPs are further exerted by the functional groups present on the surface of NPs. At this level, the physicochemical properties are shaped by the type

and density of the chemical groups, their structure, steric hindrance, and hydrophobicity. The surface charge, induced by the functional groups, can be measured by measuring zeta potential. The chemical composition of the surface can be estimated based on matrix-assisted laser desorption ionization – time of flight (MALDI-TOF) measurements. This technique is based on a desorption of a sample with laser and its subsequent ionization. Other techniques available for the measurement of chemical composition of the surface of NPs are: energy-dispersive X-ray spectroscopy (EDX), x-ray photoelectron spectroscopy (XPS), Raman spectroscopy and infrared spectroscopy.

Upon introduction in any biological media, NPs are immediately coated with biological molecules resulting in a protein corona, a layer of proteins adsorbed tightly (hard corona) and loosely (soft corona) on the surface of NPs. The protein corona is known to affect the interactions of NPs with biological systems and it has been suggested to be the main parameter that mediates any interaction of NPs (Walczyk et al. 2010; Lesniak et al. 2012; Monopoli et al. 2012). Both the amount of adsorbed proteins and their composition have been shown to affect the cellular uptake of NPs, as well as their translocation and interaction with receptors and cellular components (Tedja et al. 2012; Lesniak et al. 2010; Lundqvist 2013; Ehrenberg et al. 2009). The thickness and composition of the protein corona can be analysed with techniques like sodium dodecyl sulfate polyacrylamide gel electrophoresis (SDS-PAGE), 2-dimensional gel electrophoresis (2DE), proteomics, and liquid chromatography–mass spectrometry (LC-MS/MS). While SDS-PAGE indicates the approximate molecular mass of the proteins, LC-MS/MS gives an accurate indication of the molecular mass and allow identification of exact proteins. Additionally, with some types of dissolving NPs like silver, zinc oxide or silica NPs, it is important to measure their ion release in media. This is crucial because ions, e.g. in case of silver, exert biological functions and it is necessary to know their concentration in exposure media to distinguish the effects attributed to AgNPs from the ones of Ag^+ ions. The concentration of ions in solutions can be measured with several techniques, like a silver ion/sulphide selective electrode, or- after separation from AgNPs- with atomic absorption spectroscopy (AAS) or ICP-MS, which measure the total content of elemental silver. Ultraviolet-Visible spectroscopy (UV-Vis) gives a semi-quantitative indication of silver ions content.

AIM AND OUTLINE OF THE THESIS

The aim of the present thesis was to develop an integrated *in vitro* approach to evaluate the uptake of NPs following ingestion for the prediction of their oral bioavailability in the human body. To achieve this, an *in vitro* gastrointestinal digestion model was used, to test the fate of NPs upon digestion in the human digestion tract. Further, *in vitro* intestinal epithelial models were used to evaluate the potential translocation of NPs across the intestinal barrier to predict their potential systemic absorption. Next, the *in vitro* gastrointestinal model was combined with the intestinal model and the translocation of digested NPs was tested across the intestinal model. Lastly, an *in vivo* experiment was performed to pre-validate the integrated *in vitro* model.

Chapter 1, the present chapter of this thesis, gives an introduction to the topic of nanotoxicology, highlights the importance of careful characterization of NPs tested in the various assays and presents existing *in vitro* models of gastrointestinal digestion and human intestinal epithelium used for toxicity testing of NPs. Some of these *in vitro* models were selected and evaluated for testing NPs in the next (experimental) chapters. The aim and contents of the present thesis are also presented.

In **chapter 2**, the influence of a gastrointestinal digestion on the behaviour and properties of highly characterized AgNPs is described. AgNPs were selected for this study due to their common application in food and food-related products. To this end, an *in vitro* model of human gastrointestinal digestion was used and NPs were carefully characterized with an array of techniques after each phase of the digestion.

In **chapter 3**, the translocation of PS-NPs across *in vitro* intestinal models is described. In this study three *in vitro* intestinal epithelial cell models of increasing complexity were used to assess the translocation of differently sized (50 and 100 nm) and charged (neutral, positive and negative charge) PS-NPs. PS-NPs were selected for this study as they are commercially available with a wide variety of physicochemical properties like charge and fluorescent labelling, which makes them excellent model NPs, suitable for model development studies. A mono-culture of Caco-2 cells, a co-culture with additional mucus secreting HT29-MTX cells, and a tri-culture with additional both HT29-MTX cells and M cells were used.

In **chapter 4**, the effect of *in vitro* gastrointestinal digestion on the protein corona of NPs and their subsequent translocation across an *in vitro* intestinal barrier is investigated. PS-NPs were used with different charges (neutral, positive and negative), but also with different surface modifications (*i.e.* two types of negatively charged PS-NPs from two different suppliers) for comparison.

In **chapter 5**, an *in vivo* study is described which was performed to validate the *in vitro* integrated model described in Chapter 4. In this study the uptake and biodistribution of orally administered PS-NPs (*i.e.* the same PS-NPs as used in Chapter 4) were evaluated and results were compared with outcomes of the *in vitro* model.

Finally, **chapter 6** discusses the results described in the present thesis and provides suggestions for future research.

REFERENCES

- (1) Allahverdiyev AM, Kon KV, Abamor ES, Bagirova M, Rafailovich M. 2011. Coping with antibiotic resistance: combining nanoparticles with antibiotics and other antimicrobial agents. *Expert Rev Anti Infect Ther* 9:1035-1052.
- (2) Antunes F, Andrade F, Araujo F, Ferreira D, Sarmiento B. 2013. Establishment of a triple co-culture *in vitro* cell models to study intestinal absorption of peptide drugs. *European journal of pharmaceutics and biopharmaceutics : official journal of Arbeitsgemeinschaft fur Pharmazeutische Verfahrenstechnik e.V* 83:427-35.
- (3) Auffan M, Rose J, Bottero JY, Lowry GV, Jolivet JP, Wiesner MR. 2009. Towards a definition of inorganic nanoparticles from an environmental, health and safety perspective. *Nat Nanotechnol* 4:634-41.

- (4) Bazes A, Nollevaux G, Coco R, Joly A, Sergent T, Schneider Y-J. 2011. Development of a triculture based system for improved benefit/risk assessment in pharmacology and human food. *BMC Proceedings* 5(Suppl 8):P67.
- (5) Behrens I, Pena AI, Alonso MJ, Kissel T. 2002. Comparative uptake studies of bioadhesive and non-bioadhesive nanoparticles in human intestinal cell lines and rats: the effect of mucus on particle adsorption and transport. *Pharmaceutical research* 19:1185-93.
- (6) Bhattacharjee S, Ershov D, Gucht J, Alink GM, Rietjens IM, Zuilhof H, Marcelis AT. 2013a. Surface charge-specific cytotoxicity and cellular uptake of tri-block copolymer nanoparticles. *Nanotoxicology* 7:71-84.
- (7) Bhattacharjee S, Marcelis ATM, Zuilhof H, Woutersen RA, Rietjens IMCM, Alink GM. 2013b. Role of surface charge in bioavailability and biodistribution of tri-block copolymer nanoparticles in rats after oral exposure. *Toxicol Res-Uk* 2:187-192.
- (8) Bhattacharjee S, van Opstal EJ, Alink GM, Marcelis ATM, Zuilhof H, Rietjens IMCM. 2013c. Surface charge-specific interactions between polymer nanoparticles and ABC transporters in Caco-2 cells. *J Nanopart Res* 15.
- (9) Bihari P, Vippola M, Schultes S, Praetner M, Khandoga AG, Reichel CA, Coester C, Tuomi T, Rehberg M, Krombach F. 2008. Optimized dispersion of nanoparticles for biological in vitro and in vivo studies. *Part Fibre Toxicol* 5:14.
- (10) Bouwmeester H, Dekkers S, Noordam MY, Hagens WI, Bulder AS, de Heer C, ten Voorde SECG, Wijnhoven SWP, Marvin HJP, Sips AJAM. 2009. Review of health safety aspects of nanotechnologies in food production. *Regul Toxicol Pharm* 53:52-62.
- (11) Bouwmeester H, Lynch I, Marvin HJ, Dawson KA, Berges M, Braguer D, Byrne HJ, Casey A, Chambers G, Cliff MJ, Elia G, Fernandes TF, Fjellsbo LB, Hatto P, Juillerat L, Klein C, Kreyling WG, Nickel C, Riediker M, Stone V. 2011a. Minimal analytical characterization of engineered nanomaterials needed for hazard assessment in biological matrices. *Nanotoxicology* 5:1-11.
- (12) Bouwmeester H, Poortman J, Peters RJ, Wijma E, Kramer E, Makama S, Puspitaninganindita K, Marvin HJ, Peijnenburg AA, Hendriksen PJ. 2011b. Characterization of translocation of silver nanoparticles and effects on whole-genome gene expression using an in vitro intestinal epithelium coculture model. *ACS Nano* 5:4091-103.
- (13) Bouwmeester H, Brandhoff P, Marvin HJP, Weigel S, Peters RJB. 2014. State of the safety assessment and current use of nanomaterials in food and food production. *Trends in Food Science & Technology* xx:1-11. <http://dx.doi.org/10.1016/j.tifs.2014.08.009>.
- (14) Cedervall T, Lynch I, Lindman S, Berggard T, Thulin E, Nilsson H, Dawson KA, Linse S. 2007. Understanding the nanoparticle-protein corona using methods to quantify exchange rates and affinities of proteins for nanoparticles. *Proc Natl Acad Sci U S A* 104:2050-2055.
- (15) Chaudhry Q, Scotter M, Blackburn J, Ross B, Boxall A, Castle L, Aitken R, Watkins R. 2008. Applications and implications of nanotechnologies for the food sector. *Food Addit Contam Part A Chem Anal Control Expo Risk Assess* 25:241-258.
- (16) Cone RA. 2009. Barrier properties of mucus. *Advanced Drug Delivery Reviews* 61:75-85.
- (17) Crater JS, Carrier RL. 2010. Barrier properties of gastrointestinal mucus to nanoparticle transport. *Macromol Biosci* 10:1473-83.
- (18) Dekkers S, Krystek P, Peters RJ, Lankveld DP, Bokkers BG, van Hoeven-Arentzen PH, Bouwmeester H, Oomen AG. 2011. Presence and risks of nanosilica in food products. *Nanotoxicology* 5:393-405.
- (19) des Rieux A, Fievez V, Theate I, Mast J, Preat V, Schneider YJ. 2007. An improved in vitro model of human intestinal follicle-associated epithelium to study nanoparticle transport by M cells. *Eur J Pharm Sci* 30:380-91.
- (20) des Rieux A, Ragnarsson EGE, Gullberg E, Preat V, Schneider YJ, Artursson P. 2005. Transport of nanoparticles across an in vitro model of the human intestinal follicle associated epithelium. *Eur J Pharm Sci* 25:455-465.
- (21) Drake PL, Hazelwood KJ. 2005. Exposure-related health effects of silver and silver compounds: a review. *Ann Occup Hyg* 49:575-585.

- (22) Duran N, Marcato PD. 2013. Nanobiotechnology perspectives. Role of nanotechnology in the food industry: a review. *International Journal of Food Science and Technology* 48:1127-1134.
- (23) EFSA and Committee ES. 2011. Guidance on the risk assessment of the application of nanoscience and nanotechnologies in the food and feed chain. *EFSA J* 9:36.
- (24) Ehrenberg MS, Friedman AE, Finkelstein JN, Oberdorster G, McGrath JL. 2009. The influence of protein adsorption on nanoparticle association with cultured endothelial cells. *Biomaterials* 30:603-10.
- (25) El Badawy AM, Luxton TP, Silva RG, Scheckel KG, Suidan MT, Tolaymat TM. 2010. Impact of environmental conditions (pH, ionic strength, and electrolyte type) on the surface charge and aggregation of silver nanoparticles suspensions. *Environ Sci Technol* 44:1260-1266.
- (26) Ensign LM, Tang BC, Wang YY, Tse TA, Hoen T, Cone R, Hanes J. 2012. Mucus-Penetrating Nanoparticles for Vaginal Drug Delivery Protect Against Herpes Simplex Virus. *Sci Transl Med* 4(138): 10.1126/scitranslmed.3003453.
- (27) Fabrega J, Fawcett SR, Renshaw JC, Lead JR. 2009. Silver nanoparticle impact on bacterial growth: effect of pH, concentration, and organic matter. *Environ Sci Technol* 43:7285-7290.
- (28) Florence AT, Hillery AM, Hussain N, Jani PU. 1995. Nanoparticles as Carriers for Oral Peptide Absorption - Studies on Particle Uptake and Fate. *J Control Release* 36:39-46.
- (29) Frohlich E, Roblegg E. 2012. Models for oral uptake of nanoparticles in consumer products. *Toxicology* 291:10-7.
- (30) Greulich C, Kittler S, Epple M, Muhr G, Koller M. 2009. Studies on the biocompatibility and the interaction of silver nanoparticles with human mesenchymal stem cells (hMSCs). *Langenbecks Arch Surg* 394:495-502.
- (31) Helbig A, Silletti E, van Aken GA, Oosterveld A, Minekus M, Hamer RJ, Gruppen H. 2013. Lipid digestion of protein stabilized emulsions investigated in a dynamic in vitro gastro-intestinal model system. *Food Dig*.4:58-68.
- (32) Hilgers AR, Conradi RA, Burton PS. 1990. Caco-2 cell monolayers as a model for drug transport across the intestinal mucosa. *Pharmaceutical Research* 7(9):902-910.
- (33) Hillery AM, Jani PU, Florence AT. 1994. Comparative, quantitative study of lymphoid and non-lymphoid uptake of 60 nm polystyrene particles. *Journal of drug targeting* 2:151-6.
- (34) Hussain N, Florence AT. 1998. Utilizing bacterial mechanisms of epithelial cell entry: Invasin-induced oral uptake of latex nanoparticles. *Pharmaceutical research* 15:153-156.
- (35) Hussain N, Jani PU, Florence AT. 1997. Enhanced oral uptake of tomato lectin-conjugated nanoparticles in the rat. *Pharmaceutical research* 14:613-618.
- (36) Jani P, Halbert GW, Langridge J, Florence AT. 1989. The uptake and translocation of latex nanospheres and microspheres after oral administration to rats. *The Journal of pharmacy and pharmacology* 41:809-12.
- (37) Jani P, Halbert GW, Langridge J, Florence AT. 1990. Nanoparticle uptake by the rat gastrointestinal mucosa: quantitation and particle size dependency. *The Journal of pharmacy and pharmacology* 42:821-6.
- (38) Kerneis S, Bogdanova A, Kraehenbuhl JP, Pringault E. 1997. Conversion by Peyer's patch lymphocytes of human enterocytes into M cells that transport bacteria. *Science* 277:949-952.
- (39) Kittler S, Greulich C, Diendorf J, Koller M, Epple M. 2010. Toxicity of Silver Nanoparticles Increases during Storage Because of Slow Dissolution under Release of Silver Ions. *Chem Mater* 22:4548-4554.
- (40) Kong F, Singh RP. 2010. A human gastric simulator (HGS) to study food digestion in human stomach. *Journal of food science* 75:E627-35.
- (41) Kosińska-Cagnazzo A, Diering S, Prim D, Andlauer W. 2014. Identification of bioaccessible and uptaken phenolic compounds from strawberry fruits in in vitro digestion/Caco-2 absorption model. *Food Chemistry* 170 (2015):288-294.
- (42) Kulkarni SA, Feng SS. 2013. Effects of Particle Size and Surface Modification on Cellular Uptake and Biodistribution of Polymeric Nanoparticles for Drug Delivery. *Pharmaceutical research* 30:2512-2522.
- (43) Lesniak A, Campbell A, Monopoli MP, Lynch I, Salvati A, Dawson KA. 2010. Serum

- heat inactivation affects protein corona composition and nanoparticle uptake. *Biomaterials* 31:9511-8.
- (44) Lesniak A, Fenaroli F, Monopoli MP, Aberg C, Dawson KA, Salvati A. 2012. Effects of the presence or absence of a protein corona on silica nanoparticle uptake and impact on cells. *ACS Nano* 6:5845-57.
- (45) Li Y, McClements DJ. 2010. New mathematical model for interpreting pH-stat digestion profiles: impact of lipid droplet characteristics on in vitro digestibility. *Journal of agricultural and food chemistry* 58:8085-92.
- (46) Liu J, Hurt RH. 2010. Ion release kinetics and particle persistence in aqueous nano-silver colloids. *Environ Sci Technol* 44:2169-2175.
- (47) Lundqvist M. 2013. Nanoparticles: Tracking protein corona over time. *Nat Nanotechnol* 8:701-2.
- (48) Lundqvist M, Stigler J, Elia G, Lynch I, Cedervall T, Dawson KA. 2008. Nanoparticle size and surface properties determine the protein corona with possible implications for biological impacts. *Proc Natl Acad Sci U S A* 105:14265-14270.
- (49) Lynch I, Dawson KA. 2008. Protein-nanoparticle interactions. *Nano Today* 3:40-47.
- (50) Mahler GJ, Esch MB, Tako E, Southard TL, Archer SD, Glahn RP, Shuler ML. 2012. Oral exposure to polystyrene nanoparticles affects iron absorption. *Nat Nanotechnol* 7:264-71.
- (51) Mahler GJ, Shuler ML, Glahn RP. 2009. Characterization of Caco-2 and HT29-MTX cocultures in an in vitro digestion/cell culture model used to predict iron bioavailability. *The Journal of nutritional biochemistry* 20:494-502.
- (52) Martinez-Argudo I, Sands C, Jepson MA. 2007. Translocation of enteropathogenic *Escherichia coli* across an in vitro M cell model is regulated by its type III secretion system. *Cell Microbiol* 9:1538-1546.
- (53) Maurer EI, Sharma M, Schlager JJ, Hussain SM. 2014. Systematic analysis of silver nanoparticle ionic dissolution by tangential flow filtration: toxicological implications. *Nanotoxicology* 8(7):718-727.
- (54) Maurer-Jones MA, Mousavi MPS, Chen LD, Buhlmann P, Haynes CL. 2013. Characterization of silver ion dissolution from silver nanoparticles using fluoros-phase ion-selective electrodes and assessment of resultant toxicity to *Shewanella oneidensis*. *Chem Sci*. 4:2564-2572.
- (55) Menard O, Cattenoz T, Guillemin H, Souchon I, Deglaire A, Dupont D, Picque D. 2014. Validation of a new in vitro dynamic system to simulate infant digestion. *Food Chemistry* 145:1039-1045.
- (56) Minekus M, Smeets-Peeters M, Bernalier A, Marol-Bonnin S, Havenaar R, Marteau P, Alric M, Fonty G, Huis in't Veld JHJ. 1999. A computer-controlled system to simulate conditions of the large intestine with peristaltic mixing, water absorption and absorption of fermentation products. *Appl Microbiol Biotechnol* 53:108-114.
- (57) Monopoli MP, Aberg C, Salvati A, Dawson KA. 2012. Biomolecular coronas provide the biological identity of nanosized materials. *Nat Nanotechnol* 7:779-86.
- (58) Moyes SM, Smyth SH, Shipman A, Long S, Morris JF, Carr KE. 2007. Parameters influencing intestinal epithelial permeability and microparticle uptake in vitro. *International journal of pharmaceutics* 337:133-141.
- (59) Mwilu SK, El Badawy AM, Bradham K, Nelson C, Thomas D, Scheckel KG, Tolaymat T, Ma L, Rogers KR. 2013. Changes in silver nanoparticles exposed to human synthetic stomach fluid: effects of particle size and surface chemistry. *The Science of the total environment* 447:90-8.
- (60) Natoli M, Leoni BD, D'Agnano I, Zucco F, Felsani A. 2012. Good Caco-2 cell culture practices. *Toxicology in Vitro* 26:1243-1246.
- (61) Navarro E, Piccapietra F, Wagner B, Marconi F, Kaegi R, Odzak N, Sigg L, Behra R. 2008. Toxicity of silver nanoparticles to *Chlamydomonas reinhardtii*. *Environ Sci Technol* 42:8959-8964.
- (62) Nkabinde LA, Shoba-Zikhali LNN, Semete-Makokotlela B, Kalombo L, Swai HS, Hayeshi R, Naicker B, Hillie TK, Hamman JH. 2012. Permeation of PLGA Nanoparticles Across Different in vitro Models. *Curr Drug Deliv* 9:617-627.
- (63) Norris DA, Sinko PJ. 1997. Effect of size, surface charge, and hydrophobicity on the translocation of polystyrene microspheres through gastrointestinal mucin. *J Appl Polym Sci* 63:1481-1492.

- (64) Oberdorster G, Maynard A, Donaldson K, Castranova V, Fitzpatrick J, Ausman K, Carter J, Karn B, Kreyling W, Lai D, Olin S, Monteiro-Riviere N, Warheit D, Yang H. 2005. Principles for characterizing the potential human health effects from exposure to nanomaterials: elements of a screening strategy. *Part Fibre Toxicol* 2:8.
- (65) Oomen AG, Tolls J, Sips AJAM, Van den Hoop MAGT. 2003. Lead speciation in artificial human digestive fluid. *Arch Environ Con Tox* 44:107-115.
- (66) Park MV, Neigh AM, Vermeulen JP, de la Fonteyne LJ, Verharen HW, Briede JJ, van Loveren H, de Jong WH. 2011. The effect of particle size on the cytotoxicity, inflammation, developmental toxicity and genotoxicity of silver nanoparticles. *Biomaterials* 32:9810-7.
- (67) PEN. 2013. The project on emerging nanotechnologies. 28 October 2013 edition. <http://www.nanotechproject.org/news/archive/9242/>.
- (68) Peters RJB, van Bommel G, Herrera Rivera Z, Helsper HPG, Marvin HJP, Weigel S, Tromp PC, Oomen AG, Rietveld AG, Bouwmeester H. 2014. Characterization of titanium dioxide nanoparticles in food products: analytical methods to define nanoparticles. *J. Agric. Food Chem.* 62:6285-6293.
- (69) Prieto P, Hoffmann S, Tirelli V, Tancredi F, Gonzalez I, Bermejo M, de Angelis I. 2010. An exploratory study of two Caco-2 cell models for oral absorption: a report on their within-laboratory and between-laboratory variability, and their predictive capacity. *ATLA* 38:367-386.
- (70) Reis PM, Raab TW, Chuat JY, Leser ME, Miller R, Watzke HJ, Holmberg K. 2008. Influence of Surfactants on Lipase Fat Digestion in a Model Gastro-intestinal System. *Food biophysics* 3:370-381.
- (71) Rogers KR, Bradham K, Tolaymat T, Thomas DJ, Hartmann T, Ma L, Williams A. 2012. Alterations in physical state of silver nanoparticles exposed to synthetic human stomach fluid. *The Science of the total environment* 420:334-339.
- (72) Sager TM, Castranova V. 2009. Surface area of particle administered versus mass in determining the pulmonary toxicity of ultrafine and fine carbon black: comparison to ultrafine titanium dioxide. *Part Fibre Toxicol* 6:15.
- (73) Scaldaferri F, Pizzoferrato M, Gerardi V, Lopetuso L, Gasbarrini A. 2012. The Gut Barrier New Acquisitions and Therapeutic Approaches. *J Clin Gastroenterol* 46:S12-S17.
- (74) Seifert J, Haraszti B, Sass W. 1996. The influence of age and particle number on absorption of polystyrene particles from the rat gut. *Journal of anatomy* 189 (Pt 3):483-6.
- (75) Sung JH, Ji JH, Park JD, Yoon JU, Kim DS, Jeon KS, Song MY, Jeong J, Han BS, Han JH, Chung YH, Chang HK, Lee JH, Cho MH, Kelman BJ, Yu IJ. 2009. Subchronic inhalation toxicity of silver nanoparticles. *Toxicol Sci* 108:452-461.
- (76) Tedja R, Lim M, Amal R, Marquis C. 2012. Effects of serum adsorption on cellular uptake profile and consequent impact of titanium dioxide nanoparticles on human lung cell lines. *ACS Nano* 6:4083-93.
- (77) van de Wiele TR, Oomen AG, Wragg J, Cave M, Minekus M, Hack A, Cornelis C, Rempelberg CJM, de Zwart LL, Klinck B, van Wijnen J, Verstraete W, Sips AJAM. 2007. Comparison of five in vitro digestion models to in vivo experimental results: lead bioaccessibility in the human gastrointestinal tract. *Journal of Environmental Science and Health Part A* 42:1203-1211.
- (78) Vardakou M, Mercuri A, Barker SA, Craig DQ, Faulks RM, Wickham MS. 2011. Achieving antral grinding forces in biorelevant in vitro models: comparing the USP dissolution apparatus II and the dynamic gastric model with human in vivo data. *AAPS PharmSciTech* 12:620-6.
- (79) Versantvoort CH, Oomen AG, Van de Kamp E, Rempelberg CJ, Sips AJ. 2005. Applicability of an in vitro digestion model in assessing the bioaccessibility of mycotoxins from food. *Food Chem Toxicol* 43:31-40.
- (80) Walczyk D, Bombelli FB, Monopoli MP, Lynch I, Dawson KA. 2010. What the Cell "Sees" in Bionanoscience. *J Am Chem Soc* 132:5761-5768.
- (81) Weir A, Westerhoff P, Fabricius L, Hristovski K, von Goetz N. 2012. Titanium dioxide nanoparticles in food and personal care products. *Environ. Sci. Technol.* 46:2242-2250.

- (82) Wickham MJS, Faulks RM, Mann J, Mandalari G. 2012. The design, operation, and application of a dynamic gastric model. *Dissolution Technologies* August 2012.
- (83) Wickham M, Faulks R, Mills C. 2009. In vitro digestion methods for assessing the effect of food structure on allergen breakdown. *Mol. Nutr. Food Res.* 53:952-958.
- (84) Wijnhoven SWP, Peijnenburg WJGM, Herberts CA, Hagens WI, Oomen AG, Heugens EHW, Roszek B, Bisschops J, Gosens I, van de Meent D, Dekkers S, de Jong WH, van Zijverden M, Sips AJAM, Geertsma RE. 2009. Nano-silver - a review of available data and knowledge gaps in human and environmental risk assessment. *Nanotoxicology* 3:109-138.

2

Behaviour of silver nanoparticles and silver ions in an in vitro human gastrointestinal digestion model

Agata P. Walczak
Remco Fokkink
Ruud Peters
Peter Tromp
Zahira E. Herrera Rivera
Ivonne M.C.M. Rietjens
Peter J.M. Hendriksen
Hans Bouwmeester

Based on: Nanotoxicology 2013 Nov;7(7):1198-1210

ABSTRACT

Oral ingestion is an important exposure route for silver nanoparticles (AgNPs), but their fate during gastrointestinal digestion is unknown. This was studied for 60 nm AgNPs and silver ions (AgNO_3) using *in vitro* human digestion model. Samples after saliva, gastric and intestinal digestion were analysed with SP-ICPMS, DLS and SEM-EDX. In presence of proteins, after gastric digestion the number of particles dropped significantly, to rise back to original values after the intestinal digestion. SEM-EDX revealed that reduction in number of particles was caused by their clustering. These clusters were composed of AgNPs and chlorine. During intestinal digestion, these clusters disintegrated back into single 60 nm AgNPs. The authors conclude that these AgNPs under physiological conditions can reach the intestinal wall in their initial size and composition. Importantly, intestinal digestion of AgNO_3 in presence of proteins resulted in particle formation. These nanoparticles (of 20-30 nm) were composed of silver, sulphur and chlorine.

INTRODUCTION

Nanotechnology develops rapidly and use of consumer products containing manufactured nanoparticles (NPs) is expected to further increase in the near future (Chaudhry et al. 2008). Particularly silver nanoparticles (AgNPs) are used in a wide range of applications (e.g., textiles and wound dressings), mostly because of their antimicrobial properties (Chaudhry et al. 2008; Tien et al. 2008; Rai et al. 2009). Also in food industry, AgNPs are applied for this reason not only in materials used for processing and packaging of food (e.g., kitchenware coated with AgNPs, or foils and containers with incorporated AgNPs), but also in food itself, for example, as health supplements (Chaudhry et al. 2008; Bouwmeester et al. 2009). Aqueous dispersions of AgNPs for oral consumption are easily accessible from numerous sources (Nanoparticle Products Inventory, PEN). Therefore, consumers are very likely exposed orally to AgNPs, either intentionally or accidentally.

The interest in NPs in general is caused by their size resulting in unique physical and chemical properties that differ from their bulk counterparts, even at the same mass dose (Chaudhry et al. 2008; Allahverdiyev et al. 2011). On the other hand, the unique properties of particles at nanoscale also give rise to possible safety concerns (Oberdorster et al. 2005; Drake and Hazelwood 2005; Navarro et al. 2008; Sung et al. 2009). However, the relations between observed biological effects of NPs and their physicochemical properties remain to be elucidated. For this, a set of nanomaterial properties has been proposed that should be determined at the minimum in any biological study (Bouwmeester et al. 2009; Oberdorster et al. 2005). A specific feature of AgNPs is their dissociation of ions (Kittler et al. 2010), which distinguishes AgNPs from inert gold or titanium dioxide NPs and which makes Ag⁺ ions an inseparable element accompanying AgNPs in aqueous solutions. Depending on the conditions, release of Ag⁺ ions from AgNPs can reach 90% of their total mass (Kittler et al. 2010). Clearly in any biological study using AgNPs, also the fate and behaviour of Ag⁺ ions should be considered, as well as the possibility of Ag salt complex formation in the nanosized range.

At the moment, risk assessment of chemicals and NPs heavily relies on *in vivo* studies. There is a high societal and scientific demand to develop alternative testing strategies to reduce or refine animal studies. The recent EFSA (European Food Safety Authority) guidance on risk assessment of NPs in the food and feed chain (EFSA and Committee 2011) proposes a tiered approach for testing, in which all steps occurring after oral administration are assessed by a series of *in vitro* assays. The first step is to understand the impact of human digestion, which in turn will help defining *in vitro* exposure conditions. It has been shown that AgNPs are very responsive to environmental conditions and frequently agglomerate readily when suspended in various solvents, including water (Bihari et al. 2008; Murdock et al. 2008). Gastrointestinal digestion consists of multiple factors that might influence the dynamic nature of AgNPs, such as elevated temperature, variable pH and variable concentrations of salts and enzymes along the digestive tract. All these parameters individually are known to affect the properties of AgNPs including their surface chemistry and agglomeration state (Chaudhry et al. 2008; Fabrega et al. 2009; El Badawy

et al. 2010; Liu and Hurt 2010; Bihari et al. 2008; Greulich et al. 2009; Rogers et al. 2012), their interaction with biomolecules (Cedervall et al. 2007; Lundqvist et al. 2008; Lynch and Dawson 2008) and their dissolution rate (Liu and Hurt 2010). However, the impact of the full digestion on AgNPs has not been studied *in vitro* yet.

The aim of the present study was to test the behaviour of well-characterized 60 nm AgNPs and Ag⁺ ions derived from AgNO₃ in an *in vitro* model of human gastrointestinal digestion. For this, the authors adapted the fed digestion model described by Versantvoort et al. (2005) that allowed us to monitor changes of AgNPs after incubation in artificial saliva, gastric and intestinal juice. This model simulates the human digestion in the oral, gastric and intestinal compartments with salt and protein composition, pH differences and transit times alike the *in vivo* digestion (Brandon et al. 2006). The model has been used so far for determining the bioaccessibility of orally ingested compounds like heavy metals (Oomen et al. 2003) or other contaminants (Versantvoort et al. 2005), and silica nanoparticles (Peters et al. 2012). Samples of AgNPs and AgNO₃ were tested with dynamic light scattering (DLS) and single particle-inductively coupled plasma mass spectrometry (SP-ICPMS) at each step of the digestion process, so after saliva, gastric and intestinal incubation. Scanning electron microscopy with energy dispersive X-ray analysis (SEM-EDX) was used to characterize morphology and elemental composition of particles.

The digestion process turns out to have a critical impact on AgNPs and Ag⁺ ions. The results indicate that under physiological conditions (in the presence of proteins) AgNPs reach the intestine most likely in their original, unchanged form. Ag⁺ ions reach the intestine as silver-containing NPs. These findings have important implications for the design of *in vitro* exposure and translocation studies conducted to evaluate the health impact of orally administered AgNPs.

MATERIALS AND METHODS

Materials including nanoparticles

The 60 nm AgNPs dispersed in 2 mM citrate buffer (pH=5.1) were purchased from NanoComposix, Inc. (San Diego, CA, USA). The silver mass concentration of the stock solution was 1 mg/ml. Transmission electron microscopy (TEM) size of the NPs, as provided by the manufacturer, was 58 ± 5 nm, and the hydrodynamic size was 68 nm. For the Ag⁺ ionic experiments, the authors used AgNO₃ from Sigma (Steinbach, Germany).

LC-MS (liquid chromatography-mass spectrometry) grade water for the characterisation studies was obtained from Biosolve (Valkenswaard, The Netherlands). For the preparation of artificial digestive juices for *in vitro* digestion (fed model variant), all the chemicals were obtained from Merck (Darmstadt, Germany), except for NaCl, which was obtained from VWR (Leuven, Belgium), uric acid from Alfa Aesar (Karlsruhe, Germany), glucosaminehydrochloride from Calbiochem (Darmstadt, Germany), mucin from Roth (Karlsruhe, Germany) and lipase, bile, MgCl₂·6H₂O, glucuronic acid and amylase from Sigma.

The constituents and concentrations of the digestive juices were as described by Versantvoort et al. (2005) and are listed in Table 1.

Table 1. Composition of juices of the “fed” *in vitro* digestion model (amounts based on 1000 ml juice) (Versantvoort et al. 2005).

Saliva (pH 6.8±0.1)	Gastric juice (pH 1.3±0.1)	Duodenal juice (pH 8.1±0.1)	Bile juice (pH 8.2±0.1)
896 mg KCl	2752 mg NaCl	7012 mg NaCl	5259 mg NaCl
200 mg KSCN	306 mg NaH ₂ PO ₄ ·H ₂ O	3388 mg NaHCO ₃	5785 mg NaHCO ₃
1021 mg NaH ₂ PO ₄ ·H ₂ O	824 mg KCl	80 mg KH ₂ PO ₄	376 mg KCl
570 mg Na ₂ SO ₄	302 mg CaCl ₂	564 mg KCl	150 µl HCl (37%)
298 mg NaCl	306 mg NH ₄ Cl	50 mg MgCl ₂ ·6H ₂ O	250 mg urea
1694 mg NaHCO ₃	6.5 ml 37% HCl	180 µl HCl (37%)	167.5 mg CaCl ₂
200 mg urea	650 mg glucose	100 mg urea	1.8 g BSA*
290 mg amylase*	20 mg glucuronic acid	151 mg CaCl ₂	30 g bile*
15 mg uric acid	85 mg urea	1 g BSA*	Milli-Q water
25 mg mucin*	330 mg glucosaminehydrochloride	9 g pancreatin*	
Milli-Q water	1 g BSA*	1.5 g lipase*	
	2.5 g pepsin*	Milli-Q water	
	3 g mucin*		
	Milli-Q water		
			Sodium carbonate solution
			84.7 g NaHCO ₃
			Milli-Q water

*Protein components included in the “digestion with proteins” but not included in the “digestion without proteins”.

Sample characterisation

AgNPs and AgNO₃ samples in water and saliva were characterised with three techniques: TEM, DLS and SP-ICPMS. Samples collected from the *in vitro* digestion were measured with SP-ICPMS, and selected samples also with DLS and SEM-EDX.

TEM analysis to determine morphological properties of AgNPs was performed on a JEOL JEM 1011 microscope (JEOL, Nieuw Vennep, The Netherlands), delivering beam current at 0.45 A and fitted with a Keenview 1k-1k camera.

DLS measurements to determine the hydrodynamic sizes of AgNPs were performed on an ALV, Laser Goniometer, Model ALV/SP-125 #011, Type: Diode Pumped Solid State (DPSS). DLS measurements were conducted at a scattering angle of 90°. Each correlation function was accumulated for 30 s, which was repeated 10 times for each sample. DLS analyses the velocity distribution of particle movement by measuring dynamic fluctuations of light scattering intensity caused by the Brownian motion of the particle. The data from these measurements are then calculated via the Stokes-Einstein equation to give the hydrodynamic radius of the particles. Hydrodynamic diameters were obtained using AfterALV software. Data cut-off was applied, so that samples with intensity lower or equal to the blank (pure solvent) were assumed as not containing any particles.

SP-ICPMS was used to determine the size and particle number concentration of AgNPs. SP-ICPMS enables detection of AgNPs in relatively complex matrices. The ICP-MS machine used in this study was a Thermo Scientific X series 2 equipped with a Babington type nebulizer and a quartz impact bead spray chamber. The ICP-MS machine was operated

at a forward power of 1400 W and the gas flows were at the following settings: plasma 13 l/min, nebulizer 1.1 l/min and auxiliary 0.7 l/min. The sample flow rate to the nebulizer was set at 1.5 ml/min using the integrated peristaltic pump. Data acquisition was done using the Thermo Plasmalab software in the time resolved analysis (TRA) mode. Typical acquisition times were 60 s per measurement. Silver was measured at m/z 107. Data were transferred to a CSV (comma-separated values) file, which was processed in Microsoft Excel for calculation of particle sizes, particle size distributions and particle concentrations. Data cut-off was applied, so that samples were treated as a background when they contained a number of particles lower than or the same as in blank samples. The lower size detection limit of SP-ICPMS for AgNPs is 18-20 nm (Laborda et al. 2011), and the silver lower concentration limit is 5 ng/ml.

SEM-EDX was used to determine the morphology and elemental composition of particles in samples after the digestion. The high resolution field emission gun scanning electron microscope (FEG-SEM) used in this study was a Tescan MIRA-LMH FEG-SEM (Tescan, Brno, Czech Republic). The microscope was operated at an accelerating voltage of 15 kV, working distance (WD) of 10 mm and spot size of 5 nm. The EDX spectrometer used was a Bruker AXS spectrometer with a Quantax 800 workstation and a XFlash 4010 detector with an active area of 10 mm² and super light element window (SLEW), which allows X-ray detection of elements higher than borium ($Z > 5$). The spectral resolution of the detector was 123 eV (Mn (10 kcps) ave FWHM (full width at half maximum)). Three different magnifications were used: 10,000 x, 25,000 x and 50,000 x, so that both agglomerates and single particles could be detected. After recognising the particles in a field of view, an X-ray spectrum from each detected particle was acquired.

The lower size detection limit of SEM-EDX for AgNPs is 15-20 nm.

Characterisation of AgNPs and AgNO₃ in media

AgNPs and AgNO₃ were characterised in water and in artificial saliva (pH = 6.8 ± 0.1).

First, freshly prepared samples of AgNPs and AgNO₃ were characterised with TEM, DLS and SP-ICPMS. For the TEM measurements, a stock solution of AgNPs was suspended at 100 µg/ml in each solvent and vortexed for 10 s to provide a homogenous suspension. A 5 µl drop of AgNP suspension was deposited onto a copper formvar-coated TEM carbon grid. Samples were left to dry completely prior to analysis. All samples were analysed in triplicate.

For the DLS measurements, a stock solution of AgNPs was diluted to 10 µg/ml in each solvent, vortexed for 10 s and measured within 2 min ($t=0$ h). The concentration of 10 µg/ml was selected based on average reported concentrations in commercially available NP colloidal silver suspensions (see PEN). A stock of 10 µg/ml AgNO₃, to be used as a source of Ag⁺ ions, was prepared in water and further diluted to 1 µg/ml in each solvent, vortexed for 10 s and measured within 2 min ($t=0$ h). Samples were measured with DLS in six independent repetitions, and for each repetition 10 measurements were collected. The total DLS measurement procedure took about 5 min. For the SP-ICPMS measurements, a stock of AgNPs was suspended at 10 µg/ml in each solvent, vortexed for 10 s and within 2 min further diluted with adequate solvent to 25 and 250 ng/l. A stock solution of AgNO₃ was prepared at

10 µg/ml in water, vortexed for 10 s and within 2 min further diluted with adequate solvent to two sub-samples of 500 ng/l. The final concentrations of samples were chosen as most optimal, based on previous measurements (Peters et al. 2012). All samples were analysed with SP-ICPMS within 5-15 min ($t=0$ h). SP-ICPMS measurements were performed in triplicate and each sample of the triplicate was analysed in two analytical dilutions.

Second, the effect of ageing of NPs in the solvents was tested. To this end, DLS and SP-ICPMS measurements were repeated after incubating the AgNPs and AgNO₃ for 24 hours ($t=24$ h) in the dark, at room temperature. The samples were analysed as described above for $t=0$ h.

Characterisation of AgNPs and AgNO₃ during *in vitro* digestion

In this study, the authors used 60 nm AgNPs and AgNO₃ solution as a source of Ag⁺ ions, to check the behaviour of AgNPs and Ag⁺ ions in the *in vitro* model of human digestion. Water, not containing any forms of silver, was used as a blank sample. The *in vitro* digestion model used was adapted from Versantvoort et al. (2005), and is described there in detail (the fed model variant). Briefly, all digestive juices were prepared according to Table 1 and heated to 37°C. The digestion started by adding 1 ml of water, 10 µg/ml 60 nm AgNPs (i.e., 1661 ± 154 particles/ml) or 1 µg/ml AgNO₃ to 6 ml of saliva (pH = 6.8 ± 0.1). The mixture was incubated for 5 min at $37 \pm 2^\circ\text{C}$, rotating head-over-heels at 55 rpm, simulating peristaltic movements. Subsequently, 12 ml of gastric juice (pH=1.3) was added to the mixture and the pH of the sample was checked and, if necessary, adjusted to 2.5 ± 0.5 with NaOH (1M) or HCl (37%). The sample was further incubated rotating at 37°C for 2 h. Subsequently, 12 ml of duodenal juice (pH=8.1), 6 ml of bile (pH=8.2) and 2 ml of sodium bicarbonate solution were added. The pH of this mixture was set at 6.5 ± 0.5 with NaOH (1M) or HCl (37%) and it was rotated head-over-heels for another 2 h.

The impact of digestion was evaluated under two conditions: without proteins and with proteins. Samples without proteins were measured with SP-ICPMS and DLS. Samples with proteins could only be measured with SP-ICPMS, because DLS measurements were disturbed by the proteins present in the gastric and intestinal juices.

During the digestion procedure, samples of 0.5 ml were collected at three successive steps: after incubation in saliva, gastric and intestinal juice. Prior to SP-ICPMS analysis, samples with AgNPs were diluted with water to two sub-samples of 25 and 250 ng/l, and the samples with AgNO₃ were diluted to two sub-samples of 500 ng/l. Blank (water) samples were incubated in the digestion model and diluted in exactly the same way as the samples containing AgNPs. All samples (with AgNPs, with AgNO₃ and blanks) were incubated in triplicate, and each sample of the triplicate was analysed in two analytical dilutions.

For DLS analysis, the starting concentrations of AgNPs and AgNO₃ were increased to 50 and 5 µg/ml, respectively, in order to obtain minimum measurable concentration of 1 µg/ml in the final intestinal samples. Sub-samples of 1 ml were collected during digestion and they were measured directly with DLS.

SEM-EDX was used to characterise morphology and elemental composition of particles during digestion with proteins. Samples of AgNPs were measured after gastric and intestinal

digestion, and the samples of AgNO_3 were measured after intestinal incubation. Exclusively for these measurements, the concentrations of digested AgNPs and AgNO_3 were increased to 50 and 100 $\mu\text{g}/\text{ml}$, respectively, to increase the chances of particle detection. Aliquots of 2-5 ml of the juices were filtered over a nickel-coated polycarbonate filter with pore size 50 nm using a vacuum pump. While mounted in aluminium holders connected to the pump, the filters were rinsed with 5 ml of Milli-Q water. Subsequently, the moist filters were quickly dried and mounted on aluminium specimen holders with double-sided adhesive carbon tape. The filters were analysed immediately afterwards.

Statistics

All results are presented as an average \pm standard error. One-way analysis of variance (ANOVA) was applied to determine statistical significance for the sizes of AgNPs in media and the numbers of particles detected during the digestion experiment. Tukey *post hoc* test was used to determine the identity of the groups in which the significant difference was observed.

Groups were considered significantly different, when $p < 0.05$.

RESULTS

Characterisation of AgNPs and AgNO_3 in media

The authors characterised the behaviour of AgNPs and AgNO_3 in two solvents. Water was used as a basic simple solvent to assess the initial size of AgNPs, and artificial saliva with proteins as the first step of the digestion model to assess the size of AgNPs entering the digestion model. Three techniques were used to measure AgNPs in these media: TEM provided the diameters of the particles, DLS provided hydrodynamic diameters of particles and SP-ICPMS provided masses of the particles that were mathematically converted into sizes. TEM analysis of AgNPs in water confirmed that the size provided by the manufacturer (58 ± 5 nm) was appropriate. A representative picture of these spherical particles is shown in Figure 1. Throughout the paper, the authors used the size from TEM analysis as indicated by the manufacturer (60 nm) to describe the AgNPs. As indicated by DLS, AgNPs suspended in both media had monodisperse size distributions, as shown in Figure 2. Consequently, the data obtained from these measurements can be summarised by presenting the means \pm standard error of the diameters. The hydrodynamic size of AgNPs measured with DLS at $t=0$ was 67 ± 1 nm in water and 92 ± 3 nm in saliva. The size of AgNPs measured with SP-ICPMS at $t=0$ h was 59 ± 2 nm in water and 49 ± 1 nm in saliva. Sizes in water and saliva measured by DLS were approximately 15% and 88% larger than those indicated by both TEM and SP-ICPMS.

Subsequently, the effect of incubation of AgNPs and AgNO_3 in water and saliva for 24 h in the dark, at room temperature was studied. The sizes of AgNPs were determined with DLS and with SP-ICPMS. As measured with DLS (Figure 2), AgNPs had a hydrodynamic diameter of 70 ± 2 nm in water and 105 ± 4 nm in saliva. As measured with SP-ICPMS, AgNP sizes after 24 h incubation in both media did not differ compared with AgNPs analysed at $t=0$ h: 58 ± 4 and 52 ± 9 nm in water and saliva respectively.

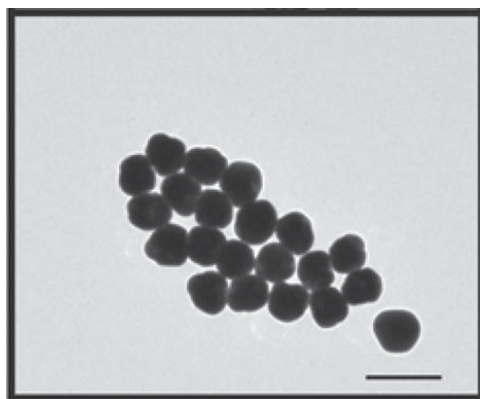


Figure 1. TEM photo of 60 nm AgNPs in water. The bar indicates 100 nm.

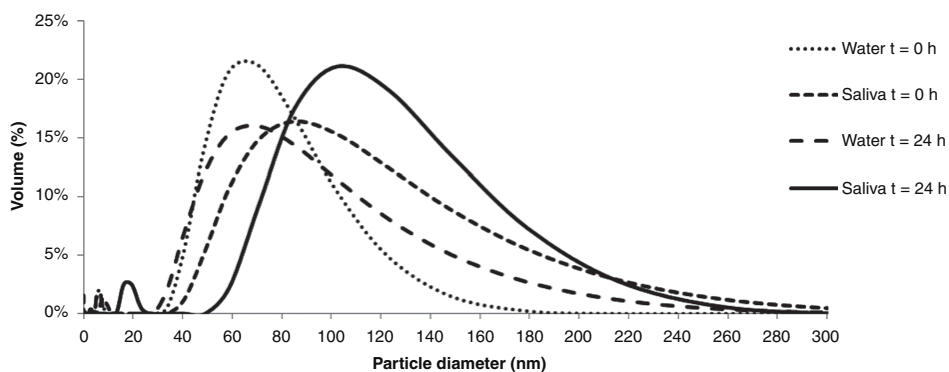


Figure 2. Hydrodynamic sizes of AgNPs in water and saliva, measured at $t=0$ h and $t=24$ h with DLS. DLS measurements were generally performed in triplicate, on two separate days ($n=6$). The results presented are an average of all measurements for each sample.

Solutions of AgNO_3 in the media did not contain any particles apart from some incidental particles of 815 ± 135 nm detected with DLS at $t=24$ h in saliva.

Characterisation of AgNPs and AgNO_3 during the *in vitro* digestion

In the next experiment, the authors tested the behaviour of 60 nm AgNPs and Ag^+ ions derived from AgNO_3 in the *in vitro* model of human digestion.

Sizes of the particles in samples were quantified with SP-ICPMS and DLS at each step of the digestion process, that is, after saliva, gastric and intestinal incubation. The impact of digestion was evaluated under two conditions: with proteins normally present during human digestion, included in the digestion juices (with SP-ICPMS) and without these proteins (with SP-ICPMS and DLS).

Digestion without proteins

As shown in Figure 3, AgNPs detected with SP-ICPMS after the incubation for 5 minutes in saliva were present nearly as numerous (1418 ± 137 /ml) as in water (1747 ± 77 /ml) with the same size distribution, with most of the particles in the size range of around 60 nm. After incubation in the gastric juice, the number of particles decreased significantly ($p < 0.05$) by 90% (to 125 ± 85 /ml) and stayed on this level (149 ± 75 /ml) during the intestinal incubation. At the same time, the sizes of the remaining particles in these gastric and intestinal samples decreased to 20-30 nm. As the lower size detection limit of SP-ICPMS for AgNPs is 18-20 nm (Peters et al. 2012; Laborda et al. 2011), it is possible that also smaller particles were present in the intestinal phase, assuming a normal size distribution.

The numbers of particles per ml determined after digestion of the AgNO_3 sample (14 ± 7 in saliva, 6 ± 9 in gastric juice and 12 ± 16 in intestinal juice) were comparable with that of AgNO_3 solutions in water (6 ± 6), and therefore considered to be the background.

Samples digested without proteins were measured also with DLS. After incubation of AgNPs in saliva, numerous particles were detected with the average hydrodynamic size of around 100 nm and with a wide size distribution (60-300 nm). After incubation in the gastric and intestinal juice no particles were detected by DLS.

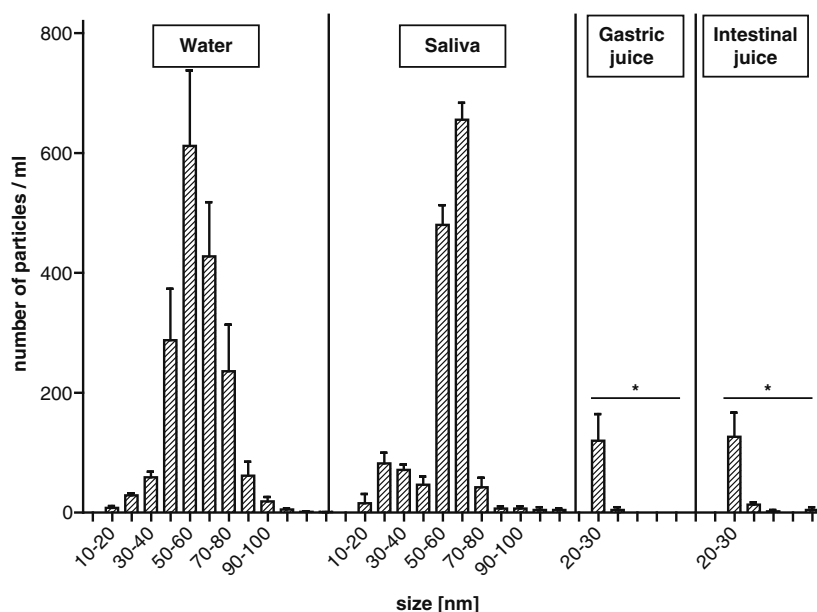


Figure 3. Size distributions of particles detected after digestion of 60 nm AgNPs, measured with SP-ICPMS. The digestion was carried out without proteins. Sizes of AgNPs are shown in water, saliva, gastric and intestinal juice. On the left axis: numbers of particles per ml detected in the samples (average \pm SEM). The total numbers of particles per ml in AgNP samples were: 1747 ± 77 in water control, 1418 ± 137 in saliva, 125 ± 85 in the gastric juice and 149 ± 75 in the intestinal juice. *Number of particles significantly different ($p < 0.05$) compared with saliva sample.

AgNO₃ samples only rarely contained NPs after saliva digestion and these had a hydrodynamic diameter of approximately 300 nm. No particles were detected after gastric and intestinal digestion (data not shown).

Digestion with proteins

SP-ICPMS analysis showed that during the whole digestion with proteins AgNPs kept similar size (around 60 nm) and size distribution (Figure 4A). The number of particles determined by SP-ICPMS in saliva (1627 ± 22 /ml) was in accordance with the number of particles detected in the control AgNP samples in water (1460 ± 51 /ml). In the gastric stage the number of particles dropped significantly ($p < 0.05$) to 374 ± 33 /ml, to rise back to 1577 ± 72 /ml after the intestinal incubation.

In AgNO₃ samples (Figure 4B), there were hardly any particles detected after saliva (12 ± 10 /ml) and gastric (13 ± 7 /ml) digestion, which was only a few more than in the water control (7 ± 4 /ml). After the intestinal incubation, however, the particles became more abundant and their numbers were highly variable between triplicates (860 ± 811 /ml). The same high variability was seen in size distributions of these particles. These outcomes suggest that formation of particles from Ag⁺ had a chaotic course. The particles formed from Ag⁺ during the intestinal incubation were much smaller (20-40 nm) than the particles in the corresponding AgNP group after intestinal incubation (around 60 nm).

Because SP-ICPMS revealed a drop in the number of AgNPs after gastric digestion with proteins and an increase in the number of AgNPs after intestinal digestion, but the size distribution was constant, further study with SEM-EDX was applied to determine appearance and composition of particles. In all cases, the detected particles contained silver. AgNPs after gastric digestion were present in two forms: as big clusters of approximately 200-500 nm and as single, well-dispersed particles (Figure 5A). The big clusters clearly consisted of grouped single AgNPs. EDX analysis of the clusters revealed the presence of chlorine, in addition to the strong silver signal (Figure 5B). Figure 6 shows the clear co-localisation of Ag and Cl in one of such clusters. Following subsequent intestinal digestion, SEM-EDX revealed the presence of single, well-dispersed silver particles with an average diameter of 48 ± 8 nm (Figure 7A). EDX analysis showed that these particles were composed of silver only (Figure 7B).

As SP-ICPMS revealed the presence of silver particles after the intestinal stage of AgNO₃ with proteins, this was also studied further with SEM-EDX. Particles were found with a size of approximately 20-30 nm (Figure 8A). EDX analysis showed that these particles were composed of silver, sulphur and chlorine (Figure 8B).

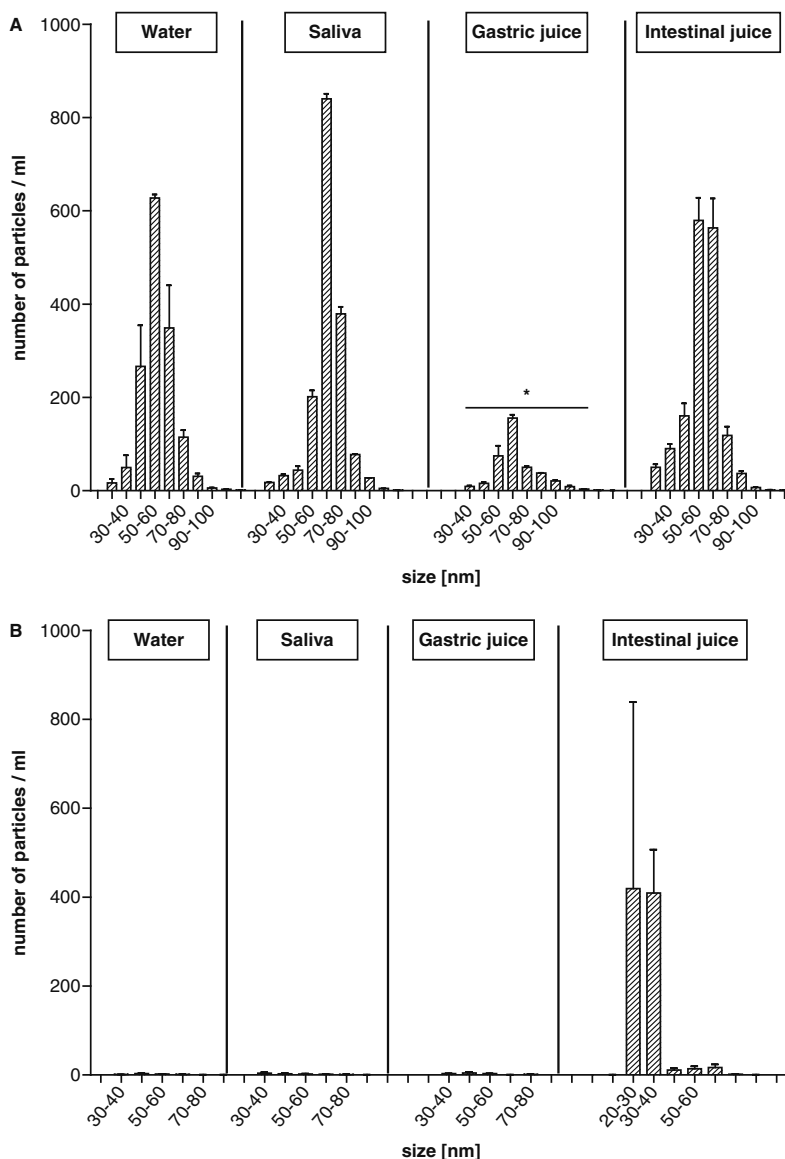


Figure 4. Size distributions of particles detected after digestion of (A) 60 nm AgNPs and (B) AgNO₃, measured with SP-ICPMS. The digestion was carried out in the presence of proteins normally present during human digestion. Sizes of AgNPs are shown in water, saliva, gastric and intestinal juice. On the left axis: numbers of particles per ml detected in the samples (average \pm SEM). The total numbers of particles per ml in AgNP samples (A) were: 1460 ± 51 in water control, 1627 ± 22 in saliva, 374 ± 33 in the gastric juice and 1577 ± 72 in the intestinal juice. The total numbers of particles per ml detected in AgNO₃ samples (B) were: 7 ± 4 in water control, 12 ± 10 in saliva, 13 ± 7 in the gastric juice and 860 ± 811 in the intestinal juice. *Number of particles significantly different ($p < 0.05$) compared with saliva sample.

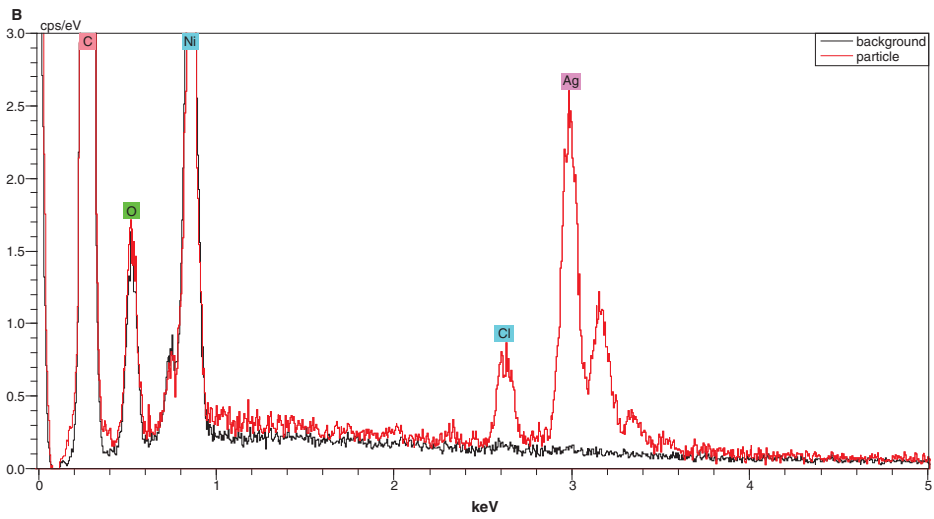
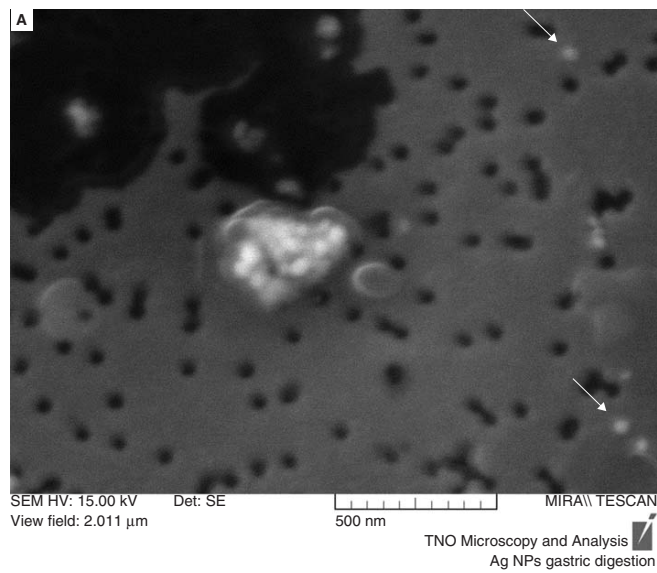


Figure 5. (A) Representative cluster of AgNPs found in gastric sample of AgNP digestion in the presence of proteins. There are also single AgNPs found in the sample (indicated with arrows). (B) X-ray spectrum obtained from the cluster, indicating the presence of silver and chlorine.

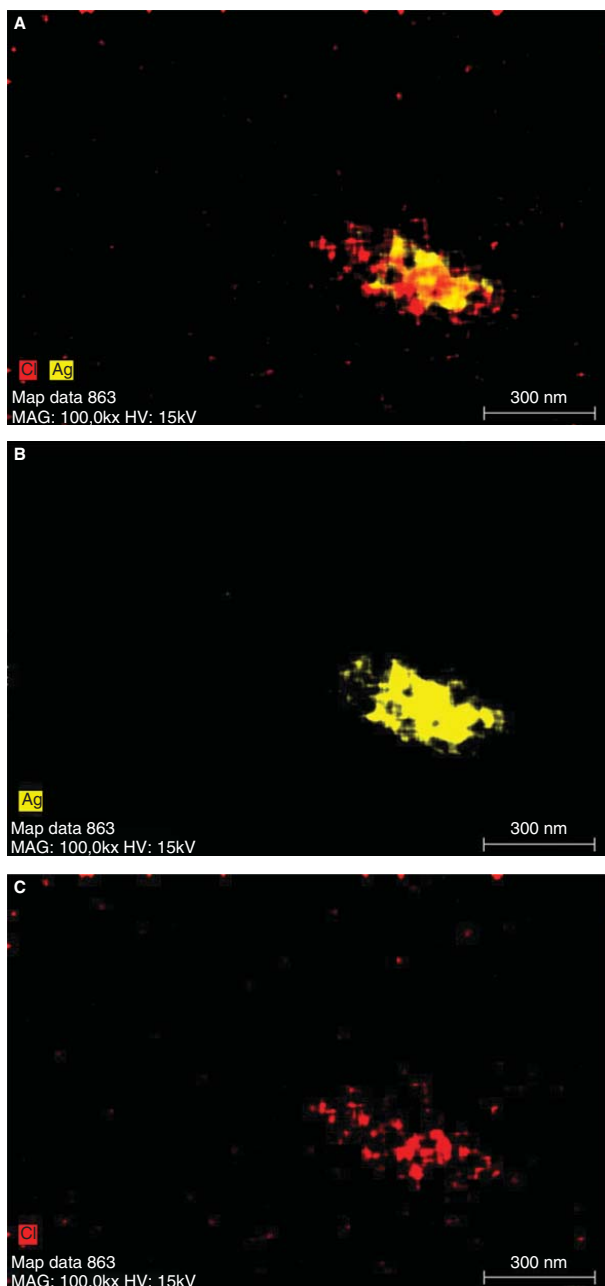


Figure 6. X-ray element mapping of the cluster of AgNPs found in gastric sample in the presence of proteins (Figure 5A). Mapping was done for (B) silver and (C) chlorine. Co-localisation of Ag and Cl in the cluster is clear (A).

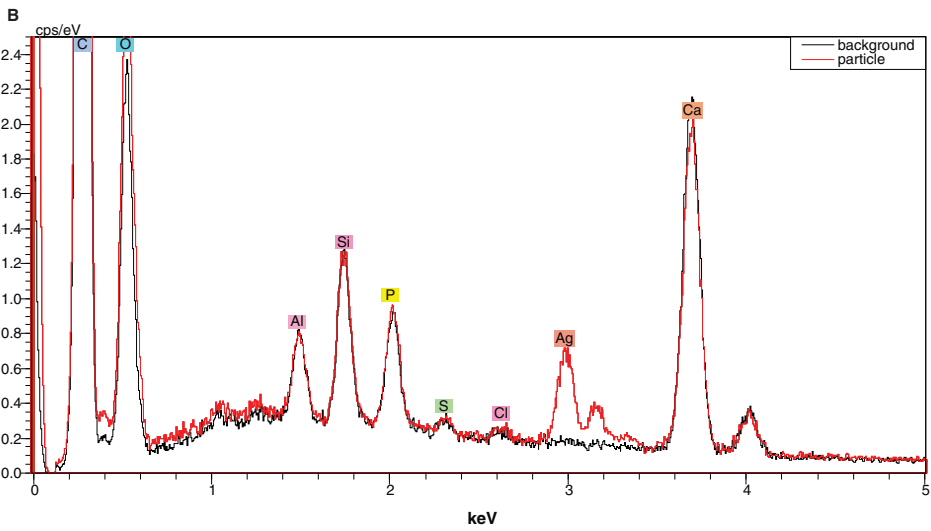
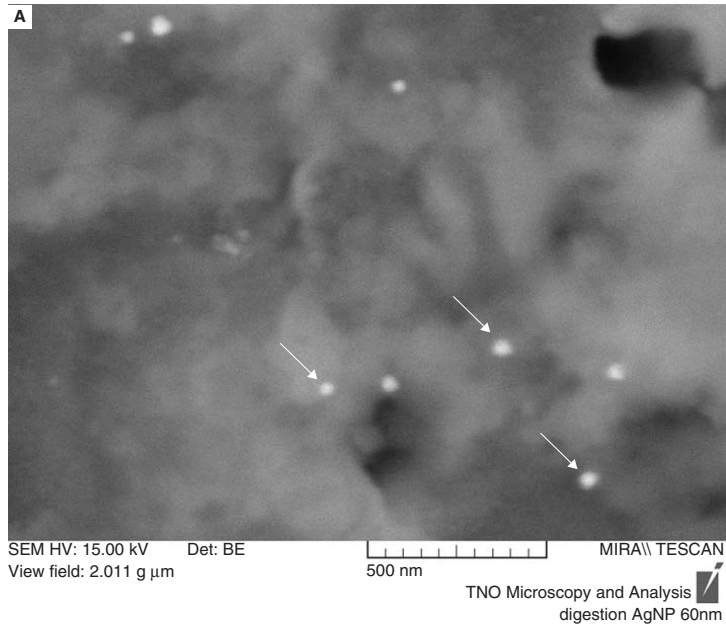


Figure 7. (A) Single particles (indicated with arrows) found in intestinal sample of AgNP digestion in the presence of proteins. (B) X-ray spectrum obtained from the particles, indicating the presence of only silver.

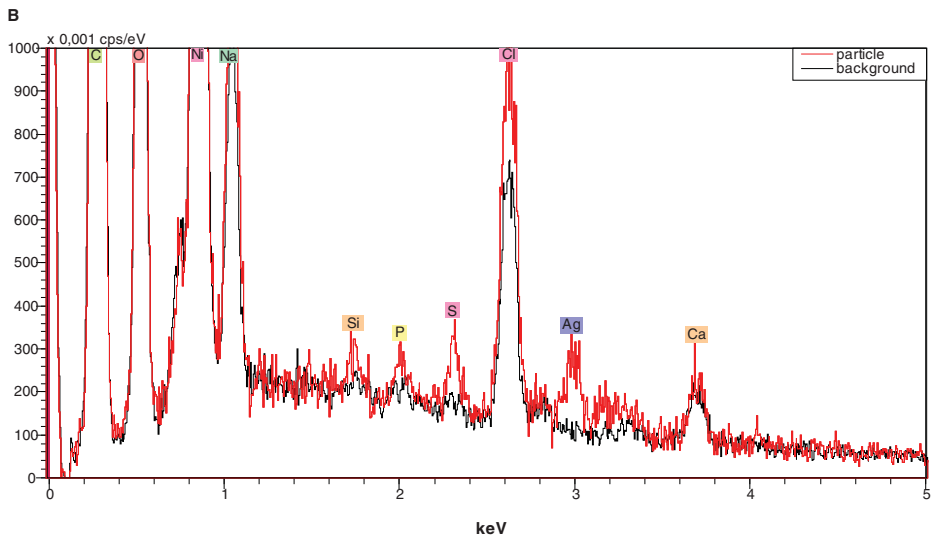
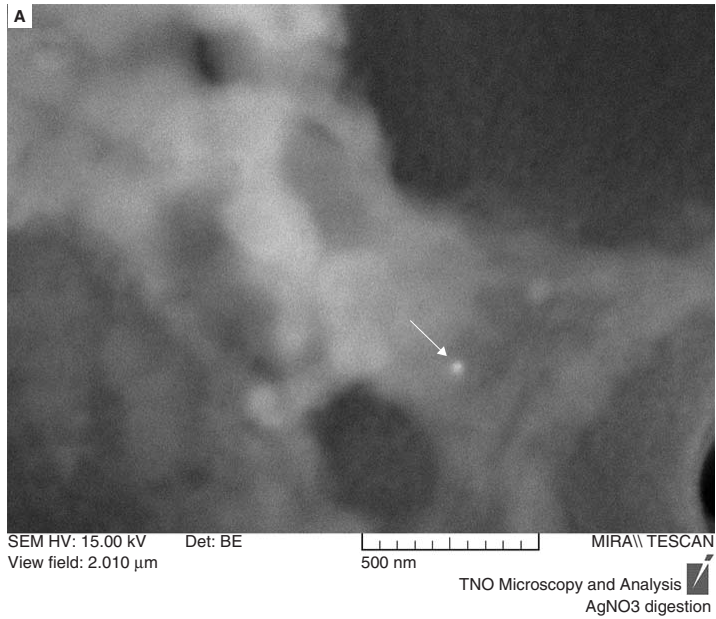


Figure 8. (A) Particle (indicated with arrow) found in intestinal sample of AgNO₃ digestion in the presence of proteins. (B) X-ray spectrum obtained from the particle, indicating the presence of silver, sulphur and chlorine.

DISCUSSION

The aim of the present study was to test the behaviour of well-characterised 60 nm AgNPs and Ag⁺ ions derived from AgNO₃ in the *in vitro* model of human digestion. First, the behaviour of AgNPs and Ag⁺ ions derived from AgNO₃ in water and saliva was tested with three different techniques. AgNPs were confirmed to be approximately 60 nm in water. In general, sizes measured with DLS were somewhat larger (by approximately 15- 88%) than those indicated by both TEM and SP-ICPMS. With TEM and SP-ICPMS only the silver content of AgNPs is measured. Therefore, sizes obtained from TEM and SP-ICPMS can differ from sizes obtained from DLS, which measures the hydrodynamic sizes of particles (Nath and Chilkoti 2004). Comparing results from DLS and TEM/SP-ICPMS allows to differentiate indirectly the silver core of NP from its non-silver coating. The DLS sizes of AgNPs in saliva were slightly larger than in water (by approximately 37%) and larger than SP-ICPMS sizes in saliva (by approximately 88%). Likely these differences can be explained by the hydrodynamic size measured by DLS or by the formation of a protein corona around the particles (Walczyk et al. 2010), which is not detected with SP-ICPMS. The sizes of AgNPs were stable during the 24 h of incubation in saliva. It has been reported before that media containing proteins stabilize the particles (Greulich et al. 2009; Murdock et al. 2008). The stability of AgNPs in media and the retention of their size during the time frame of the experiments are necessary for reliability and reproducibility of the results.

In this study, the authors used the well-established model for gastrointestinal digestion described previously (Versantvoort et al. 2005; Peters et al. 2012), consisting of subsequent incubation in oral, gastric and intestinal conditions. The main outcome of this study is that 60 nm AgNPs ingested in the concentration of 10 µg/ml (i.e., 1661 ± 153 particles/ml) in the presence of proteins, survive the extreme conditions of gastrointestinal digestion and reach the intestine. It can be concluded that the human intestinal epithelium is very likely exposed to 60 nm AgNPs as ingested, with minimal changes in size. At the same time, ingestion of Ag⁺ ions at 1 µg/ml also results in intestinal exposure to particles, but these are most likely complexes of silver, sulphur and chlorine (Table 2).

The results indicate that in the absence of proteins during digestion the behaviour of both AgNPs and AgNO₃ is completely different compared with the digestion in the presence of proteins. In the absence of proteins, after both gastric and intestinal digestion, only a small fraction of initial AgNP concentration was detected with SP-ICPMS, and the sizes of particles were smaller (20-30 nm). With DLS no particles were detected in these samples. This suggests that without the “protection” of proteins, particles dissolve in the low gastric pH, as proposed before (Chen and Schluesener 2008; Loeschner et al. 2011). It is known that high temperature, low pH and high ionic strength can facilitate the dissolution of AgNPs (Zelyanskii et al. 2001; Kittler et al. 2010; Liu and Hurt 2010; Huynh and Chen 2011).

After the gastric digestion with proteins, the number of AgNPs measured by SP-ICPMS decreased, but SEM analysis indicated clusters of AgNPs. It was shown by SEM that most of the AgNPs were present in the form of big clusters (200-500 nm diameter), each containing easily distinguishable single NPs. AgNPs are known to agglomerate in media of high ionic

Table 2. Summary of the results of *in vitro* digestion of 60 nm AgNPs and AgNO₃.

Type of material	Digestive conditions	Digestive stage (number of particles/ml and mean size of NPs as determined by SP-ICPMS)		
		Saliva	Gastric	Intestinal
AgNPs	Without proteins	1418 ± 137	125 ± 85*	149 ± 75*
		60 nm	20-30 nm#	20-30 nm#
	With proteins	1627 ± 22	374 ± 33*	1577 ± 72
		60 nm	60 nm and large clusters of 200-500 nm shown by SEM-EDX	60 nm
Ag ions	Without proteins	ND	ND	ND
	With proteins	ND	ND	860 ± 811 nm 20-40 nm

#The lower size detection limit of SP-ICPMS is 18-20 nm; *Number of particles significantly different ($p < 0.05$) compared with saliva sample; ND, number of nanoparticles/ml in the respective digestive juices was comparable with the number of nanoparticles/ml in water; AgNPs, silver nanoparticles; SEM-EDX, scanning electron microscopy with energy dispersive X-ray analysis; SP-ICPMS, single particle-inductively coupled plasma mass spectrometry.

strength (Bihari et al. 2008; Greulich et al. 2009; Foldbjerg et al. 2009; El Badawy et al. 2010) and this could be the reason underlying their agglomeration in the gastric juice. High ionic strength enhances AgNP dissolution (Huynh and Chen 2011), which in turn facilitates the agglomeration process (Li et al. 2010). Subsequent EDX analysis showed the co-localisation of silver and chlorine. It suggests that chlorine was involved in connecting separate AgNPs inside clusters with chlorine interparticle “bridges”. Formation of such chlorine bridges is reported in solutions where AgNPs come in contact with chlorine ions (Li et al. 2010; Huynh and Chen 2011). Formation of agglomerates with incorporation of chlorine has been recently reported after digestion of 40 nm AgNPs at a concentration of 25 µg/ml in a simple *in vitro* model of the human stomach (Rogers et al. 2012). Both in their and this model, AgNP agglomeration was observed after gastric digestion. Apparently, neither the difference in size (40 vs. 60 nm) nor in concentration (25 vs. 10 µg/ml) influences the occurrence of agglomeration of AgNPs during gastric digestion. However, in this model after gastric digestion some fraction of AgNPs remained in well-dispersed, single form of unchanged size. This is in line with the results obtained from SP-ICPMS that revealed the presence of AgNPs with sizes distributed around 60 nm. Strikingly, no clusters of AgNPs were detected with SP-ICPMS. Theoretically, SP-ICPMS should be able to measure AgNPs up to µm sizes (Pace et al. 2011). Possibly, the clusters did not reach the detector of the ICPMS, probably because the clusters sedimented before analysis.

Importantly, after the intestinal digestion in the presence of proteins, well-dispersed, single AgNPs were detected with SP-ICPMS with size distribution around 60 nm. Additional

EDX analysis showed that these were pure silver NPs, without co-localisation of any other element. Apparently, the increase of pH from gastric to intestinal stage, even though in combination with high ionic strength, induced the process of cluster disintegration resulting in reappearance of single particles. Similar intestinal disintegration of particles clustered previously in the stomach has recently been shown for silica nanoparticles (Peters et al. 2012). Reversible clustering and disassembling of NPs due to changes in pH was shown to be caused by changes in the protein coating of the NPs (Meziani and Sun 2003).

Interestingly, after intestinal digestion of AgNO_3 in the presence of proteins, silver-containing particles were found by SP-ICPMS, while no particles were detected at the earlier digestion stages. The particles were small, with diameter of 20-30 nm. Because this size is close to the lower size detection limit of SP-ICPMS, it is possible that there were a number of smaller particles in the sample, assuming a normal size distribution. Since the lower size detection limit for SEM is around 15-20 nm, a 10 times higher AgNO_3 concentration was used for the SEM experiment. Particles containing Ag were detected, and EDX analysis showed that these particles were composed of silver, chlorine and sulphur. Silver is known to have a very high affinity with both chlorine and sulphur. AgCl and Ag_2S are formed readily in solutions containing Ag^+ ions and Cl^- or S^{2-} (Li and Zhu 2006; Cheng et al. 2004; Loeschner et al. 2011; Levard et al. 2011; Danscher and Stoltenberg 2006; Choi et al. 2009).

Data from *in vivo* studies indicate that upon oral administration of AgNPs and Ag^+ ions, particles accumulate in tissues and these particles were shown to consist of silver and sulphur (Danscher and Stoltenberg 2006; Jonas et al. 2007; Loeschner et al. 2011). Additionally, oral exposure to Ag^+ ions has been recently shown to result in formation of sulphur containing silver granules in the intestinal epithelium (Loeschner et al. 2011). The authors suggested that these complexes were formed in lysosomes, but our results indicate that these complexes might already be formed in the intestinal lumen during digestion.

The fact that during intestinal digestion Ag^+ ions give rise to particle formation, most probably Ag_2S and/or AgCl salt particles, might influence their potential uptake and toxicity. The toxic effects of silver ions should be reduced by the formation of insoluble silver salts (Loeschner et al. 2011). On the other hand, the effects of silver salts (Ag_2S) on the intestine are unknown and, given the results of the present study, need to be investigated.

CONCLUSION

From this study, the authors conclude that gastrointestinal digestion impacts AgNPs and Ag^+ ions so that they change during gastrointestinal digestion. AgNPs agglomerate to a high extent during gastric passage, a process facilitated by chlorine interparticle bridges. Nevertheless, these agglomerates break down when changing into intestinal conditions, releasing the original AgNPs retaining their original size in the intestinal juice. Thus, it is concluded that orally ingested 60 nm AgNPs, digested under physiologically relevant conditions (i.e., in the presence of proteins), ultimately can reach the intestinal wall in their size and dispersion. The results of the present study also revealed that ingestion of Ag^+ ions

results in formation of NPs containing silver, sulphur and chlorine. Therefore, ingestion of both AgNPs and Ag⁺ ions ultimately leads to intestinal exposure to NPs, albeit with a different chemical composition. The outcomes of this study should be used for designing future *in vitro* and *in vivo* experiments, to serve future risk assessments of orally ingested silver nanoparticles and ions.

ACKNOWLEDGEMENTS

This project was funded by ZonMw (grant no. 40-40100-94-9016), the Dutch Ministry of Economy, Agriculture and Innovation. This work is supported by NanoNextNL, a micro- and nanotechnology consortium of the Government of the Netherlands and 130 partners. The authors would like to thank Rob Bakker for making TEM pictures and Elly Wijma for operating SP-ICPMS.

REFERENCES

- (1) Allahverdiyev AM, Kon KV, Abamor ES, Bagirova M, Rafailovich M. 2011. Coping with antibiotic resistance: combining nanoparticles with antibiotics and other antimicrobial agents. *Expert Rev Anti Infect Ther* 9:1035-1052.
- (2) Bihari P, Vippola M, Schultes S, Praetner M, Khandoga AG, Reichel CA, Coester C, Tuomi T, Rehberg M, Krombach F. 2008. Optimized dispersion of nanoparticles for biological *in vitro* and *in vivo* studies. *Part Fibre Toxicol* 5:14.
- (3) Bouwmeester H, Dekkers S, Noordam MY, Hagens WI, Bulder AS, de Heer C, ten Voorde SECG, Wijnhoven SWP, Marvin HJP, Sips AJAM. 2009. Review of health safety aspects of nanotechnologies in food production. *Regul Toxicol Pharm* 53:52-62.
- (4) Brandon EF, Oomen AG, Rompelberg CJ, Versantvoort CH, van Engelen JG, Sips AJ. 2006. Consumer product *in vitro* digestion model: Bioaccessibility of contaminants and its application in risk assessment. *Regul Toxicol Pharmacol* 44:161-171.
- (5) Cedervall T, Lynch I, Foy M, Berggard T, Donnelly SC, Cagney G, Linse S, Dawson KA. 2007. Detailed identification of plasma proteins adsorbed on copolymer nanoparticles. *Angew Chem Int Ed Engl* 46:5754-5756.
- (6) Chaudhry Q, Scotter M, Blackburn J, Ross B, Boxall A, Castle L, Aitken R, Watkins R. 2008. Applications and implications of nanotechnologies for the food sector. *Food Addit Contam Part A Chem Anal Control Expo Risk Assess* 25:241-258.
- (7) Chen X, Schluesener HJ. 2008. Nanosilver: a nanoproduct in medical application. *Toxicol Lett* 176:1-12.
- (8) Cheng D, Xia H, Chan HS. 2004. Facile fabrication of AgCl@polypyrrole-chitosan core-shell nanoparticles and polymeric hollow nanospheres. *Langmuir* 20:9909-9912.
- (9) Choi O, Clevenger TE, Deng B, Surampalli RY, Ross L, Jr., Hu Z. 2009. Role of sulfide and ligand strength in controlling nanosilver toxicity. *Water Res* 43:1879-86.
- (10) Danscher G, Stoltenberg M. 2006. Silver enhancement of quantum dots resulting from (1) metabolism of toxic metals in animals and humans, (2) *in vivo*, *in vitro* and immersion created zinc-sulphur/zinc-selenium nanocrystals, (3) metal ions liberated from metal implants and particles. *Prog Histochem Cytochem* 41:57-139.
- (11) Drake PL, Hazelwood KJ. 2005. Exposure-related health effects of silver and silver compounds: a review. *Ann Occup Hyg* 49:575-585.
- (12) EFSA, Committee ES. 2011. Guidance on the Risk Assessment of the Application of Nanoscience and Nanotechnologies in the Food and Feed Chain. *EFSA Journal* 9:36.
- (13) El Badawy AM, Luxton TP, Silva RG, Scheckel KG, Suidan MT, Tolaymat TM.

2010. Impact of environmental conditions (pH, ionic strength, and electrolyte type) on the surface charge and aggregation of silver nanoparticles suspensions. *Environ Sci Technol* 44:1260-1266.
- (14) Fabrega J, Fawcett SR, Renshaw JC, Lead JR. 2009. Silver nanoparticle impact on bacterial growth: effect of pH, concentration, and organic matter. *Environ Sci Technol* 43:7285-7290.
- (15) Foldbjerg R, Olesen P, Hougaard M, Dang DA, Hoffmann HJ, Autrup H. 2009. PVP-coated silver nanoparticles and silver ions induce reactive oxygen species, apoptosis and necrosis in THP-1 monocytes. *Toxicol Lett* 190:156-162.
- (16) Greulich C, Kittler S, Eppe M, Muhr G, Koller M. 2009. Studies on the biocompatibility and the interaction of silver nanoparticles with human mesenchymal stem cells (hMSCs). *Langenbecks Arch Surg* 394:495-502.
- (17) Huynh KA, Chen KL. 2011. Aggregation kinetics of citrate and polyvinylpyrrolidone coated silver nanoparticles in monovalent and divalent electrolyte solutions. *Environ Sci Technol* 45:5564-71.
- (18) Jonas L, Bloch C, Zimmermann R, Stadie V, Gross GE, Schad SG. 2007. Detection of silver sulfide deposits in the skin of patients with argyria after long-term use of silver-containing drugs. *Ultrastructural pathology* 31:379-384.
- (19) Kittler S, Greulich C, Diendorf J, Koller M, Eppe M. 2010. Toxicity of Silver Nanoparticles Increases during Storage Because of Slow Dissolution under Release of Silver Ions. *Chem Mater* 22:4548-4554.
- (20) Laborda F, Jimenez-Lamana J, Bolea E, Castillo JR. 2011. Selective identification, characterization and determination of dissolved silver(I) and silver nanoparticles based on single particle detection by inductively coupled plasma mass spectrometry. *J Anal Atom Spectrom* 26:1362-1371.
- (21) Levard C, Reinsch BC, Michel FM, Oumahi C, Lowry GV, Brown GE. 2011. Sulfidation processes of PVP-coated silver nanoparticles in aqueous solution: impact on dissolution rate. *Environ Sci Technol* 45:5260-5266.
- (22) Li L, Zhu YJ. 2006. High chemical reactivity of silver nanoparticles toward hydrochloric acid. *J Colloid Interface Sci* 303:415-418.
- (23) Li X, Lenhart JJ, Walker HW. 2010. Dissolution-accompanied aggregation kinetics of silver nanoparticles. *Langmuir* 26:16690-16698.
- (24) Liu J, Hurt RH. 2010. Ion release kinetics and particle persistence in aqueous nano-silver colloids. *Environ Sci Technol* 44:2169-2175.
- (25) Loeschner K, Hadrup N, Qvortrup K, Larsen A, Gao X, Vogel U, Mortensen A, Lam HR, Larsen EH. 2011. Distribution of silver in rats following 28 days of repeated oral exposure to silver nanoparticles or silver acetate. *Part Fibre Toxicol* 8:18.
- (26) Lundqvist M, Stigler J, Elia G, Lynch I, Cedervall T, Dawson KA. 2008. Nanoparticle size and surface properties determine the protein corona with possible implications for biological impacts. *Proc Natl Acad Sci U S A* 105:14265-70.
- (27) Lynch I, Dawson KA. 2008. Protein-nanoparticle interactions. *Nano Today* 3:40-47.
- (28) Meziani MJ, Sun YP. 2003. Protein-conjugated nanoparticles from rapid expansion of supercritical fluid solution into aqueous solution. *J Am Chem Soc* 125:8015-8018.
- (29) Murdock RC, Braydich-Stolle L, Schrand AM, Schlager JJ, Hussain SM. 2008. Characterization of nanomaterial dispersion in solution prior to in vitro exposure using dynamic light scattering technique. *Toxicol Sci* 101:239-253.
- (30) Nanoparticle Products Inventory, PEN, <http://www.nanotechproject.org/>
- (31) Nath N, Chilkoti A. 2004. Label-free biosensing by surface plasmon resonance of nanoparticles on glass: optimization of nanoparticle size. *Anal Chem* 76:5370-5378.
- (32) Navarro E, Picciapietra F, Wagner B, Marconi F, Kaegi R, Odzak N, Sigg L, Behra R. 2008. Toxicity of silver nanoparticles to *Chlamydomonas reinhardtii*. *Environ Sci Technol* 42:8959-8964.
- (33) Oberdorster G, Maynard A, Donaldson K, Castranova V, Fitzpatrick J, Ausman K, Carter J, Karn B, Kreyling W, Lai D, Olin S, Monteiro-Riviere N, Warheit D, Yang H. 2005. Principles for characterizing the potential human health effects from exposure to nanomaterials: elements of a screening strategy. *Part Fibre Toxicol* 2:8.

- (34) Oomen AG, Tolls J, Sips AJAM, Van den Hoop MAGT. 2003. Lead speciation in artificial human digestive fluid. *Arch Environ Con Tox* 44:107-115.
- (35) Pace HE, Rogers NJ, Jarolimek C, Coleman VA, Higgins CP, Ranville JF. 2011. Determining transport efficiency for the purpose of counting and sizing nanoparticles via single particle inductively coupled plasma mass spectrometry. *Anal Chem* 83:9361-9369.
- (36) Peters R, Kramer E, Oomen AG, Herrera Rivera ZE, Oegema G, Tromp PC, Fokkink R, Rietveld A, Marvin HJ, Weigel S, Peijnenburg AA, Bouwmeester H. 2012. Presence of Nano-Sized Silica during In Vitro Digestion of Foods Containing Silica as a Food Additive. *ACS Nano* 6(3):2441-2451.
- (37) Rai M, Yadav A, Gade A. 2009. Silver nanoparticles as a new generation of antimicrobials. *Biotechnol Adv* 27:76-83.
- (38) Rogers KR, Bradham K, Tolaymat T, Thomas DJ, Hartmann T, Ma L, Williams A. 2012. Alterations in physical state of silver nanoparticles exposed to synthetic human stomach fluid. *The Science of the total environment* 420:334-339.
- (39) Sung JH, Ji JH, Park JD, Yoon JU, Kim DS, Jeon KS, Song MY, Jeong J, Han BS, Han JH, Chung YH, Chang HK, Lee JH, Cho MH, Kelman BJ, Yu IJ. 2009. Subchronic inhalation toxicity of silver nanoparticles. *Toxicol Sci* 108:452-461.
- (40) Tien DC, Tseng KH, Liao CY, Tsung TT. 2008. Colloidal silver fabrication using the spark discharge system and its antimicrobial effect on *Staphylococcus aureus*. *Med Eng Phys* 30:948-952.
- (41) Versantvoort CH, Oomen AG, Van de Kamp E, Rempelberg CJ, Sips AJ. 2005. Applicability of an in vitro digestion model in assessing the bioaccessibility of mycotoxins from food. *Food Chem Toxicol* 43:31-40.
- (42) Walczyk D, Bombelli FB, Monopoli MP, Lynch I, Dawson KA. 2010. What the Cell "Sees" in Bionanoscience. *J Am Chem Soc* 132:5761-5768.
- (43) Zelyanskii AV, Zhukova LV, Kitaev GA. 2001. Solubility of AgCl and AgBr in HCl and HBr. *Inorg Mater+* 37:523-526.

3

Translocation of differently sized and charged polystyrene nanoparticles in in vitro intestinal cell models of increasing complexity

Agata P. Walczak
Evelien Kramer
Peter J.M. Hendriksen
Peter Tromp
Johannes P.F.G. Helsper
Meike van der Zande
Ivonne M.C.M. Rietjens
Hans Bouwmeester

Based on: Nanotoxicology 2014 Aug 5:1-9

ABSTRACT

Intestinal translocation is a key factor for determining bioavailability of nanoparticles (NPs) after oral uptake. Therefore, we evaluated three *in vitro* intestinal cell models of increasing complexity which might affect the translocation of NPs: a mono-culture (Caco-2 cells), a co-culture with mucus secreting HT29-MTX cells and a tri-culture with M-cells. Cell models were exposed to well characterized differently sized (50 and 100 nm) and charged (neutral, positively and negatively) polystyrene NPs. In addition, two types of negatively charged NPs with different surface chemistries were used. Size strongly affected the translocation of NPs, ranging up to 7.8% for the 50 nm NPs and 0.8% for the 100 nm NPs. Surface charge of NPs affected the translocation, however, surface chemistry seems more important, as the two types of negatively charged 50 nm NPs had an over 30-fold difference in translocation. Compared to the Caco-2 mono-culture, presence of mucus significantly reduced the translocation of neutral 50 nm NPs, but significantly increased the translocation of one type of negatively charged NPs. Incorporation of M-cells shifted the translocation rates for both NPs closer to those in the mono-culture model. The relative pattern of NP translocation in all three models was similar, but the absolute amounts of translocated NPs differed per model. We conclude that for comparing the relative translocation of different NPs, using one intestinal model is sufficient. To choose the most representative model for risk assessment, *in vivo* experiments are now needed to determine the *in vivo* translocation rates of the used NPs.

INTRODUCTION

Nanotechnology in the food industry develops quickly and the large number of products containing nanoparticles (NPs) on the market is expected to further increase (Chaudhry et al. 2008) resulting in consumer exposure to NPs. Classically, human safety assessment of chemicals and NPs relies heavily on *in vivo* studies (EFSA and Committee 2011). Given the enormous diversity of NPs, these cannot all be evaluated using animal studies. In addition, there is a strong societal demand to develop alternative testing approaches (3Rs: replacement, reduction and refinement) to reduce animal studies. An *in vitro* screening method should be developed for linking the physicochemical properties of NPs with their translocation across cells for prioritizing NPs for further animal testing. Therefore, the aim of this study was to evaluate three *in vitro* intestinal epithelial cell models of increasing complexity to compare their barrier properties for differently sized and charged polystyrene (PS)-NPs.

Physicochemical properties of NPs play a crucial role in the interactions between NPs and cells (Shang et al. 2014). No single metric is postulated to govern translocation, but size and surface modifications certainly play a role (Oomen et al. 2014; Zhao et al. 2011). Therefore, these parameters are targeted for boosting the physicochemical properties of NPs to increase their commercial, including medical, applications (Pozzi et al. 2014; Prijic et al. 2012; Sharma et al. 2013; Yang et al. 2014). Smaller NPs generally translocate more efficiently through cell layers than larger particles (Elbakry et al. 2012; Mahler et al. 2012; Oh et al. 2011; Schubbe et al. 2012; Varela et al. 2012). The exact contribution of the surface charge on translocation has not yet been elucidated. A positive surface charge of NPs is often associated with a higher translocation efficiency, as shown for PS-NPs in MDCK-II cells (Fazlollahi et al. 2011) and in an intestinal co-culture model of Caco-2 and M cells (des Rieux et al. 2005).

Size, surface chemistry and charge have been shown to significantly affect the coating of NPs by proteins present in cell culture media, resulting in a protein corona (Lundqvist et al. 2008; Meder et al. 2012). The composition and amount of proteins adsorbed onto NPs influence their biological interactions (Lesniak et al. 2010; Lundqvist 2013; Tedja et al. 2012). For instance, the amount of adsorbed proteins onto NPs has been suggested to positively correlate with the NP cellular uptake (Ehrenberg et al. 2009).

To study NP translocation across the human intestinal epithelium *in vitro*, in previous studies cells were grown on a semi-permeable membrane, separating apical and basolateral chambers. Presently, models with different degrees of complexity are being employed, starting with the simplest and most commonly used mono-culture of Caco-2 cells (Nkabinde et al. 2012). These mono-cultures, however, lack a mucus layer which, especially for charged NPs, might be a very important barrier because of electrostatic repulsion (for negatively charged NPs) and mucus entrapment (for positively charged NPs) (Hussain et al. 2001; Lai et al. 2007; Norris et al. 1998; Szentkuti 1997). Therefore, co-culture models that include mucus producing goblet cells have been proposed (i.e. the combination of Caco-2 and HT29-MTX cells) (Chen et al. 2010; Hilgendorf et al. 2000; Walter et al. 1996). Finally, *in vitro* models incorporating human intestine microfold (M) cells have also

been developed. M-cells, localized in the intestinal Peyer's patches, are responsible for the uptake and translocation and immune presentation of relatively larger particles and they have been accommodated in co- and tri-culture models. In these models, Caco-2 cells are differentiated into M-cells by a temporary co-culture with Raji cells (des Rieux et al. 2005). All these models have been used for testing the translocation of NPs (Bouwmeester et al. 2011; des Rieux et al. 2005; Mahler et al. 2012), but have never been compared with each other in one study to evaluate their applicability for NP testing.

In this study, we compared three *in vitro* intestinal epithelial cell models of increasing complexity to assess the translocation of differently sized and charged PS-NPs. We used a mono-culture of Caco-2 cells, a co-culture with additional mucus secreting HT29-MTX cells and a tri-culture with additional both HT29-MTX cells and M-cells. These three models were exposed to fluorescently labelled 50 and 100 nm PS-NPs with neutral, negative, or positive charge, resulting from different surface modifications.

MATERIALS AND METHODS

NPs

Neutral, amine- and carboxyl-modified PS-NPs, 50 and 100 nm (referred to as 50 (0), 50 (+), 50 (-M), 100 (0), 100 (+) and 100 (-)) with a red fluorophore core (Ex/Em: 530/590 nm) were purchased from Magsphere (Pasadena, CA, USA). Carboxyl-modified PS-NPs, 50 nm (referred to as 50 (-P)) with a yellow-green fluorophore core (Ex/Em: 485/530 nm) were purchased from Polysciences (Warrington, PA, USA). The mass concentration of all stock solutions was 2.5 %.

NP characterization

PS-NP morphology, size and surface charge were characterized with scanning electron microscopy (SEM), dynamic light scattering (DLS) and zeta-potential measurements. In addition, a chemical analysis of NPs was performed by matrix-assisted laser desorption/ionization-time-of-flight mass spectrometry (MALDI-TOF) and the adsorbed protein corona was analysed by sodium dodecyl sulphate polyacrylamide gel electrophoresis (SDS-PAGE) following its desorption from the NPs, performed as described hereafter.

SEM analysis was performed using a high resolution field emission gun (FEG) SEM (Tescan MIRA-LMH FEG-SEM; Tescan, Brno, Czech Republic). Samples were prepared by depositing 20 μ l of a 20 μ g/ml NP suspension in water onto a nickel-coated polycarbonate filter which was left to dry completely and then coated with a 5 nm layer of chromium. Size distributions were determined using Scandium SIS image analysis software (Olympus Soft Imaging Solutions GmbH, Germany). The mean diameter \pm SD of 80-600 particles is given.

DLS measurements were performed as previously described (Walczak et al. 2013). The zeta-potential was measured using a Malvern Zetasizer 2000 (Malvern Instruments, Malvern, UK). Each sample was measured in 5 runs, 1.5 min each. For DLS and zeta-potential measurements, 100 μ g/ml NP suspensions in water or cell culture medium were used. All samples were analysed in triplicate and the results are presented as the mean \pm SD.

For MALDI-TOF analyses suspensions of NPs at 2 mg/ml were prepared in 5 mM sodium acetate and mixed with MALDI-TOF matrix solution at a 1:1 (v:v) ratio, from which 1 μ l was spotted on a Bruker 384 ground steel target plate and air-dried. MALDI-TOF matrix solution contained 2,5-dihydrobenzoic acid (20 mg/ml) in 50% aqueous acetonitril. MALDI-TOF analyses were performed in positive mode on a Bruker Ultraflex extreme II mass spectrometer (Bruker Daltonics, Bremen, Germany). For each MALDI-TOF MS spectrum 3 x 500 shots were recorded.

The absence of detectable leakage of the fluorescent dye from the used NPs was confirmed by centrifugation of NPs after 24 h incubation in cell culture medium at 37°C, using filter tubes (Amicon Ultra-4 3kDa Ultracel-PL memb 24/Pk; Millipore BV, the Netherlands).

Assessment of the protein corona of NPs

The 50 nm PS-NPs at a concentration of 1.66 mg/ml and the 100 nm PS-NPs at an equal total surface area were incubated in cell culture medium for 24 h at 37°C (Lundqvist et al. 2008). Subsequently, to remove non-firmly bound proteins, the samples were washed three times by centrifugation (18 000 rcf, 15°C, 40 min), re-suspension of the pellet in 1 ml PBS (Gibco; Bleiswijk, the Netherlands) and transferring to a new tube. The final pellet was re-suspended in a loading buffer (Laemmli Sample Buffer, BIO-RAD; Veenendaal, the Netherlands) containing β -mercaptoethanol (Sigma; Steinbach, Germany). The samples were boiled for 5 min and the centrifugation step was repeated once more to separate the NPs from proteins desorbed from their surface. Protein containing supernatant was then loaded onto a SDS-PAGE gel. Each lane contained the amount of protein corresponding to equal NP surface areas, protein samples obtained from the 100 nm NPs were 1.5 x diluted. Intensity of each whole lane in the gel was digitally analysed and the amount of protein per lane was estimated. Based on this, a second gel was prepared with each lane containing an equal amount of protein.

One-dimensional polyacrylamide gel electrophoresis was performed at 90 V for about 80 min on 12% polyacrylamide gels of 1 mm thickness (Mini-PROTEAN TGX Gels, BIO-RAD). A protein ladder of 10-250 kDa was included in each gel (Precision Plus Protein Dual Color Standards, BIO-RAD). The gels were washed in 40% methanol in water containing 10% acetic acid for 15 min and were subsequently stained with Bio-Safe Coomassie Stain G-250 (BIO-RAD) for 1.5 hrs. Afterwards, the gels were destained by extensive washing in distilled water.

The experiments were repeated three times with comparable results. The gels were scanned (Odyssey, Li-Cor ISO 9001, Bad Homburg, Germany) and gel densitometry was performed using the Odyssey software (Odyssey Biosciences, Bad Homburg, Germany).

Cell models

Caco-2 and Raji B cell lines were obtained from the American Type Culture Collection and were used in experiments at passage numbers 29-38 and 8-24, respectively. A human colon adenocarcinoma mucus secreting cell line (HT29-MTX) was obtained from the European Collection of Cell Cultures and was used at passages 20-29. Caco-2 and HT29-MTX cells

were cultured with Dulbecco's Modified Eagle Medium (DMEM) (Lonza, Verviers, Belgium) without phenol red, supplemented with 10% heat-inactivated fetal bovine serum (FBS) (Gibco), 1% penicillin-streptomycin (Sigma), 1% MEM non-essential amino acids (Gibco) and 1% GlutaMAX (Gibco). The complete medium is further referred to as DMEM+. The medium was changed every 2-3 days and cells were subcultured upon reaching 80% confluence. Raji cells were cultured in RPMI 1640 medium (Gibco), supplemented with 10% heat-inactivated FBS and 1% penicillin-streptomycin. The medium was changed every 3-4 days by centrifugation of the cells at 1200 rpm (Heraeus Labofuge 400R) for 7 min and resuspending the cells in fresh medium.

For translocation experiments cells were seeded at a density of 40 000 cells/cm² in transwell polyester inserts (3 µm pore size, 1.12 cm² surface area, Corning, the Netherlands). All cell models were used for experiments on day 21. For the mono-culture, Caco-2 cells were used. For the co- and tri-cultures, Caco-2 and HT29-MTX cells were seeded at a ratio of 3:1. For the tri-cultures, an inverted model (des Rieux et al. 2007) was used as follows: on day 6 of Caco-2/HT29-MTX culture the inserts were inverted and further cultured as described before (Bouwmeester et al. 2011), and on day 16, 40 000 Raji cells were added into the basolateral chamber of the insert. On day 21, Raji cells were removed and the inserts were placed in plates in their original orientation to be used in experiments.

Cell model characterization: assessment of cell barrier integrity

The integrity of the cell barrier in all cell models was assessed before and after NP exposure by measuring the transepithelial electrical resistance (TEER) with a STX01 electrode connected to a Millicell ERS-2 Epithelial Volt-Ohm Meter (Millipore, Bedford, MA). After each cell culture medium refreshment, cells were allowed to equilibrate for 30 min at 37°C before TEER measurements. Only inserts with TEER values above 200 Ω x cm² were used in experiments.

Cell layer integrity was also evaluated using Lucifer Yellow (Sigma) and two FITC-dextrans (low- and high-molecular weight of 4 and 10 kDa, respectively; Sigma), in the presence and absence of EGTA (Sigma), which opens tight junctions. Lucifer Yellow and dextran solutions at a concentration of 1 mg/ml in DMEM+ were added apically to the cells (500 µl/insert). Controls were incubated with 2.5 mM EGTA in DMEM+ (apically and basolaterally) for 1 h at 37°C. Afterwards, cells were allowed to equilibrate in DMEM+ for 30 min and the TEER was measured. Then, EGTA/DMEM+ was added again in the basolateral chamber, while the integrity marker solutions were added apically. After 1 h incubation at 37°C, the basolateral medium was collected and analysed for fluorescence at 485/530 nm.

Cell model characterization: histological evaluation

For histological evaluation, after 21 days in culture, cells in the insert were fixed with 4% paraformaldehyde (pH 7.4), followed by washing with PBS and addition of 0.5 ml filtered 10 mg/ml Alcian blue solution (8GX; Sigma) in 3% acetic acid (pH 2.5). After 20 min of incubation at room temperature, the cells were extensively washed with PBS. The insert

membrane with cells was cut out of the plastic insert holder, mounted onto a glass slide using a drop of PBS, and visualized by microscopy.

NP in vitro translocation experiments

After 21 days in culture, cells were exposed apically to 500 μ l/insert of NPs at 250 μ g/ml. After 24 h exposure, the basolateral medium was collected and fluorescence was measured with a Synergy HT Multi-Detection Microplate Reader at excitation/emission wavelengths of 530/590 and 485/530 nm, for red and yellow-green NPs, respectively. The obtained values were converted into NP concentrations, based on a concentration standard calibration curve included in every experiment.

All experiments were conducted in triplicate for each treatment and repeated twice. The reported percentages of translocation are the NP amounts in basolateral samples divided by the NP amounts to which cells were exposed in the apical chamber. The results of translocation are presented as an average \pm standard error of the mean (SEM).

Statistics

Data were analysed with Prism software (v5.02; GraphPad Software, Inc., La Jolla, CA, USA). A one-way analysis of variance test and *post hoc* Tukey test were used to determine significant differences between the groups. Groups were considered significantly different when $p < 0.05$.

RESULTS

NP characterization

We characterized the PS-NPs in water using SEM. The spherical shape of the NPs was confirmed (Figure 1 and Table 1). All types of 50 nm NPs had similar size distributions except for the 50 nm (+) NPs, which had a larger average size of 50.6 nm, compared with the other 50 nm NPs (Figure 1, Table 1 and Supplementary Figure S1). The 100 nm (0) and 100 nm (+) had similar size distributions, while the 100 nm (-) NPs had a fraction of 34.6% of smaller (15-35 nm) NPs causing a smaller average projected area diameter (54.2 nm) as compared with the other 100 nm NPs.

With DLS we measured the hydrodynamic diameters of all NPs in water and DMEM+. In water, the size ranged from 52.4 to 56.2 nm and from 96.3 to 121.4 nm, for the 50 and 100 nm NPs, respectively (Table 2). In DMEM+ at $t=0$ h hydrodynamic diameters were in all cases, except for the 100 (+) NPs, significantly larger than in water, ranging from 114.9 to 187.6 nm for 50 nm NPs and from 138.5 to 255.3 nm for 100 nm NPs. Only the hydrodynamic sizes of the 100 (0) and 100 (+) NPs were significantly different from each other in DMEM+ at $t=0$ h. Incubation of the NPs for 24 h in DMEM+ did not significantly affect the hydrodynamic sizes compared with $t=0$ h (Table 2).

The zeta-potential measurements of the (+) and (-) NPs in water confirmed their positive and negative charges (Table 3). The neutral NPs had a negative charge of -26.0 mV and -59.1 mV for the 50 and 100 nm NPs, respectively. The two types of negatively charged

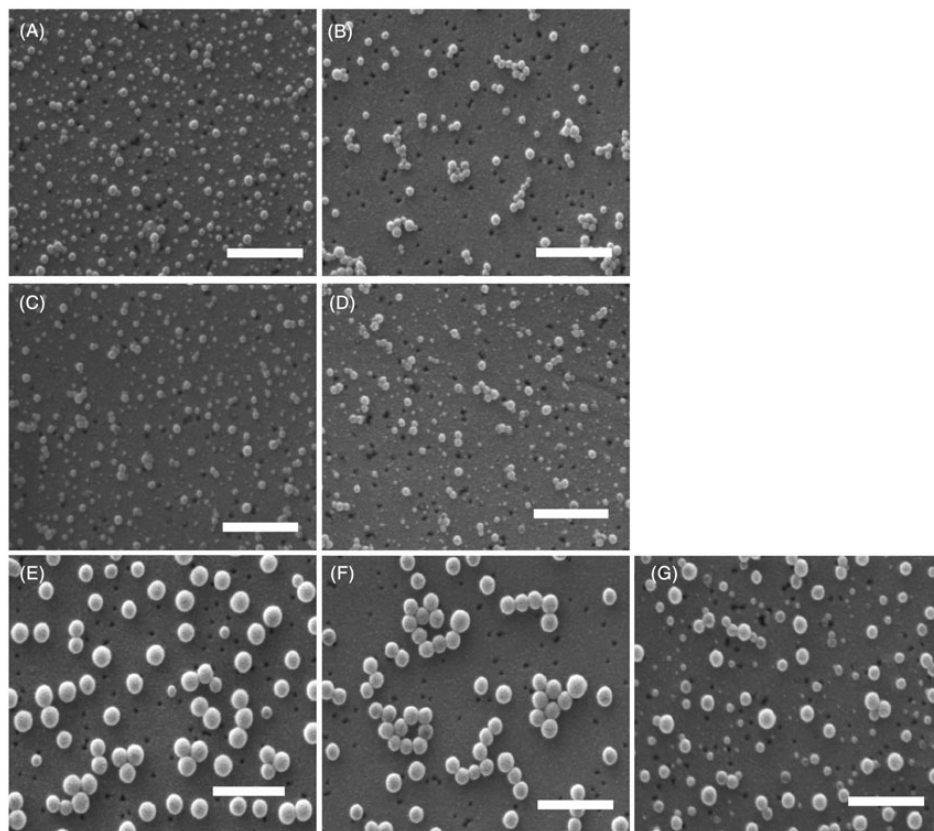


Figure 1. Scanning electron micrographs of 50 and 100 nm PS-NPs in water: (A) 50nm (0), (B) 50nm (+), (C) 50nm (-M), (D) 50nm (-P), (E) 100nm (0), (F) 100nm (+), (G) 100nm (-). Magnification 100 000 x. The bar indicates 500 nm.

Table 1. Projected area diameters (Dpa) (nm) of PS-NPs in water at $t=0$ h, as determined by SEM.

NPs	<i>n</i>	Sphericity	Dpa (nm)	Size range (nm)
50 nm (0)	170	0.70	31.2 ± 12.7	$\leq 15 - 70$
50 nm (+)	80	0.78	50.6 ± 9.3	20 - 80
50 nm (-M)	100	0.66	35.0 ± 15.3	$\leq 15 - 70$
50 nm (-P)	290	0.70	31.6 ± 13.6	$\leq 15 - 70$
100 nm (0)	350	0.89	108.1 ± 18.0	40 - 140
100 nm (+)	80	0.88	100.2 ± 10.7	60 - 140
100 nm (-)	600	0.79	54.2 ± 28.0	$\leq 15 - 130$

n, Number of measured NPs; (0), neutral NPs; (+), positively charged NPs; (-), negatively charged NPs.

50 nm NPs had the same zeta-potential. The initially different charges of NPs in water all converted into rather equal negative charges after suspension in DMEM+ (ranging from -9.4 mV to -19.5 mV) and did not significantly change after 24 h (Table 3).

The two types of negatively charged 50 nm NPs were compared by MALDI-TOF analysis (Figure 2). According to the manufacturers, both NPs contain carboxylic groups on their surface, but the MALDI-TOF spectrum of the (-M) NPs showed several peaks (at m/z -values of 411.3, 463.3 and 565.3) that were not detected in the spectrum of the (-P) NPs and vice versa at m/z -values of 351.2, 371.2, 547.2, 719.4 and 756.6. These analyses show that (-M) and (-P) NPs were different in their chemical composition.

Table 2. Hydrodynamic diameters (nm) of PS-NPs in water and DMEM+.

NPs	In water (nm)	In DMEM+ ($t=0$ h) (nm)	In DMEM+ ($t=24$ h) (nm)
50 nm (0)	52.5 \pm 0.5	187.6 \pm 7.7 ^a	143.0 \pm 11.1
50 nm (+)	56.2 \pm 0.7	144.4 \pm 2.5 ^a	161.0 \pm 47.6
50 nm (-M)	52.4 \pm 0.2	114.9 \pm 5.0 ^a	88.7 \pm 1.6
50 nm (-P)	52.4 \pm 0.9	183.7 \pm 22.7 ^a	166.3 \pm 48.4
100 nm (0)	114.0 \pm 2.4 ^b	255.3 \pm 67.8 ^{a,b}	227.5 \pm 72.6
100 nm (+)	121.4 \pm 2.1 ^b	138.5 \pm 1.2 ^b	144.3 \pm 3.7
100 nm (-)	96.3 \pm 2.6 ^b	198.5 \pm 27.8 ^a	205.7 \pm 31.2

The measurements in water were done at $t=0$ h, and the measurements in DMEM+ were done at $t=0$ h and 24 h. (0), Neutral NPs; (+), positively charged NPs; (-), negatively charged NPs. ^aSignificant difference between sizes in water and DMEM+. $n=3$. ^bSignificant difference between NP types.

Table 3. Zeta-potential (mV) of PS-NPs in water and DMEM+.

NPs	In water (mV)	In DMEM+ ($t=0$ h) (mV)	In DMEM+ ($t=24$ h) (mV)
50 nm (0)	-26.0 \pm 16.2	-13.3 \pm 1.5 ^a	-11.9 \pm 0.9
50 nm (+)	26.6 \pm 13.9	-9.4 \pm 1.5 ^a	-12.2 \pm 0.8
50 nm (-M)	-27.7 \pm 19.3	-10.2 \pm 0.8 ^a	-10.2 \pm 1.1
50 nm (-P)	-27.8 \pm 17.4	-12.7 \pm 1.3	-12.4 \pm 0.9
100 nm (0)	-59.1 \pm 5.4	-19.5 \pm 20.5 ^a	-12.3 \pm 1.4
100 nm (+)	64.9 \pm 1.6	-10.1 \pm 1.3 ^a	-10.1 \pm 1.7
100 nm (-)	-51.78 \pm 4.9	-12.4 \pm 2.0 ^a	-12.5 \pm 1.2

The measurements in water were done at $t=0$ h, and the measurements in DMEM+ were done at $t=0$ h and 24 h. (0), Neutral NPs; (+), positively charged NPs; (-), negatively charged NPs. ^aSignificant difference between zeta-potential in water and DMEM+. $n=2$.

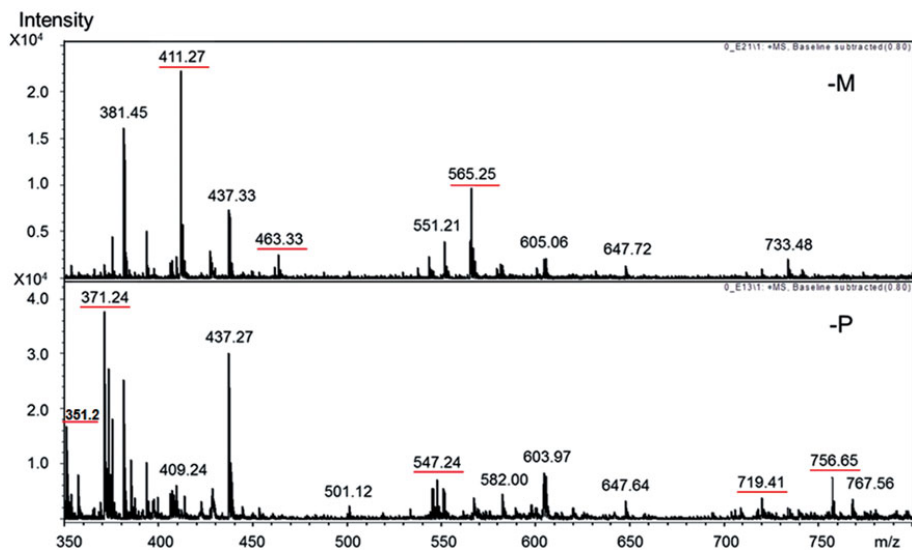


Figure 2. MALDI-TOF analyses of chemical groups on the surface of two types of negatively charged 50 nm PS-NPs: (-M) NPs and (-P) NPs. Underlined with red are the numbers of peaks different between the two NPs.

Assessment of the protein corona of NPs

To assess the proteins adsorbed onto the NPs that were used for exposure, we extracted the protein corona after incubation in DMEM+ for 24 h at 37°C. Only protein corona of NPs was analyzed, which was ensured by applying three washing and centrifugation steps (Lundqvist et al. 2011; Monopoli et al. 2011). A control DMEM+ sample without NPs, treated the same as the NP samples, did not show any protein bands on the gel (data not shown), confirming that the proteins shown on the gels are only the proteins of the NP protein corona. Figure 3(A) shows the gel loaded with samples normalized on the NP surface area and it clearly demonstrates differences in the total protein content, visible in the band intensity profiles of the NPs. The highest protein content was found on 100 nm (-) and 100 nm (0) NPs with intensities of whole lanes of 809 and 773, respectively. However, in the 100 nm (+) sample hardly any protein was detected (39). Also, 50 nm (+) NPs had a relatively low protein content (132), while the other 50 nm NPs had much more protein adsorbed on the surface: the highest in (-P) (528), followed by (-M) and (0) with similar contents (375 and 330, respectively). Remarkably, there was a 1.5-fold difference in the amount of adsorbed protein between the two negatively charged 50 nm NPs.

Figure 3(B) shows the samples normalized on the total protein content and it reveals relatively minor differences in the types of adsorbed proteins between NPs, which can be derived from the band intensity profiles. A difference in band pattern between the 50 nm (-M) and (-P) NPs shows that (-M) NPs had more adsorbed proteins >250 kDa, and (-P) NPs had more proteins of ~ 67 kDa. The gels show that the protein coronas contained

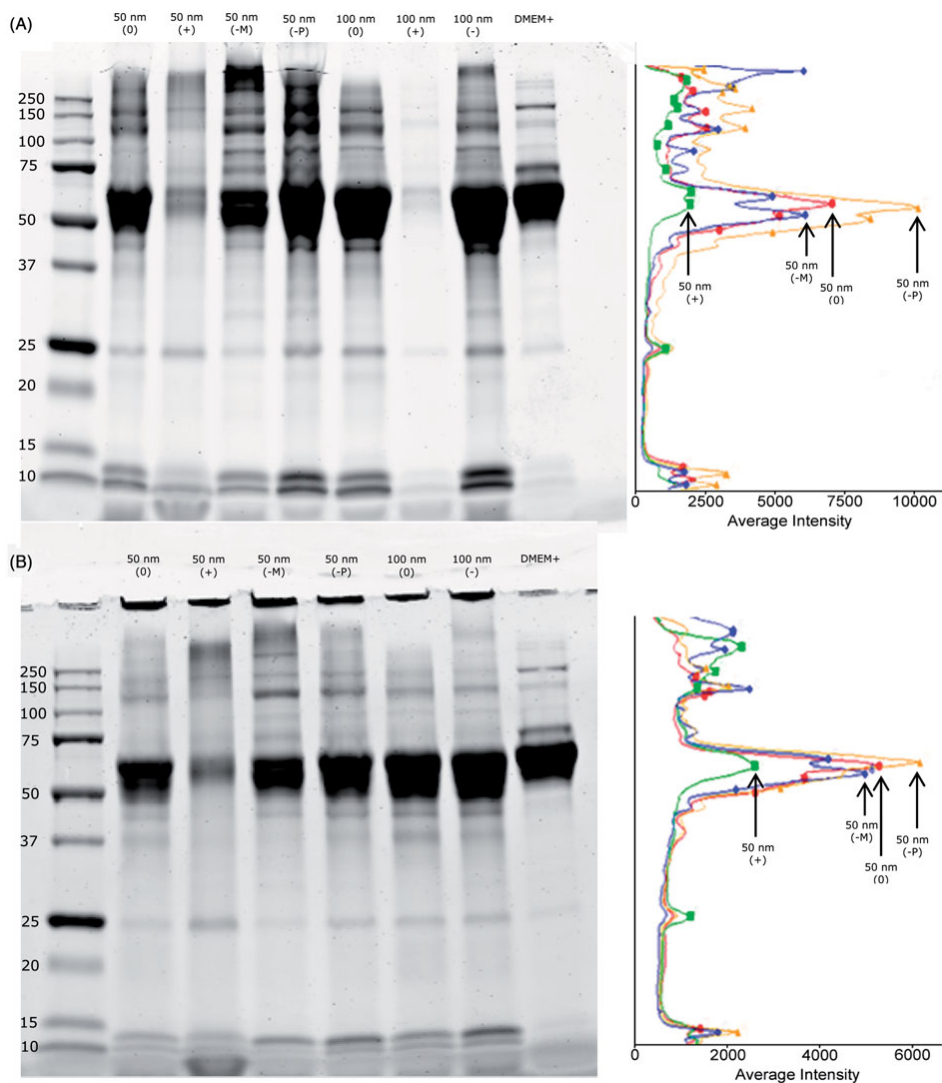


Figure 3. SDS-PAGE showing the protein corona of PS-NPs after 24 h incubation in DMEM+: (A) samples normalized on the NP surface area; the protein samples obtained from the 100 nm NPs were 1.5 x diluted compared with 50 nm NP samples to avoid overloading the gel. The molecular weights of the proteins in the standard ladder are given on the left side. The sample order is indicated above the lanes. DMEM+: medium control. On the right: profile of band intensities of 50 nm NPs: (0): red, (+): green, (-M): blue, (-P): yellow. (B) Samples normalized on the total protein content. Lane 50 nm (+) contains less protein than the other lanes and lane 100 nm (+) is absent, both due to the lack of sufficient amounts of protein. On the right: profile of band intensities as described in A.

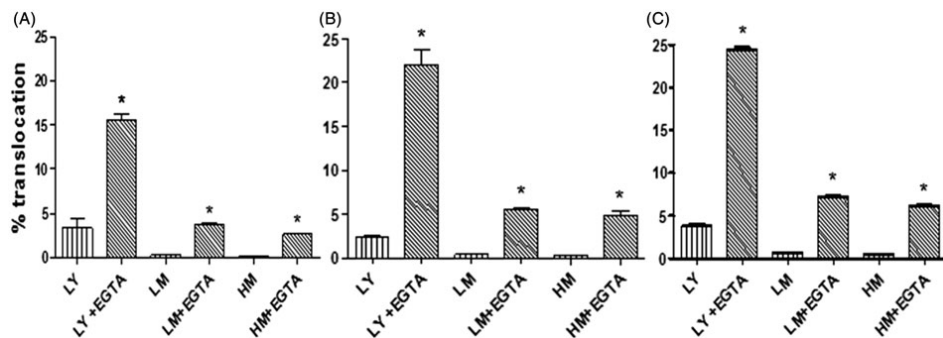


Figure 4. Translocation of membrane integrity markers in mono- (A), co- (B) and tri- culture (C) as used for the NP translocation studies. LY: Lucifer Yellow, LM: low-molecular-weight dextran, HM: high-molecular-weight dextran. *: significant difference between the translocation without and with EDTA. $n=3$.

mostly proteins present at high abundance in DMEM+, in different ratios. However, protein coronas contained also other proteins, not visible in DMEM+ lane, with molecular weights of: ~10, 12, 26, 43 and >250 kDa. This indicates that NPs enriched some of the medium proteins in pellet by preferential binding.

Cell model characterization: assessment of cell barrier integrity

In this study, we compared three types of intestinal cell barrier models in a two chamber design. TEER values were measured in cell cultures during culturing to monitor confluency and cell layer integrity. TEER values increased over the first days after seeding and then remained constant ($>200 \Omega \times \text{cm}^2$) until day 21, as reported previously (Hilgendorf et al. 2000). On day 21, cell barrier integrity was additionally assessed by translocation studies using Lucifer Yellow and dextrans as translocation markers. As shown in Figure 4, all three models allowed only a limited marker translocation, similar to that reported before (Nolleaux et al. 2006), which was not significantly different between the models. Upon opening of the tight junctions with EGTA as used before (Bouwmeester et al. 2011; Rothen-Rutishauser et al. 2002), permeability increased significantly. Exposure to NPs at 250 $\mu\text{g}/\text{ml}$ for 24 h did not affect the TEER values of the cell layers (data not shown).

Cell model characterization: presence of mucus on co-culture

To visualize the mucus on top of the co-culture cell surface, the cell layer was stained with Alcian blue. Figure 5 shows the presence of mucus in blue (Figure 5B), in a pattern typical for mucus on the co-culture cell layer, but not on the mono-culture (Figure 5A).

NP in vitro translocation experiments

Mono-, co- and tri-culture models were exposed to six types of PS-NPs. In each model, the translocation of each type of 50 nm NPs was significantly different ($p<0.05$) from that of the other NPs. In the Caco-2 mono-culture, the 50 nm (0) NPs translocated to the highest

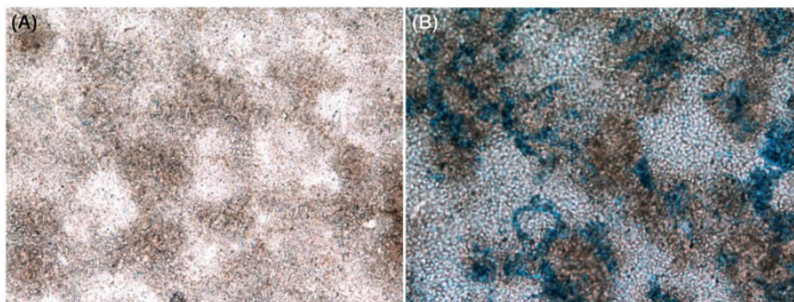


Figure 5. Mucus staining with Alcian blue: (A) mono-culture (Caco-2 cells) and (B) co-culture (Caco-2 + HT29-MTX cells).

extent (7.8% of the apically applied amount), followed by 50 nm (-P) NPs (4.0%), 50 nm (+) NPs (0.6%) and finally 50 nm (-M) NPs (0%). As shown in Figure 6, this order of translocation percentage (i.e. 50 nm (0) > 50 nm (-P) > 50 nm (+) > 50 nm (-M)) was similar in the tri-culture model. In the co-culture model, the presence of mucus significantly reduced the translocation of 50 nm (0) NPs, but significantly increased the translocation of 50 nm (-P) compared with the mono-culture model. Incorporation of M-cells in the model shifted the translocation rates for both NPs closer (but still significantly different) to those in the Caco-2 mono-culture. Strikingly, the two types of negatively charged 50 nm NPs had significantly different translocation properties in all cell models, where 50 nm (-P) NPs translocated 210.5 x more than (-M) NPs in mono-culture, 78.3 x in co-culture and 30 x in tri-culture. Size affected the translocation as well, as the translocation of neutral and positively charged 100 nm NPs (0.51 %, 0.46 %, 0.76 % for (0) NPs and 0.21 %, 0.46 %, 0.51 % for (+) NPs in the mono-, co- and tri-culture models, respectively) was much lower than that of their equivalent 50 nm NPs. Negatively charged 100 nm NPs translocated to a similar extent as their 50 nm (-M) counterparts (0.07 %, 0.19 %, 0.15 % vs 0.02 %, 0.08 %, 0.17 %, respectively). The relative order of translocation percentage of the 100 nm NPs was similar to that of their corresponding 50 nm NPs (from Magsphere).

DISCUSSION

We investigated the influence of size and surface modifications of PS-NPs on their translocation properties in the three cell models. Clearly, translocation was strongly affected by the size, with 100 nm NPs reaching up to 0.8% translocation and 50 nm NPs reaching up to 7.8%. Translocation was also strongly affected by the surface chemistry, most clearly seen in the results for the 50 nm NPs, which all translocated significantly differently, varying from 0 % to 7.8%. In all three cell models, the 50 nm (0) and 50 nm (-P) NPs translocated to the highest extent.

It is striking that we observed such large differences between the translocation of two types of negatively charged 50 nm NPs, even though their size, surface charge (both in water

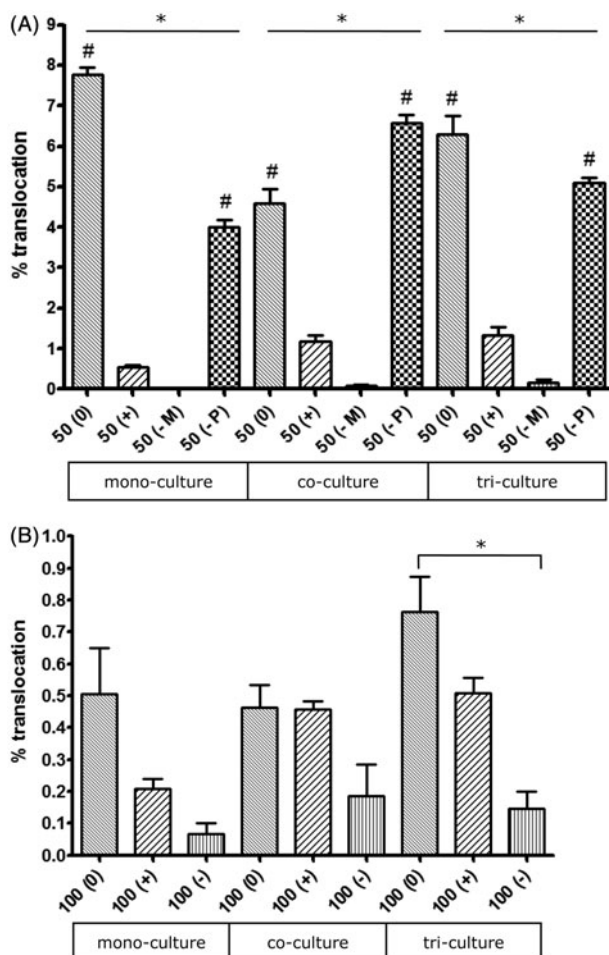


Figure 6. Translocation of 50 nm (A) and 100 nm (B) PS-NPs in three cell models: mono-, co- and tri-culture. (0): neutral NPs, (+): positively charged NPs, (-): negatively charged NPs; *: significantly different translocation within models, #: significantly different translocation between models.

and DMEM+) and relative protein composition of their coronas were similar. However, the corona of the (-P) NPs contained 1.5 times more protein than the (-M) NPs, therefore the total amount of protein in corona in this case may be a factor governing the translocation potential. We looked further into the surface chemical composition of these NPs. For this we used MALDI-TOF, which allows the characterization of surface properties of NPs. MALDI-TOF spectrum showed that the composition of the surface chemical groups is different. It has already been shown that steric shielding of the charge and steric interaction of chemical groups on the surface of NPs, as well as molecular weight and density of the coating (Gref et al. 2000) can affect their biological responses (Bhattacharjee et al. 2013; Yoncheva et al. 2005) and protein corona (Gessner et al. 2003; Jedlovsky-Hajdu et al.

2012). Likely, the difference in the surface chemistry of these NPs caused differences in protein binding capacity. The differences in surface chemistry or in protein binding resulted in different behaviour in biological test systems.

All three NPs of 100 nm with different surface modifications also translocated differently. SEM analysis showed that 100 nm (-) NPs had a fraction of 34.6% of smaller (15-35 nm) NPs and also their hydrodynamic size in water was smaller as compared with the other 100 nm NPs. However, they translocated to the lowest extent. The 100 nm (0) NPs translocated to the highest extent, even though they had the largest hydrodynamic size in DMEM+. Additionally, their charge in water was in fact strongly negative. This suggests the influence of surface chemistry rather than charge on translocation.

The size and zeta-potential of all NPs were determined in water and in DMEM+, as used in the translocation studies. As expected, NPs in DMEM+ had larger hydrodynamic sizes than in water, which did not change significantly upon 24 h incubation. While in water charges of the NPs were different, they all obtained a rather equal negative charge in DMEM+. This shift, shown before (Cho et al. 2014; Ehrenberg et al. 2009; Fleischer and Payne 2012; Mahler et al. 2012; Meder et al. 2012), probably results from the protein adsorption on the NPs or from measuring protein aggregates of medium rather than NPs. A mucus layer as used in the co- and tri-culture model is an important barrier especially for charged NPs (Hussain et al. 2001; Lai et al. 2007; Norris et al. 1998; Szentkuti 1997). We indeed confirmed this for the translocation of the 50 nm (0) NPs that had a negative zeta-potential in water, but not for the 50 nm (-P) NPs that also had a negative zeta-potential in water. Incorporation of M-cells shifted the translocation rates for both NPs closer to those in the mono-culture model.

Translocation of NPs is a complex process dependent on many factors, one of them being the protein corona, which influences the interactions of NPs with cell membranes and cellular uptake (Lesniak et al. 2010; Lundqvist 2013; Tedja et al. 2012). In this study, we show that NPs with different surface modifications adsorbed different amounts of proteins. It has been shown that the protein adsorptive capacity of NPs, rather than the identity of bound proteins, could predict their cellular interactions and cellular uptake (Ehrenberg et al. 2009). In our study, the 50 nm NPs with largest amount of adsorbed protein, (0) and (-P), translocated to the highest extent. The difference in the amount of adsorbed protein could also explain the difference in translocation between 50 nm (-M) and (-P) NPs. However, the 50 nm (+) and 100 nm (+) NPs had much less adsorbed proteins and translocated to a higher extent than 50 nm (-M) and 100 nm (-) NPs. This indicates that the amount of protein in the corona is not the only parameter influencing translocation of the NPs across the intestinal barrier.

The types of proteins adsorbed onto all NPs were highly comparable, while their ratios were different for different NPs, which are illustrated by their protein band patterns. Similar protein composition with only different protein ratios have been shown previously in the coronas of NPs, regardless of their surface modification (Cho et al. 2014; Jedlovsky-Hajdu et al. 2012). The major components of the corona of tested NPs were proteins most abundantly present in the medium as shown by comparison of the proteins in the NP corona and those in the DMEM+ control lane. The most prominent band on our gels had

a mass of 50-70 kDa and this was likely a combination of albumin (72 kDa) and fibrinogen chains: gamma (50 kDa), beta (60 kDa) and alpha (72 kDa) (Monopoli et al. 2011). The band of ~150 kDa was likely IgG (Lee et al. 2012). Albumin, IgG and fibrinogen are the most abundant proteins in plasma (Anderson and Anderson 2002) and they are the main serum proteins identified in the protein corona of NPs (Aggarwal et al. 2009; Cho et al. 2014). Fibrinogen is known to adsorb more abundantly onto negatively charged surfaces (Bernabeu and Caprani 1990) and in our gel the band 50-70 kDa was thickest in negatively charged NP samples. Additionally, there were bands of: ~90 kDa (most likely complement factors/components or/and transferrin), ~26 kDa (most likely apolipoprotein A-1) and ~12 kDa (most likely Ig kappa chain C region) (Monopoli et al. 2011).

CONCLUSION

In the current study, three different intestinal *in vitro* cell models were used with increasing complexity to study the translocation properties of differently sized and charged PS-NPs. We show that the relative pattern of NP translocation in all three used intestinal models was similar, but the absolute amounts of translocated NPs differed per model, significantly for 50 nm (0) and (-M) NPs. There was no coherence that one specific model had more efficient translocation than others, because it depended on NP type. Therefore, we conclude that for comparing the relative translocation of different NPs, using one intestinal model would be sufficient. However, for screening studies in a tiered risk assessment approach, when absolute translocation values are needed, it should be kept in mind that depending on the chosen model, the outcomes will differ. To choose the most representative model for risk assessment, *in vivo* experiments are now needed in order to assess which of the three models is most closely reflecting the *in vivo* translocation.

Our results point out that size is an important metric governing translocation. Surface charge expressed as zeta-potential could be used, but only if determined in water. Clearly, the chemical composition at the surface seems more important than the zeta-potential as illustrated by the two negatively charged PS-NPs that had comparable zeta-potential in water but different surface chemistries. More efforts should now be devoted to relate the chemical surface properties of NPs with the same surface charge but different surface modification to their different biological behaviours. Our findings suggest that ingested PS-NPs, depending on their size and physicochemical properties, could potentially translocate across intestinal barrier.

ACKNOWLEDGEMENTS

This project was funded by ZonMw (grant no. 40-40100-94-9016) to APW, the Dutch Ministry of Economic Affairs (PJM, JPM, PT and HB). This work is supported by NanoNextNL (EK, MZ), a micro- and nanotechnology consortium of the Government of The Netherlands and 130 partners. The authors would like to thank Norbert de Ruijter for the help in generating photos of mucus staining.

REFERENCES

- (1) Aggarwal P, Hall JB, McLeland CB, Dobrovolskaia MA, McNeil SE. 2009. Nanoparticle interaction with plasma proteins as it relates to particle biodistribution, biocompatibility and therapeutic efficacy. *Adv Drug Deliver Rev* 61:428-437.
- (2) Anderson NL, Anderson NG. 2002. The human plasma proteome - History, character, and diagnostic prospects. *Mol Cell Proteomics* 1:845-867.
- (3) Bernabeu P, Caprani A. 1990. Influence of Surface-Charge on Adsorption of Fibrinogen and or Albumin on a Rotating-Disk Electrode of Platinum and Carbon. *Biomaterials* 11:258-264.
- (4) Bhattacharjee S, Ershov D, Gucht J, Alink GM, Rietjens IM, Zuilhof H, Marcelis AT. 2013. Surface charge-specific cytotoxicity and cellular uptake of tri-block copolymer nanoparticles. *Nanotoxicology* 7:71-84.
- (5) Bouwmeester H, Poortman J, Peters RJ, Wijma E, Kramer E, Makama S, Puspitaninganindita K, Marvin HJ, Peijnenburg AA, Hendriksen PJ. 2011. Characterization of translocation of silver nanoparticles and effects on whole-genome gene expression using an in vitro intestinal epithelium coculture model. *ACS Nano* 5:4091-103.
- (6) Chaudhry Q, Scotter M, Blackburn J, Ross B, Boxall A, Castle L, Aitken R, Watkins R. 2008. Applications and implications of nanotechnologies for the food sector. *Food Addit Contam Part A Chem Anal Control Expo Risk Assess* 25:241-258.
- (7) Chen XM, Elisia I, Kitts DD. 2010. Defining conditions for the co-culture of Caco-2 and HT29-MTX cells using Taguchi design. *J Pharmacol Tox Met* 61:334-342.
- (8) Cho WS, Thielbeer F, Duffin R, Johansson EMV, Megson IL, MacNee W, Bradley M, Donaldson K. 2014. Surface functionalization affects the zeta potential, coronal stability and membranolytic activity of polymeric nanoparticles. *Nanotoxicology* 8:202-211.
- (9) des Rieux A, Fievez V, Theate I, Mast J, Preat V, Schneider YJ. 2007. An improved in vitro model of human intestinal follicle-associated epithelium to study nanoparticle transport by M cells. *Eur J Pharm Sci* 30:380-91.
- (10) des Rieux A, Ragnarsson EG, Gullberg E, Preat V, Schneider YJ, Artursson P. 2005. Transport of nanoparticles across an in vitro model of the human intestinal follicle associated epithelium. *Eur J Pharm Sci* 25:455-65.
- (11) EFSA, Committee ES. 2011. Guidance on the Risk Assessment of the Application of Nanoscience and Nanotechnologies in the Food and Feed Chain. *EFSA Journal* 9:36.
- (12) Ehrenberg MS, Friedman AE, Finkelstein JN, Oberdorster G, McGrath JL. 2009. The influence of protein adsorption on nanoparticle association with cultured endothelial cells. *Biomaterials* 30:603-10.
- (13) Elbakry A, Wurster EC, Zaky A, Liebl R, Schindler E, Bauer-Kreisel P, Blunk T, Rachel R, Goepferich A, Breunig M. 2012. Layer-by-layer coated gold nanoparticles: size-dependent delivery of DNA into cells. *Small* 8:3847-56.
- (14) Fazlollahi F, Angelow S, Yacobi NR, Marchelletta R, Yu AS, Hamm-Alvarez SF, Borok Z, Kim KJ, Crandall ED. 2011. Polystyrene nanoparticle trafficking across MDCK-II. *Nanomedicine: nanotechnology, biology, and medicine* 7:588-94.
- (15) Fleischer CC, Payne CK. 2012. Nanoparticle surface charge mediates the cellular receptors used by protein-nanoparticle complexes. *J Phys Chem B* 116:8901-7.
- (16) Gessner A, Lieske A, Paulke BR, Muller RH. 2003. Functional groups on polystyrene model nanoparticles: Influence on protein adsorption. *J Biomed Mater Res A* 65A:319-326.
- (17) Gref R, Luck M, Quellec P, Marchand M, Dellacherie E, Harnisch S, Blunk T, Muller RH. 2000. 'Stealth' corona-core nanoparticles surface modified by polyethylene glycol (PEG): influences of the corona (PEG chain length and surface density) and of the core composition on phagocytic uptake and plasma protein adsorption. *Colloids and surfaces. B, Biointerfaces* 18:301-313.
- (18) Hilgendorf C, Spahn-Langguth H, Regardh CG, Lipka E, Amidon GL, Langguth P. 2000. Caco-2 versus Caco-2/HT29-MTX co-cultured cell lines: Permeabilities via

- diffusion, inside- and outside-directed carrier-mediated transport. *J Pharm Sci* 89:63-75.
- (19) Hussain N, Jaitley V, Florence AT. 2001. Recent advances in the understanding of uptake of microparticulates across the gastrointestinal lymphatics. *Adv Drug Deliver Rev* 50:107-142.
- (20) Jedlovsky-Hajdu A, Bombelli FB, Monopoli MP, Tombacz E, Dawson KA. 2012. Surface coatings shape the protein corona of SPIONS with relevance to their application in vivo. *Langmuir* 28:14983-91.
- (21) Lai SK, O'Hanlon DE, Harrold S, Man ST, Wang YY, Cone R, Hanes J. 2007. Rapid transport of large polymeric nanoparticles in fresh undiluted human mucus. *Proc Natl Acad Sci U S A* 104:1482-7.
- (22) Lee SH, Hoshino Y, Randall A, Zeng ZY, Baldi P, Doong RA, Shea KJ. 2012. Engineered Synthetic Polymer Nanoparticles as IgG Affinity Ligands. *J Am Chem Soc* 134:15765-15772.
- (23) Lesniak A, Campbell A, Monopoli MP, Lynch I, Salvati A, Dawson KA. 2010. Serum heat inactivation affects protein corona composition and nanoparticle uptake. *Biomaterials* 31:9511-8.
- (24) Lundqvist M. 2013. Nanoparticles: Tracking protein corona over time. *Nat Nanotechnol* 8:701-2.
- (25) Lundqvist M, Stigler J, Cedervall T, Berggard T, Flanagan MB, Lynch I, Elia G, Dawson K. 2011. The Evolution of the Protein Corona around Nanoparticles: A Test Study. *ACS Nano* 5:7503-7509.
- (26) Lundqvist M, Stigler J, Elia G, Lynch I, Cedervall T, Dawson KA. 2008. Nanoparticle size and surface properties determine the protein corona with possible implications for biological impacts. *Proc Natl Acad Sci U S A* 105:14265-70.
- (27) Mahler GJ, Esch MB, Tako E, Southard TL, Archer SD, Glahn RP, Shuler ML. 2012. Oral exposure to polystyrene nanoparticles affects iron absorption. *Nat Nanotechnol* 7:264-71.
- (28) Meder F, Daberkow T, Treccani L, Wilhelm M, Schowalter M, Rosenauer A, Madler L, Rezwani K. 2012. Protein adsorption on colloidal alumina particles functionalized with amino, carboxyl, sulfonate and phosphate groups. *Acta biomaterialia* 8:1221-9.
- (29) Monopoli MP, Walczyk D, Campbell A, Elia G, Lynch I, Bombelli FB, Dawson KA. 2011. Physical-chemical aspects of protein corona: relevance to in vitro and in vivo biological impacts of nanoparticles. *J Am Chem Soc* 133:2525-34.
- (30) Nkabinde LA, Shoba-Zikhali LNN, Semete-Makokotela B, Kalombo L, Swai HS, Hayeshi R, Naicker B, Hillie TK, Hamman JH. 2012. Permeation of PLGA Nanoparticles Across Different in vitro Models. *Curr Drug Deliv* 9:617-627.
- (31) Nollevaux G, Deville C, El Moulaj B, Zorzi W, Deloyer P, Schneider YJ, Peulen O, Dandriofosse G. 2006. Development of a serum-free co-culture of human intestinal epithelium cell-lines (Caco-2/HT29-5M21). *Bmc Cell Biol* 7.
- (32) Norris DA, Puri N, Sinko PJ. 1998. The effect of physical barriers and properties on the oral absorption of particulates. *Adv Drug Deliver Rev* 34:135-154.
- (33) Oh E, Delehanty JB, Sapsford KE, Susumu K, Goswami R, Blanco-Canosa JB, Dawson PE, Granek J, Shoff M, Zhang Q, Goering PL, Huston A, Medintz IL. 2011. Cellular uptake and fate of PEGylated gold nanoparticles is dependent on both cell-penetration peptides and particle size. *ACS Nano* 5:6434-48.
- (34) Oomen AG, Bos PM, Fernandes TF, Hund-Rinke K, Boraschi D, Byrne HJ, Aschberger K, Gottardo S, von der Kammer F, Kuhnelt D, Hristozov D, Marcomini A, Migliore L, Scott-Fordsmand J, Wick P, Landsiedel R. 2014. Concern-driven integrated approaches to nanomaterial testing and assessment-report of the NanoSafety Cluster Working Group 10. *Nanotoxicology* 8:334-48.
- (35) Pozzi D, Colapicchioni V, Caracciolo G, Piovesana S, Capriotti AL, Palchetti S, De Grossi S, Riccioli A, Amenitsch H, Lagana A. 2014. Effect of polyethyleneglycol (PEG) chain length on the bio-nano-interactions between PEGylated lipid nanoparticles and biological fluids: from nanostructure to uptake in cancer cells. *Nanoscale* 6:2782-92.
- (36) Prijic S, Prosen L, Cemazar M, Scancar J, Romih R, Lavrencak J, Bregar VB, Coer A, Krzan M, Znidarsic A, Sersa G. 2012. Surface modified magnetic nanoparticles for

- immuno-gene therapy of murine mammary adenocarcinoma. *Biomaterials* 33:4379-4391.
- (37) Rothen-Rutishauser B, Riesen FK, Braun A, Gunthert M, Wunderli-Allenspach H. 2002. Dynamics of tight and adherens junctions under EGTA treatment. *J Membrane Biol* 188:151-162.
- (38) Schubbe S, Schumann C, Cavalius C, Koch M, Muller T, Kraegeloh A. 2012. Size-Dependent Localization and Quantitative Evaluation of the Intracellular Migration of Silica Nanoparticles in Caco-2 Cells. *Chem Mater* 24:914-923.
- (39) Shang L, Nienhaus K, Nienhaus GU. 2014. Engineered nanoparticles interacting with cells: size matters. *Journal of nanobiotechnology* 12:5.
- (40) Sharma B, Peetla C, Adjei IM, Labhasetwar V. 2013. Selective biophysical interactions of surface modified nanoparticles with cancer cell lipids improve tumor targeting and gene therapy. *Cancer Lett* 334:228-236.
- (41) Szentkuti L. 1997. Light microscopical observations on lumenally administered dyes, dextrans, nanospheres and microspheres in the pre-epithelial mucus gel layer of the rat distal colon. *J Control Release* 46:233-242.
- (42) Tedja R, Lim M, Amal R, Marquis C. 2012. Effects of serum adsorption on cellular uptake profile and consequent impact of titanium dioxide nanoparticles on human lung cell lines. *ACS Nano* 6:4083-93.
- (43) Varela JA, Bexiga MG, Aberg C, Simpson JC, Dawson KA. 2012. Quantifying size-dependent interactions between fluorescently labeled polystyrene nanoparticles and mammalian cells. *Journal of nanobiotechnology* 10:39.
- (44) Walczak AP, Fokkink R, Peters R, Tromp P, Herrera Rivera ZE, Rietjens IM, Hendriksen PJ, Bouwmeester H. 2012. Behaviour of silver nanoparticles and silver ions in an in vitro human gastrointestinal digestion model. *Nanotoxicology* 7:1198-1210.
- (45) Walter E, Janich S, Roessler BJ, Hilfinger JM, Amidon GL. 1996. HT29-MTX/Caco-2 cocultures as an in vitro model for the intestinal epithelium: In vitro in vivo correlation with permeability data from rats and humans. *J Pharm Sci* 85:1070-1076.
- (46) Yang ZX, Kang SG, Zhou RH. 2014. Nanomedicine: de novo design of nanodrugs. *Nanoscale* 6:663-677.
- (47) Yoncheva K, Gomez S, Campanero MA, Gamazo C, Irache JM. 2005. Bioadhesive properties of pegylated nanoparticles. *Expert opinion on drug delivery* 2:205-18.
- (48) Zhao Y, Sun X, Zhang G, Trewyn BG, Slowing, II, Lin VS. 2011. Interaction of mesoporous silica nanoparticles with human red blood cell membranes: size and surface effects. *ACS Nano* 5:1366-75.

SUPPLEMENTARY MATERIAL

3

TRANSLOCATION OF DIFFERENTLY SIZED AND CHARGED POLYSTYRENE NANOPARTICLES...

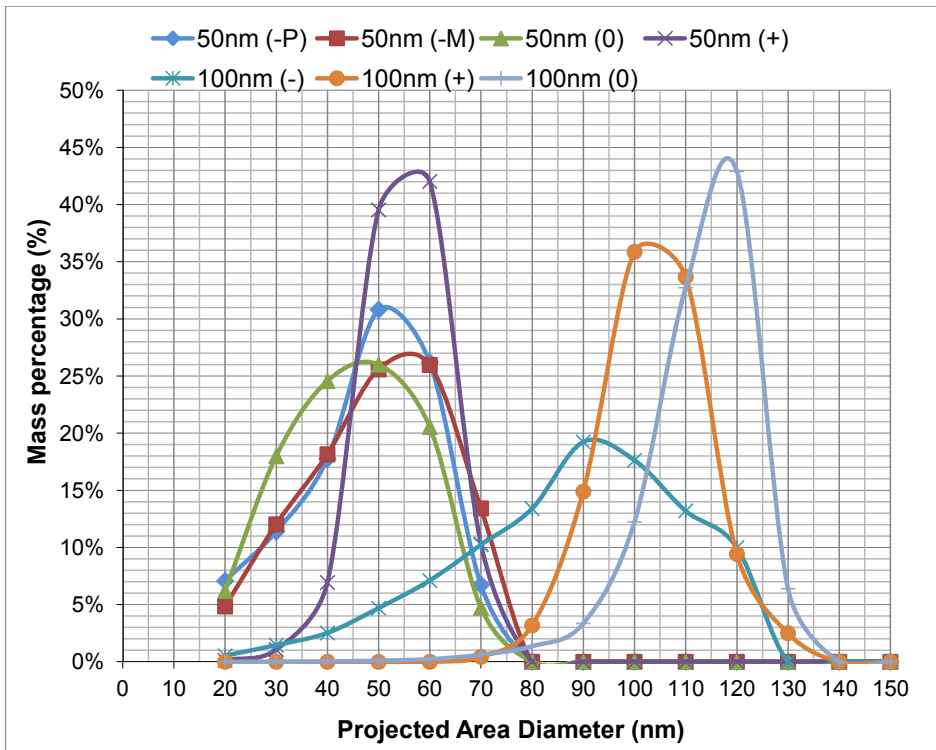


Figure S1. Size distributions [nm] of PS-NPs in water at $t=0$ h, as determined by SEM. (0): neutral NPs, (+): positively charged NPs, (-): negatively charged NPs.

4

In vitro gastrointestinal digestion increases the translocation of polystyrene nanoparticles in an in vitro intestinal co-culture model

Agata P. Walczak
Evelien Kramer
Peter J.M. Hendriksen
Richard Helsdingen
Meike van der Zande
Ivonne M.C.M. Rietjens
Hans Bouwmeester

Based on: Nanotoxicology, in press

ABSTRACT

The conditions of the gastrointestinal tract may change the physicochemical properties of nanoparticles (NPs) and therewith the bioavailability of orally taken NPs. Therefore, we assessed the impact of *in vitro* gastrointestinal digestion on the protein corona of polystyrene NPs (PS-NPs) and their subsequent translocation across an *in vitro* intestinal barrier. A co-culture of intestinal Caco-2 and HT29-MTX cells was exposed to 50 nm PS-NPs of different charges (“neutral”, positive and negative) in two forms: pristine and digested in an *in vitro* gastrointestinal digestion model. *In vitro* digestion significantly increased the translocation of all, except the “neutral”, PS-NPs. Upon *in vitro* digestion, translocation was 4-fold higher for positively charged NPs and 80- and 1.7-fold higher for two types of negatively charged NPs. Digestion significantly reduced the amount of protein in the corona of three out of four types of NPs. This reduction of proteins was 4.8-fold for “neutral”, 3.5-fold for positively charged and 1.8-fold for one type of negatively charged PS-NPs. *In vitro* digestion also affected the composition of the protein corona of PS-NPs by decreasing the presence of higher molecular weight proteins and shifting the protein content of the corona to low molecular weight proteins. These findings are the first to report that *in vitro* gastrointestinal digestion significantly affects the protein corona and significantly increases the *in vitro* translocation of differently charged PS-NPs. These findings stress the importance of including the *in vitro* digestion in future *in vitro* intestinal translocation screening studies for risk assessment of orally taken NPs.

INTRODUCTION

Nanotechnology develops rapidly and the number of consumer products containing nanoparticles (NPs) is constantly growing. Consumer oral exposure to NPs through some of these products (e.g. lipsticks, toothpaste, food packaging materials, food additives, juice clarifiers, health supplements) is likely [1, 2]. Currently, the safety evaluation of NPs still relies mainly on animal studies and there is a high societal demand to develop alternative *in vitro* methods to reduce animal studies. A combination of alternative *in vitro* methods should lead to development of a tiered safety assessment approach [3]. For this, *in vitro* models of intestinal epithelium have been evaluated using model NPs like polystyrene NPs (PS-NPs). Several *in vitro* studies report translocation of PS-NPs across the intestinal barrier [4-7]. However, so far these studies did not consider the effects of the different physicochemical environments in the digestive tract on NP behaviour. Critical factors in the gastrointestinal tract include dynamics of pH and ionic strength. These factors are known to affect the physicochemical characteristics of NPs [8, 9] and this has also been observed during *in vitro* gastrointestinal digestion of NPs [10-13].

The ultimate metrics that drive NP translocation have not been established yet, but important characteristics that determine the translocation are size, charge and surface modifications [7, 14-17]. Upon contact with biological fluids, NPs immediately get coated with biomolecules like proteins forming a protein corona [18-21], of which the amount and composition determine the translocation [22, 23]. A direct correlation between different surface modifications of NPs and the amount and type of proteins in the corona has also been shown [7, 24, 25]. While it is unlikely that the digestive enzymes present in the *in vitro* digestion model affect the NPs themselves, it can be expected that these enzymes do affect the protein corona of the NPs. However, the effect of gastrointestinal digestion on the protein corona composition of NPs and the consequences of this digestion on their subsequent translocation across the epithelial intestinal barrier have not been studied so far.

In this study, we aimed to assess the effect of *in vitro* gastrointestinal digestion on the protein corona of NPs and their subsequent translocation across an *in vitro* intestinal barrier. PS-NPs were selected for this study because of their stability and availability in a wide range of surface modifications. Different charges (“neutral”, positive and negative), but also different surface modifications (i.e. two types of negatively charged PS-NPs from two different suppliers) were used for comparison. The combination of *in vitro* gastrointestinal digestion with *in vitro* intestinal translocation should give a more complete *in vitro* model for prediction of bioavailability of orally administered NPs.

MATERIALS AND METHODS

NPs and chemicals

“Neutral”, amine- and carboxyl-modified 50 nm PS-NPs (referred to as 50 nm (“0”), 50 nm (+), 50 nm (-M)) with a red fluorophore core (Ex/Em: 530/590) were purchased

from Magsphere (Pasadena, CA, USA). Carboxyl-modified 50 nm PS-NPs (referred to as 50 nm (-P)) with a yellow-green fluorophore core (Ex/Em: 485/530) were purchased from Polysciences (Warrington, Pennsylvania, USA). The mass concentration of all stock solutions was 2.5 %. Throughout the paper we have chosen to use the manufacturer indication to identify the different types of nanoparticles in the text.

For the preparation of artificial digestive juices for *in vitro* digestion (fed model variant) [26] all chemicals were obtained from Merck (Darmstadt, Germany), except for NaCl, which was obtained from VWR (Leuven, Belgium), uric acid from Alfa Aesar (Karlsruhe, Germany), glucosaminehydrochloride from Calbiochem (Darmstadt, Germany), mucin from Roth (Karlsruhe, Germany) and lipase, bile, $MgCl_2 \cdot 6H_2O$, glucuronic acid and amylase from Sigma (Steinbach, Germany). The constituents and concentrations of the digestive juices were as described before [10].

NP characterization

PS-NP morphology, size and surface charge were characterized with scanning electron microscopy (SEM), dynamic light scattering (DLS) and zeta-potential measurements. In addition, the adsorbed protein corona was analysed by sodium dodecyl sulfate polyacrylamide gel electrophoresis (SDS-PAGE) following its desorption from the PS-NPs, performed as described hereafter.

SEM analysis was performed using a high resolution field emission gun (FEG)SEM (Tescan MIRA-LMH FEG-SEM; Tescan, Brno, Czech Republic). Samples were prepared by depositing 20 μ l of a 20 μ g/ml NP suspension in water onto a nickel-coated polycarbonate filter which was left to dry completely and then coated with a 5 nm layer of chromium. Size distributions were determined using Scandium SIS image analysis software (Olympus Soft Imaging Solutions GmbH, Germany). The mean diameter \pm SD of 80-600 particles is given.

DLS measurements were performed as previously described [10]. The zeta-potential was measured using a Malvern Zetasizer 2000 (Malvern Instruments, UK). Each sample was measured in 5 runs, 1.5 minutes each. For DLS and zeta-potential measurements, 100 μ g/ml NP suspensions in water or cell culture medium were used. All samples were analysed in triplicate and the results are presented as the mean \pm SD.

Digestion of PS-NPs

Four types of 50 nm PS-NPs with different surface modifications were subjected to the *in vitro* human gastrointestinal digestion model. Deionized water, not containing any NPs, was used as a negative control. Briefly, all digestive juices were prepared as described before [10] and heated to 37°C. The digestion started by adding 0.25 ml of deionized water or 25 mg/ml PS-NPs to 1 ml of saliva (pH=6.8 \pm 0.1). The mixture was incubated for 5 min at 37 \pm 2°C, rotating head-over-heels at 55 rpm, simulating peristaltic movements. Subsequently, 2 ml of gastric juice (pH=1.3) was added to the mixture and the pH of the sample was checked and, if necessary, adjusted to 2.5 \pm 0.5 with NaOH (1M) or HCl (37%). The sample was further incubated rotating at 37°C for 2 h. Subsequently, 2 ml of duodenal juice (pH=8.1) and 1 ml of bile (pH=8.2) were added. This complete mixture of digestive juices is referred

to as chyme hereafter. The pH of this mixture was set at 6.5 ± 0.5 with NaOH (1M) or HCl (37%) and it was rotated head-over-heels for another 2 h.

Absence of detectable leakage of the fluorescent dye from the used PS-NPs was shown upon digestion. For this, PS-NPs were incubated in the gastric juice for 2 hrs at 37°C, after which the suspensions were brought to neutral pH. Subsequently, suspensions at 250 µg/ml were centrifuged (30 min, 3000 g, 20°C) in filter tubes (Amicon Ultra-4 3kDa Ultracel-PL memb 24/Pk; Millipore BV, Netherlands) to remove the PS-NPs and the filtrates were measured for fluorescence.

Cell model

The human colonic adenocarcinoma (Caco-2) cell line was obtained from the American Type Culture Collection and was used in all experiments at passage numbers 29-38. The HT29-MTX (human colon adenocarcinoma mucus secreting) cell line was obtained from the European Collection of Cell Cultures and was used at passages 20-29. Cells were cultured in Dulbecco's Modified Eagle Medium (DMEM) (Lonza) without phenol red, supplemented with 10% heat-inactivated fetal bovine serum (FBS) (Gibco), 1% penicillin-streptomycin (Sigma), 1% MEM non-essential amino acids (Gibco) and 1% GlutaMAX (Gibco). The complete medium is further referred to as DMEM+. The medium was changed every 2-3 days and cells were subcultured upon reaching 80% confluence.

For the translocation experiments, cells were seeded at a density of 40 000 cells per cm² in Transwell polyester inserts (3 µm pore size, 1.12 cm² surface area, Corning, Amsterdam, The Netherlands), at ratio 3:1 Caco-2/HT29-MTX. Cells were used for experiments on day 21.

Cytotoxicity of PS-NPs

For the cytotoxicity test, Caco-2 and HT29-MTX cells in ratio 3:1 were seeded in 96-well plate at the concentration of 10⁵ cells/ml in DMEM+ (100 µl/well) and were incubated at 37°C for 24 h. Then, PS-NPs were added to the wells (100 µl/well) to achieve the desired concentrations at the total volume of 200 µl/well. PS-NPs in pristine form were suspended in DMEM+, and PS-NPs in digested form in chyme, as appearing after digestion, were diluted 4 x with DMEM+ to keep the chyme concentration at the non-cytotoxic level (based on previous experiments done in our group, data not shown). After 24 h of exposure at 37°C, 10 µl WST-1 reagent (Roche Diagnostics GmbH, Germany) was added to each well and the plates were shaken for 1 min. After subsequent 2 h incubation at 37°C, the absorbance was measured at 440 nm with a plate reader and the background absorbance at 690 nm was subtracted. Viability for each concentration of PS-NPs was expressed as a percentage of the control. DMEM+ was used as a negative control for pristine PS-NPs, and chyme/DMEM+ (1:3) was used as a negative control for digested PS-NPs. Triton-X100 (0.25%) (Sigma) was used as a positive control and decreased the viability to 7.1 ± 0.5 %.

Assessment of cell barrier integrity upon exposure to PS-NPs

The integrity of the cell barrier in the *in vitro* cell model was assessed before and after exposure to PS-NPs by measuring the TEER (transepithelial electrical resistance) values with a chopstick-like STX01 electrode connected to a Millicell ERS-2 Epithelial Volt- Ohm

Meter (Millipore, Bedford, MA). After each cell culture medium refreshment, cells were allowed to equilibrate for 30 min at 37°C before TEER measurements were performed. Only the inserts with initial TEER values above 200 $\Omega \cdot \text{cm}^2$ were used in experiments. Cell layer integrity directly after exposure to PS-NPs was additionally evaluated with Lucifer Yellow. To this end, Lucifer Yellow at a concentration of 1 mg/ml in DMEM+ was added apically to the cells (500 μl /insert) and after 1 h incubation at 37°C, the basolateral medium was collected and analysed for fluorescence at 485/530 nm.

Assessment of the protein corona of PS-NPs

The 50 nm PS-NPs at a concentration of 1.66 mg/ml were incubated in cell culture medium for 24 h at 37°C [22]. Subsequently, to remove non-firmly bound proteins, the samples were washed three times by centrifugation (18000 g, 15°C, 40 min), re-suspension of the pellet in 1 ml PBS (Gibco; Bleiswijk, The Netherlands) and each time transferring to a new tube. The final pellet was re-suspended in a loading buffer (Laemmli Sample Buffer, BIO-RAD; Veenendaal, The Netherlands) containing β -mercaptoethanol (Sigma). The samples were boiled for 5 min and the centrifugation step was repeated once more to separate the PS-NPs from proteins desorbed from their surface. The total protein content in the samples was measured with RC DC Protein Assay (BIO-RAD). Briefly, 62.5 μl reagent I was added to 12.5 μl sample and incubated for 1 min at room temperature. Subsequently, 62.5 μl of reagent II was added and tubes were centrifuged at 15000 x g for 4 min. Supernatant was discarded, liquid drained from the tubes, and 63.5 μl reagent A was added and incubated for 5 min, followed by adding 500 μl reagent B, vortexing and incubation for 15 min at room temperature before measurement of absorbance at 750 nm. The absorbance was converted into protein concentration based on a standard curve of BSA that was included in each experiment. All experiments were conducted in triplicate for each treatment and repeated at least twice. As controls, DMEM+ and chyme/DMEM+ (nonincubated) were used. The reported amounts of protein in the coronas are obtained after subtraction of the values obtained for washed controls: DMEM+ washed (cell culture medium) for pristine PS-NPs and chyme/DMEM+ washed (chyme diluted with the cell culture medium) for digested PS-NPs. The amounts of protein are presented as an average \pm standard error of the mean.

Protein containing supernatant was then loaded onto an SDS-PAGE gel. Each lane with NP samples, both pristine and digested, contained an equal amount of protein. One-dimensional polyacrylamide gel electrophoresis was performed at 90 V for about 80 min on 12% polyacrylamide gels of 1 mm thickness (Mini-PROTEAN TGX Gels, BIO-RAD). A protein ladder of 10-250 kDa was included in each gel (Precision Plus Protein Dual Color Standards, BIO-RAD). The gels were washed in 40% methanol in water containing 10% acetic acid for 15 min and were subsequently stained with Bio-Safe Coomassie Stain G-250 (BIO-RAD) for 1.5 hrs. Afterwards, the gels were destained by extensive washing in distilled water.

The experiments were repeated three times with comparable results. The gels were scanned (Odyssey, Li-cor ISO 9001) and gel densitometry was performed using the Odyssey software (Li-cor Biosciences).

PS-NP *in vitro* translocation experiments

For the translocation studies, pristine and digested PS-NPs were used. Pristine (stock) PS-NPs were suspended in DMEM+ at a concentration of 250 µg/ml. The NPs-chyme suspensions directly after the *in vitro* digestion were suspended in DMEM+ in a 1:3 ratio (at 250 µg/ml). These suspensions were directly applied apically on cells (500 µl/insert), at day 21 of culture. After 24 h of exposure, the basolateral medium was collected and fluorescence was measured with a Synergy HT Multi-Detection Microplate Reader (Biotek Instruments Inc., Winooski, VT, USA) at excitation/emission wavelengths of 530/590 nm and 485/530 nm, for red and yellow-green PS-NPs, respectively. The obtained values were converted into NP concentrations, based on a concentration standard calibration curve included in each experiment.

All experiments were conducted in triplicate for each treatment and repeated twice. The reported percentages of translocation are the NP amounts in basolateral samples divided by the NP amounts to which cells were exposed in the apical chamber. The results of translocation are presented as an average \pm standard error of the mean.

Statistics

Data were analysed with Prism software (v5.02; GraphPad Software, Inc., La Jolla, USA). A one-way analysis of variance ANOVA test and *post hoc* Tukey test were used to determine significant differences between the groups. Groups were considered significantly different when $p < 0.05$.

RESULTS

NP characterization

PS-NPs with different surface modifications were characterized in water using SEM. The spherical shape of the PS-NPs was confirmed (Figure 1). All types of 50 nm PS-NPs had similar size distributions with an average size of 31.6 - 35.0 nm, except for the 50 nm (+) NPs, which had a larger average size of 50.6 nm (Figure 1 and Table 1).

The hydrodynamic diameters of the PS-NPs were characterized in water and DMEM+ using DLS. In water the PS-NPs were monodispersed as indicated by their polydispersity indices (Table 1) and their hydrodynamic diameters ranged from 52.4 to 56.2 nm. In DMEM+ at $t=0$ h (each measurement takes 5 minutes) hydrodynamic diameters were in all cases significantly larger than in water, ranging from 114.9 to 187.6 nm (Table 1). Incubation of the PS-NPs for 24 h in DMEM+ did not significantly affect the hydrodynamic sizes compared to $t=0$ h (Table 1).

The zeta-potential measurements of the 50 nm (+) and 50 nm (-) NPs in water confirmed their positive and negative charges (Table 1). The two types of negatively charged 50 nm PS-NPs (-M and -P) had the same zeta-potential (i.e. -27.7 and -27.8 mV), while the zeta-potential of the positively charged PS-NPs was 26.6 mV. The "neutral" PS-NPs had a negative charge of -26.0 mV in water. The initially different charges of PS-NPs in water all converted into rather equal negative charges after suspension in DMEM+ (ranging from -9.4 mV to -13.3 mV) and did not significantly change after 24 h (Table 1).

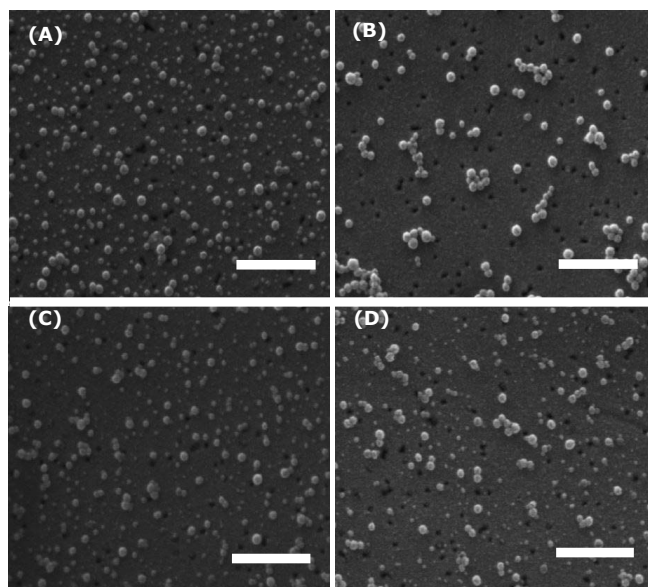


Figure 1. Scanning electron micrographs of PS-NPs in water: A) 50 nm (“0”), B) 50 nm (+), C) 50 nm (-M), D) 50 nm (-P). Magnification 100.000 x. The bar indicates 500 nm.

Cytotoxicity of PS-NPs

To determine if *in vitro* digestion affects PS-NP toxicity, a WST-1 viability assay was used on a proliferating co-cultured Caco-2 and HT29-MTX cells. “neutral” PS-NPs, in both pristine and digested form, did not affect the cell viability up to a concentration of 250 $\mu\text{g}/\text{ml}$ (Fig. 2). Negatively charged PS-NPs (both -M and -P) in pristine form did not affect the cell viability up to a concentration of 125 $\mu\text{g}/\text{ml}$, while at 250 $\mu\text{g}/\text{ml}$ the viability decreased to $86 \pm 5\%$ (-M) and $81 \pm 5\%$ (-P). In digested form the negatively charged NPs did not affect the cell viability up to 250 $\mu\text{g}/\text{ml}$. Positively charged PS-NPs, both pristine and digested, showed significant cytotoxicity, starting at a concentration of 25 $\mu\text{g}/\text{ml}$ and 50 $\mu\text{g}/\text{ml}$, respectively. Both pristine and digested positively charged NPs reduced the cell viability to 7% at 250 $\mu\text{g}/\text{ml}$.

Assessment of cell barrier integrity upon exposure to PS-NPs

In this study we used a co-culture cell model (Caco-2 and HT29-MTX cells) in a transwell design. In this model cells are covered with mucus, as shown in our previous study [7]. The TEER value was measured during culture to monitor confluency and cell layer integrity. TEER values increased over the first days after seeding and then remained at a constant level ($>200 \Omega \cdot \text{cm}^2$) until day 21, as reported previously [27]. Additionally, the TEER values were measured after exposure of the cell layers to 250 $\mu\text{g}/\text{ml}$ of PS-NPs for 24 h. As shown in Figure 3, the TEER value of exposed cell layers was not significantly affected compared to the non-exposed controls (DMEM+ and chyme/DMEM+) with exception of digested 50 nm (+) NPs that significantly decreased the TEER to 71.2% of that of the non-exposed cell control.

Table 1. Physicochemical characterization of 50 nm PS-NPs.

PS-NPs	SEM ^a (nm)		DLS ^b (nm)		Zeta-potential ^c (mV)					
	Water		Water		DMEM+ (t=0 h)			DMEM+ (t=24 h)		
	Water	Mean ± SD	PDI	Mean ± SD	PDI	Mean ± SD	PDI	Mean ± SD	PDI	DMEM+ (t=0 h)
50nm ("0")	33.4 ± 12.7	52.5 ± 0.5	0.05	187.6 ± 7.7*	0.43	143.0 ± 11.1	0.34	-26.0 ± 16.2	-13.3 ± 1.5*	-11.9 ± 0.9
50nm (+)	50.6 ± 9.3	56.2 ± 0.7	0.05	144.4 ± 2.5*	0.29	161.0 ± 47.6	0.34	26.6 ± 13.9	-9.4 ± 1.5*	-12.2 ± 0.8
50nm (-M)	35.0 ± 15.3	52.4 ± 0.2	0.17	114.9 ± 5.0*	0.32	88.7 ± 1.6	0.31	-27.7 ± 19.3	-10.2 ± 0.8*	-10.2 ± 1.1
50nm (-P)	31.6 ± 13.6	52.4 ± 0.9	0.04	183.7 ± 22.7*	0.39	166.3 ± 48.4	0.31	-27.8 ± 17.4	-12.7 ± 1.3	-12.4 ± 0.9

^aDiameters [nm] of PS-NPs in water, as measured with SEM (n=80-380). ^bHydrodynamic diameters [nm] of PS-NPs in water and DMEM+, as determined by DLS. The measurements in water were done at t=0 h, and the measurements in DMEM+ were done at t=0 h and 24 h (n=3); ^cZeta-potential [mV] of PS-NPs in water and DMEM+, as determined by a zeta-sizer. The measurements in water were done at t=0 h, and the measurements in DMEM+ were done at t=0 h and 24 h (n=2). Abbreviations: ("0"); "neutral" PS-NPs, (+); positively charged PS-NPs, (-M and -P); negatively charged PS-NPs from Magsphere and Polysciences, respectively; PDI: Polydispersity index. *Significant difference between sizes in water and DMEM+ (n=3).

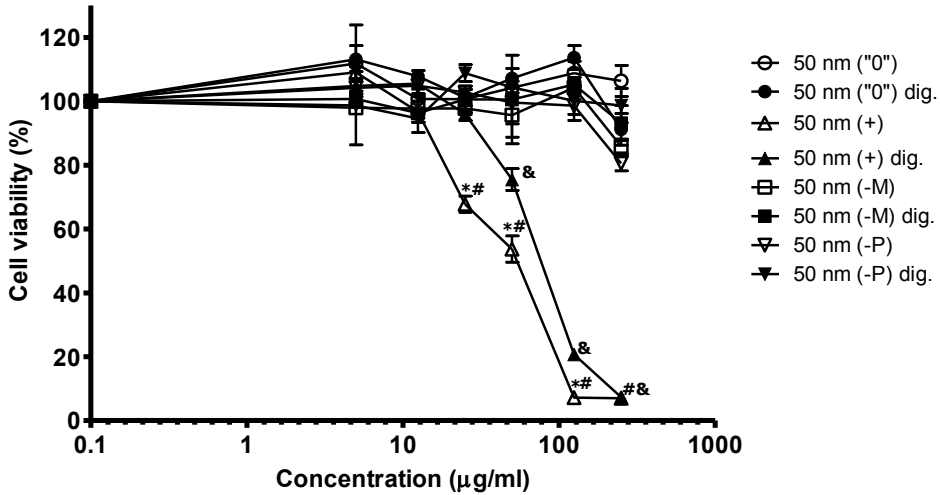


Figure 2. Effect on cell viability of a co-culture of Caco-2 and HT29-MTX cells upon exposure to 50 nm PS-NPs for 24 h. Abbreviations: ("0"): "neutral" PS-NPs, (+): positively charged PS-NPs, (-M and -P): negatively charged PS-NPs, dig: digested samples. Error bars show the standard error of mean ($n=3$). *: significant difference between the pristine and digested form of the same PS-NPs; #: significant difference with all other pristine PS-NPs; &: significant difference with all other digested PS-NPs. $n=3$.

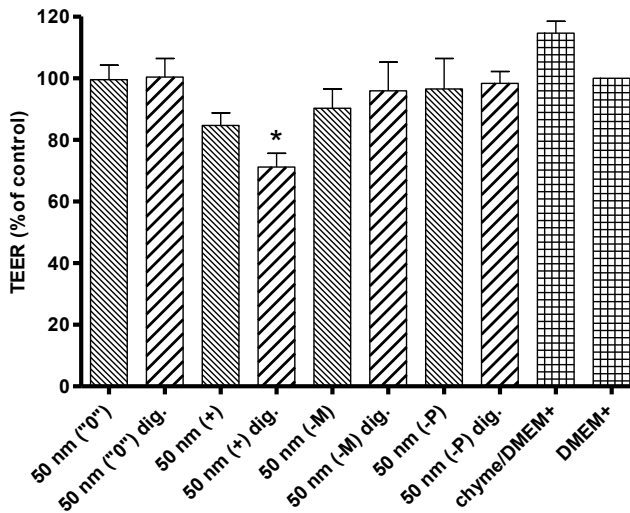


Figure 3. TEER values in a co-culture of Caco-2 and HT29-MTX cells upon exposure to pristine and digested 50 nm PS-NPs at 250 µg/ml for 24 h, as a percentage of the negative control (DMEM+). Abbreviations: ("0"): "neutral" PS-NPs, (+): positively charged PS-NPs, (-M and -P): negatively charged PS-NPs; dig: digested samples. *Significantly different from the chyme/DMEM+ control ($n=3$).

Cell barrier integrity after exposure to PS-NPs was additionally assessed by translocation studies using Lucifer Yellow. As shown in Figure 4, Lucifer Yellow permeability, after exposure to pristine and digested PS-NPs at 250 $\mu\text{g}/\text{ml}$ for 24 h, was not significantly affected compared to the DMEM+ and chyme/DMEM+ controls (3.3% and 2.5% permeability, respectively) and stayed in the range of 2.8 to 6.3% for all PS-NPs except for the digested 50 nm (+) NPs, for which the permeability reached 11.7%, which was significantly higher than the controls and than the other digested NP samples ($p < 0.001$), but not significantly higher than the non-digested 50 nm (+) NPs ($p = 0.06$).

Assessment of the protein corona of PS-NPs

To assess the proteins adsorbed onto the PS-NPs, we extracted the protein corona from all 4 types of PS-NPs, both pristine and digested, which were incubated in DMEM+ for 24 h at 37°C. A control DMEM+ sample treated similarly as the PS-NP samples contained only very low amount of total protein (0.03 $\mu\text{g}/\mu\text{l}$; data not shown), confirming that the proteins shown for pristine PS-NPs are only the proteins of the NP protein corona. A control chyme/DMEM+ sample treated similarly as the PS-NP samples contained an average total protein amount of 0.3 $\mu\text{g}/\mu\text{l}$ (data not shown), indicating that some of the proteins in the digested samples did not originate from the protein coronas of the PS-NPs. In order to correct for this, the amount of protein in this control sample was subtracted from the measured amounts of protein in the digested NP samples, which is presented in Figure 5.

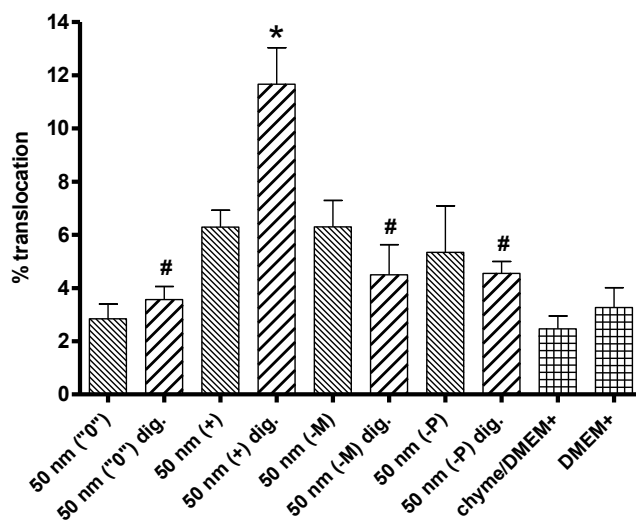


Figure 4. Translocation of Lucifer Yellow across a co-culture of Caco-2 and HT29-MTX cells upon exposure to pristine and digested 50 nm PS-NPs at 250 $\mu\text{g}/\text{ml}$ for 24 h. Abbreviations: ("0"): "neutral" PS-NPs, (+): positively charged PS-NPs, (-M and -P): negatively charged PS-NPs; dig: digested samples. *Significantly different from the chyme/DMEM+ control ($n=3$); #Significantly different from 50 nm (+) dig. NPs.

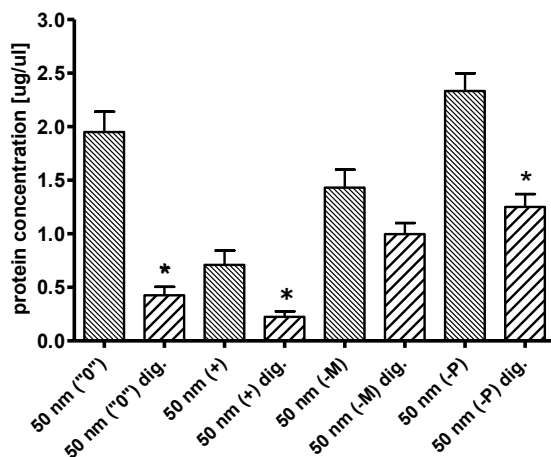


Figure 5. Total protein content [$\mu\text{g}/\mu\text{l}$] in samples of the protein corona desorbed from the surface of pristine and digested 50 nm PS-NPs incubated in DMEM+ for 24 h. Abbreviations: ("0"): "neutral" PS-NPs, (+): positively charged PS-NPs, (-M and -P): negatively charged PS-NPs; dig: digested samples. *Significant difference between the pristine and digested form of the same PS-NPs ($n=3$).

As shown in Figure 5, differences in surface chemistry resulted in different amounts of proteins in the protein corona of pristine PS-NPs in the following order: $2.3 \mu\text{g}/\mu\text{l}$ (-P) $> 1.9 \mu\text{g}/\mu\text{l}$ ("0") $> 1.4 \mu\text{g}/\mu\text{l}$ (-M) $> 0.7 \mu\text{g}/\mu\text{l}$ (+). Also the coronas of different digested PS-NPs contained different amounts of protein: $1.3 \mu\text{g}/\mu\text{l}$ (-P) $> 1.0 \mu\text{g}/\mu\text{l}$ (-M) $> 0.4 \mu\text{g}/\mu\text{l}$ ("0") $> 0.2 \mu\text{g}/\mu\text{l}$ (+). All digested PS-NPs had less adsorbed protein than their pristine equivalents, which reached significance for ("0") ($p=0.01$), (+) ($p<0.02$) and (-P) ($p=0.02$) NPs. The corona of the (-P) NPs contained more protein than that of (-M) NPs, both in pristine (1.6 x more) and digested (1.3 x more) form.

Figure 6A shows the SDS-PAGE gel loaded with samples normalized on the total protein content and it reveals minor differences in the types of adsorbed proteins between different pristine PS-NPs. However, the protein patterns between the pristine PS-NPs and their digested equivalents are very different. The band at 50-70 kDa, which is very thick and dominating in the pristine PS-NP samples, is much weaker and less dominant in the digested PS-NP samples. Figure 6B shows the comparison of the band intensity profiles between pristine and digested form of equivalent PS-NPs. It clearly demonstrates a strong decrease of the protein band at 50-70 kDa in all digested PS-NPs compared to their pristine equivalents and the appearance of a thick band at ~ 12 kDa, which is absent in pristine PS-NP samples. Proteins of ~ 12 kDa were also found in the chyme/DMEM+ control sample, though the band was weaker than in the NP samples. Compared to the chyme/DMEM+ washed control sample, digested NP samples contained the same bands, however their intensity was stronger, and all NP samples also contained additional bands, of which the band at ~ 18 kDa (in -M and -P NPs) and the band at ~ 45 kDa (in -M, -P and "0" NPs) were most pronounced. The band at ~ 45 kDa was the only band which made the chyme/

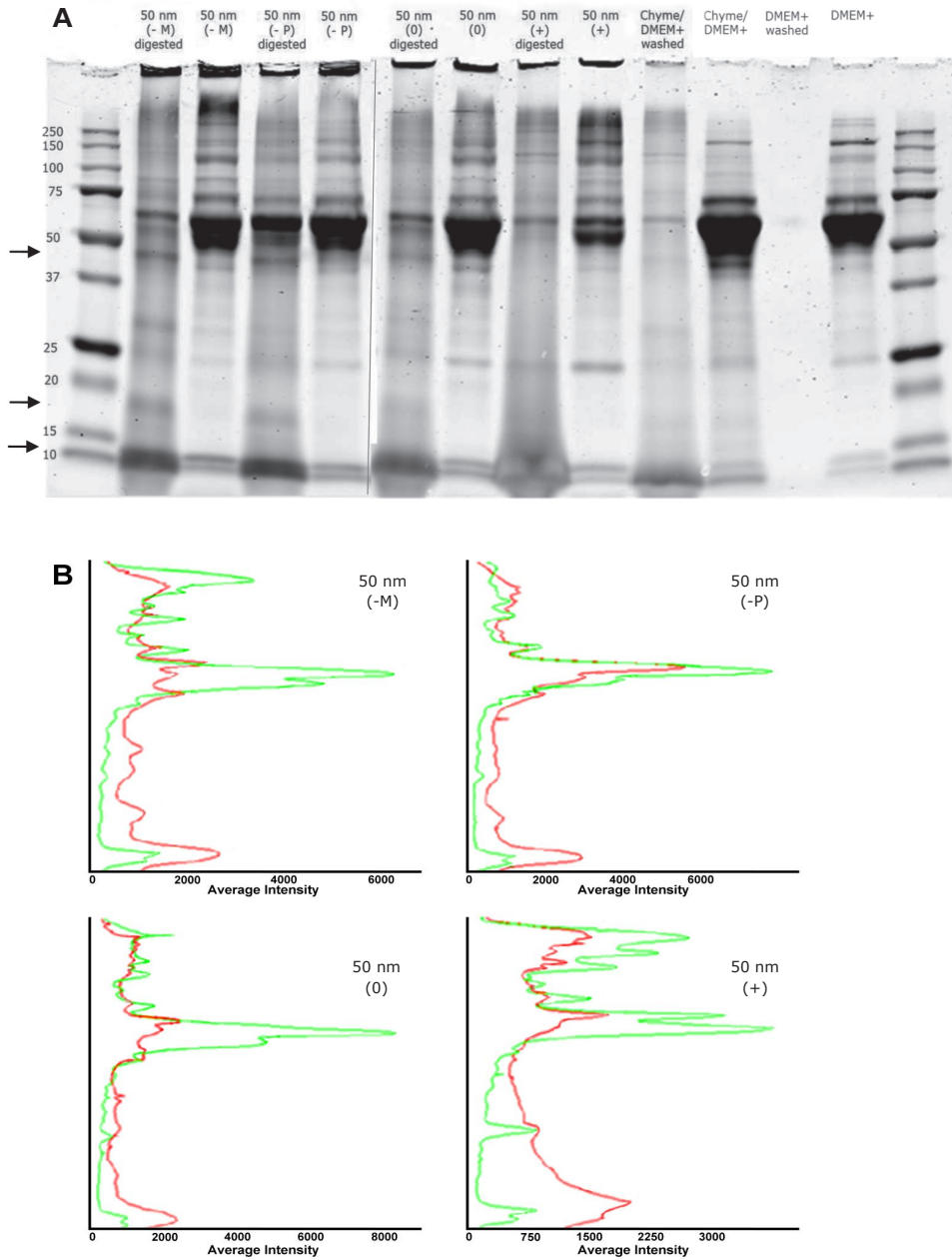


Figure 6. A) SDS-PAGE showing the protein pattern of the corona of pristine and digested 50 nm PS-NPs. NP samples were normalized on the total protein amount (11 μ g). The molecular weights of the proteins in the standard ladder are given on the left side. The sample order is indicated above the lanes. Abbreviations: DMEM+: medium control (11 μ g protein); Chyme/DMEM+: chyme/medium control (11 μ g protein); DMEM+ washed (0.9 μ g protein) and Chyme+DMEM+ washed (7 μ g protein): samples processed in the same way as NP samples. Arrows indicate bands typical for digested NPs (as explained in the text). B) Profiles of band intensities of PS-NPs: pristine (green) and digested (red).

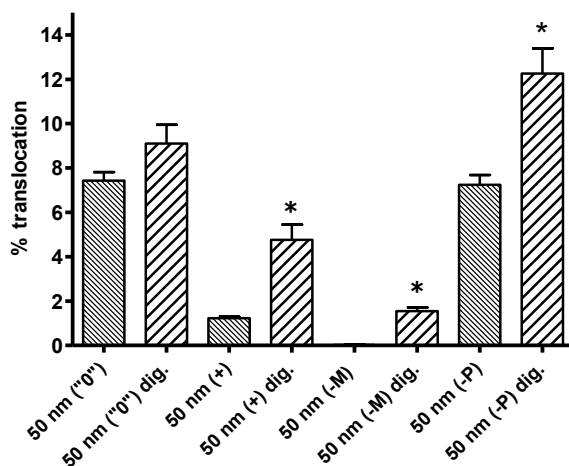


Figure 7. Translocation of pristine and digested 50 nm PS-NPs across a co-culture of Caco-2 and HT29-MTX cells upon exposure at 250 $\mu\text{g}/\text{ml}$ for 24 h. Abbreviations: ("0"): "neutral" PS-NPs, (+): positively charged PS-NPs, (-M and -P): negatively charged PS-NPs; dig: digested PS-NPs; n.d.: not detectable. *Significant difference between the pristine and digested form of the same PS-NPs ($n=3$).

DMEM+ sample different from the DMEM+ sample, indicating that the protein of this molecular weight was typical for the chyme. High molecular weight proteins (>250 kDa), present in pristine (+) and (-M) NPs, were absent after digestion. Digested samples resulted in more smeary lanes than pristine samples. While there was a substantial difference between samples of pristine PS-NPs and digested PS-NPs, all digested PS-NP samples were not much different between one another regarding the types of adsorbed proteins, and they differed only regarding the ratios of these component proteins.

PS-NP in vitro translocation experiments

The co-culture model of Caco-2 and HT29-MTX cells was exposed to four types of 50 nm PS-NPs at 250 $\mu\text{g}/\text{ml}$ for 24 h, each NP in pristine and digested form. As shown in Figure 7, without digestion the ("0") and (-P) NPs had the highest translocation rate (7.4 and 7.2% of the applied dose, respectively), while the translocation rate of the (+) NPs (1.2%; $p<0.001$) and (-M) NPs (0.02%; $p<0.001$) was much lower. Digestion increased the translocation of all PS-NPs, from 7.4 to 9.1% for the ("0") PS-NPs (not significant), and significantly from 1.2 to 4.8% ($p=0.02$), 0.02 to 1.6% ($p<0.001$) and 7.2 to 12.3% ($p=0.03$), for the (+), (-M) and (-P) PS-NPs, respectively. Translocation between different types of digested PS-NPs was significantly ($p<0.05$) different for all PS-NPs, with the exception of ("0" dig.) and (-P dig.) PS-NPs ($p=0.06$). Remarkably, the two types of negatively charged PS-NPs showed a completely different translocation behaviour in both pristine and digested form, where translocation of the pristine and digested 50 nm (-P) NPs was 360x and 7.7x higher respectively than that of the (-M) NPs.

DISCUSSION

The aim of this study was to assess the impact of *in vitro* gastrointestinal digestion on *in vitro* intestinal translocation of differently charged 50 nm PS-NPs. To this end, PS-NPs with four different surface modifications were studied in an *in vitro* gastrointestinal digestion model coupled to an *in vitro* intestinal barrier model consisting of Caco-2 and HT29-MTX cells. *In vitro* digestion significantly increased translocation of (+), (-M) and (-P) NPs 4-, 80- and 1.7-fold, respectively. One type of negatively charged PS-NPs (-P) translocated significantly more than the other type of negatively charged (-M) PS-NPs in both pristine (as also previously reported [7]) (360x), and digested form (7.7x). Interestingly, (-M) NPs, which almost did not translocate at all in pristine form (0.02% of the applied amount), translocated at 1.6% of applied amount in digested form.

We determined the translocation of differently charged pristine and digested PS-NPs after 24 h of exposure. The integrity of the co-culture cell layer following exposure was evaluated to ensure the validity of presented results. “Neutral” and negatively charged NPs, up to an exposure concentration of 250 µg/ml, did not affect the cell layer integrity, as shown by TEER values and Lucifer Yellow permeability. Responsiveness of TEER measurements in our systems was shown in our previous experiments, where opening of the tight junctions by exposure to EGTA resulted in significantly increased leakage of Lucifer Yellow [7]. Other studies looked at TEER values and translocation at earlier time points, and report that directly at the onset of polymer NP exposure the integrity of Caco-2 and co-culture monolayers was not affected [28] and a gradual cumulative translocation was observed [28-30]. Thus translocation due to initial loss of monolayer integrity can be excluded for the “neutral” and negatively charged PS-NPs. Positively charged PS-NPs significantly decreased TEER values (which has been seen before in the same cell model by [4]) and significantly increased Lucifer Yellow permeability, but only in the digested form. The dose of 250 µg/ml was selected to be able to detect the rather low expected translocation rates, which was based on previous results [7]. To further explore potential cytotoxicity of the NPs, we exposed proliferating cells to PS-NPs and measured the cell viability. As reported before for polymeric NPs [17, 31] and silicon NPs [32], only pristine and digested forms of positively charged PS-NPs decreased the viability of the proliferating cells. Proliferating Caco-2 cells are more sensitive to toxicity of NPs than differentiated cells as used in the translocation experiment, as has been shown using AgNPs [33, 34]. As for the digested PS-NP effects on TEER values and Lucifer Yellow permeability were observed on the 21 day old co-culture of Caco-2 and HT29-MTX, cytotoxic effects of these PS-NPs at the dose used cannot be excluded.

Not only did *in vitro* digestion increase the translocation but it also affected the protein corona of PS-NPs. Digested NPs contained less protein in their corona compared to their pristine equivalents: 4.8 x for (“0”), 3.5 x for (+), 1.4 x for (-M) and 1.8 x for (-P), and in the case of (“0”), (+) and (-P) NPs this difference was significant ($p < 0.03$) even after incubation of the digested NPs for 24h in cell culture medium. The effect of gastrointestinal conditions on the protein corona of NPs has not been reported before. However, proteolytic

enzyme phospholipase A2 (from macrophage phagolysosomes) has been shown to decrease the amount of proteins in the corona of polymeric NPs after overnight incubation [35]. Furthermore, it has been shown that the NP surface chemistry plays an important role in determining the NP protein corona [7, 21, 22]. In line with this, we show that different surface chemistries of PS-NPs adsorbed different amounts of proteins, both in pristine and digested forms. Digested PS-NPs had less adsorbed protein and they translocated more than pristine PS-NPs, which suggests a direct correlation between these two parameters. On the other hand, the difference in translocation between different pristine PS-NPs did not correlate directly with the difference in the amount of adsorbed protein. The same holds for the different digested PS-NPs. In literature, there is also no clear consensus as a negative correlation between the amount of adsorbed protein on NPs and their cellular interaction and uptake has been reported [36-38], as well as the opposite [37, 39-41]. Further detailed studies are required to elucidate the influence of the composition of the corona on cellular interactions and uptake mechanisms.

Digestion also affected the composition of the protein corona of NPs, which was demonstrated by differences in protein band patterns between pristine and digested PS-NPs. The main composition of the protein corona of pristine PS-NPs was independent of functionalization, as shown before for PS-NPs [7, 25, 35] and resulted in similar protein band pattern, with only minor differences in the ratios of component proteins, for all pristine PS-NPs. The major components of the corona of pristine NPs were proteins most abundantly present in cell culture medium (see DMEM+ control). The most prominent protein band on the gel had a mass of around 50-70 kDa, and comprised likely the fibrinogen gamma chain (50 kDa), fibrinogen beta chain (60 kDa), fibrinogen alpha chain (72 kDa) and albumin (72 kDa) as previously reported to be present in the protein corona of 50 nm PS-NPs [42]. Previous studies also showed that albumin and fibrinogen were the main components of the corona of differently functionalized 50, 100 and 200 nm PS-NPs [42, 43] incubated in plasma.

The pattern of protein bands in digested NPs, regarding protein types and their relative amounts, was clearly different from that of pristine NPs. Compared to pristine NPs, coronas of digested PS-NPs contained less proteins of high molecular weight and of 50-70 kDa and more low molecular weight proteins. The lanes with digested samples were smeary, suggesting partially broken down proteins. The intensity of the band at ~26 kDa, being most likely apolipoprotein A-1 [42], was clearly decreased in digested ("0") and digested (+) NPs compared to their equivalent pristine PS-NPs. In (-P) and (-M) NPs this band was hardly visible. Strikingly, digested PS-NP samples contained additional bands at ~18 kDa (in -M and -P NPs) and at ~45 kDa (in -M, -P and 0 NPs) that were not present in the washed control nor in the coronas of the pristine PS-NPs. As shown before for pristine PS-NPs [7], the composition of the protein corona of digested NPs was independent of the functionalization. All together, these results clearly indicate that *in vitro* digestion affects the protein corona by enzymatic breakdown of the proteins. The breakdown occurs either directly on the NP surface to already adsorbed proteins, or in suspension, which results in subsequent adsorption of the digested protein fragments onto the NPs.

CONCLUSION

In our study we demonstrated that digestion of differently charged 50 nm PS-NPs influenced both their translocation behaviour and their protein corona. The latter being affected in two aspects, regarding its amount and composition of proteins. Translocation of all digested PS-NPs was clearly increased compared to the translocation of their pristine equivalent PS-NPs, significantly for (+), (-M) and (-P) PS-NPs. Digested PS-NPs contained less protein in their corona than their equivalent pristine PS-NPs, significantly for ("0"), (+) and (-P) PS-NPs. Furthermore, digestion had a remarkable effect on the composition of the protein corona of PS-NPs in a way that it resulted in a shift from larger proteins (present in coronas of pristine NPs) towards low molecular weight proteins.

This study clearly illustrates that gastrointestinal digestion affects *in vitro* translocation behaviour of different types of PS-NPs. The implications are at least twofold, i) polymer NPs are increasingly explored to enhance the bioavailability of loaded drugs or poorly soluble compounds [44]- manipulating their surface modification will greatly enhance the uptake potency and ii) integration of *in vitro* digestion and *in vitro* intestinal translocation models is crucial to obtain relevant information from screening studies for risk assessment.

ACKNOWLEDGEMENTS

This project was funded by ZonMw (grant no. 40-40100-94-9016) to APW, the Dutch Ministry of Economic Affairs (RH, PJMH and HB). This work is supported by NanoNextNL (EK, MZ), a micro- and nanotechnology consortium of the Government of The Netherlands and 130 partners.

REFERENCES

- (1) Chaudhry Q, Scotter M, Blackburn J, Ross B, Boxall A, Castle L, Aitken R, Watkins R: Applications and implications of nanotechnologies for the food sector. *Food additives & contaminants Part A, Chemistry, analysis, control, exposure & risk assessment* 2008, 25:241-258.
- (2) PEN: The project on emerging nanotechnologies. 28 October 2013 edition. <http://www.nanotechproject.org/news/archive/9242/>; 2013.
- (3) EFSA, Committee ES: Guidance on the Risk Assessment of the Application of Nanoscience and Nanotechnologies in the Food and Feed Chain. *EFSA Journal* 2011, 9:36.
- (4) Mahler GJ, Esch MB, Tako E, Southard TL, Archer SD, Glahn RP, Shuler ML: Oral exposure to polystyrene nanoparticles affects iron absorption. *Nature Nanotechnology* 2012, 7:264-271.
- (5) Behrens I, Pena AI, Alonso MJ, Kissel T: Comparative uptake studies of bioadhesive and non-bioadhesive nanoparticles in human intestinal cell lines and rats: the effect of mucus on particle adsorption and transport. *Pharm Res* 2002, 19:1185-1193.
- (6) Martinez-Argudo I, Sands C, Jepson MA: Translocation of enteropathogenic *Escherichia coli* across an *in vitro* M cell model is regulated by its type III secretion system. *Cellular Microbiology* 2007, 9:1538-1546.
- (7) Walczak AP, Kramer E, Hendriksen PJ, Tromp P, Helsper JP, van der Zande M, Rietjens IM, Bouwmeester H: Translocation of differently sized and charged polystyrene nanoparticles in *in vitro* intestinal

- cell models of increasing complexity. *Nanotoxicology* 2014, 5:1-9.
- (8) El Badawy AM, Luxton TP, Silva RG, Scheckel KG, Suidan MT, Tolaymat TM: Impact of environmental conditions (pH, ionic strength, and electrolyte type) on the surface charge and aggregation of silver nanoparticles suspensions. *Environmental science & technology* 2010, 44:1260-1266.
 - (9) Bihari P, Vippola M, Schultes S, Praetner M, Khandoga AG, Reichel CA, Coester C, Tuomi T, Rehberg M, Krombach F: Optimized dispersion of nanoparticles for biological in vitro and in vivo studies. *Particle and fibre toxicology* 2008, 5:14.
 - (10) Walczak AP, Fokkink R, Peters R, Tromp P, Herrera Rivera ZE, Rietjens IM, Hendriksen PJ, Bouwmeester H: Behaviour of silver nanoparticles and silver ions in an in vitro human gastrointestinal digestion model. *Nanotoxicology* 2013, 7(7):1198-1210.
 - (11) Mwilu SK, El Badawy AM, Bradham K, Nelson C, Thomas D, Scheckel KG, Tolaymat T, Ma L, Rogers KR: Changes in silver nanoparticles exposed to human synthetic stomach fluid: effects of particle size and surface chemistry. *Sci Total Environ* 2013, 447:90-98.
 - (12) Rogers KR, Bradham K, Tolaymat T, Thomas DJ, Hartmann T, Ma L, Williams A: Alterations in physical state of silver nanoparticles exposed to synthetic human stomach fluid. *Sci Total Environ* 2012, 420:334-339.
 - (13) Peters R, Kramer E, Oomen AG, Herrera Rivera ZE, Oegema G, Tromp PC, Fokkink R, Rietveld A, Marvin HJ, Weigel S, et al: Presence of Nano-Sized Silica during In Vitro Digestion of Foods Containing Silica as a Food Additive. *ACS nano* 2012, 6(3):2441-2451.
 - (14) Oomen AG, Bos PM, Fernandes TF, Hund-Rinke K, Boraschi D, Byrne HJ, Aschberger K, Gottardo S, von der Kammer F, Kuhnel D, et al: Concern-driven integrated approaches to nanomaterial testing and assessment--report of the NanoSafety Cluster Working Group 10. *Nanotoxicology* 2014, 8:334-348.
 - (15) Zhao Y, Sun X, Zhang G, Trewyn BG, Slowing, II, Lin VS: Interaction of mesoporous silica nanoparticles with human red blood cell membranes: size and surface effects. *ACS Nano* 2011, 5:1366-1375.
 - (16) des Rieux A, Ragnarsson EG, Gullberg E, Preat V, Schneider YJ, Artursson P: Transport of nanoparticles across an in vitro model of the human intestinal follicle associated epithelium. *European Journal of Pharmaceutical Sciences* 2005, 25:455-465.
 - (17) Bhattacharjee S, Ershov D, Gucht J, Alink GM, Rietjens IM, Zuillhof H, Marcelis AT: Surface charge-specific cytotoxicity and cellular uptake of tri-block copolymer nanoparticles. *Nanotoxicology* 2013, 7:71-84.
 - (18) Peng Q, Zhang S, Yang Q, Zhang T, Wei XQ, Jiang L, Zhang CL, Chen QM, Zhang ZR, Lin YF: Preformed albumin corona, a protective coating for nanoparticles based drug delivery system. *Biomaterials* 2013, 34:8521-8530.
 - (19) Zhang H, Burnum KE, Luna ML, Petritis BO, Kim JS, Qian WJ, Moore RJ, Heredia-Langner A, Webb-Robertson BJ, Thrall BD, et al: Quantitative proteomics analysis of adsorbed plasma proteins classifies nanoparticles with different surface properties and size. *Proteomics* 2011, 11:4569-4577.
 - (20) Dell'Orco D, Lundqvist M, Oslakovic C, Cedervall T, Linse S: Modeling the time evolution of the nanoparticle-protein corona in a body fluid. *PLoS one* 2010, 5:e10949.
 - (21) Tenzer S, Docter D, Kuharev J, Musyanovych A, Fetz V, Hecht R, Schlenk F, Fischer D, Kiouptsi K, Reinhardt C, et al: Rapid formation of plasma protein corona critically affects nanoparticle pathophysiology. *Nat Nanotechnol* 2013, 8:772-781.
 - (22) Lundqvist M, Stigler J, Elia G, Lynch I, Cedervall T, Dawson KA: Nanoparticle size and surface properties determine the protein corona with possible implications for biological impacts. *Proceedings of the National Academy of Sciences of the United States of America* 2008, 105:14265-14270.
 - (23) Meder F, Daberkow T, Treccani L, Wilhelm M, Schowalter M, Rosenauer A, Madler L, Rezwani K: Protein adsorption on colloidal alumina particles functionalized with amino, carboxyl, sulfonate and phosphate groups. *Acta Biomater* 2012, 8:1221-1229.
 - (24) Gessner A, Lieske A, Paulke B, Muller R: Influence of surface charge density on protein adsorption on polymeric nanoparticles: analysis by two-dimensional

- electrophoresis. *Eur J Pharm Biopharm* 2002, 54:165-170.
- (25) Jedlovsky-Hajdu A, Bombelli FB, Monopoli MP, Tombacz E, Dawson KA: Surface coatings shape the protein corona of SPIONs with relevance to their application in vivo. *Langmuir* 2012, 28:14983-14991.
- (26) Versantvoort CH, Oomen AG, Van de Kamp E, Rempelberg CJ, Sips AJ: Applicability of an in vitro digestion model in assessing the bioaccessibility of mycotoxins from food. *Food and chemical toxicology : an international journal published for the British Industrial Biological Research Association* 2005, 43:31-40.
- (27) Hilgendorf C, Spahn-Langguth H, Regardh CG, Lipka E, Amidon GL, Langguth P: Caco-2 versus Caco-2/HT29-MTX co-cultured cell lines: Permeabilities via diffusion, inside- and outside-directed carrier-mediated transport. *Journal of Pharmaceutical Sciences* 2000, 89:63-75.
- (28) He B, Lin P, Jia Z, Du W, Qu W, Yuan L, Dai W, Zhang H, Wang X, Wang J, et al: The transport mechanisms of polymer nanoparticles in Caco-2 epithelial cells. *Biomaterials* 2013, 34:6082-6098.
- (29) Araujo F, Shrestha N, Shahbazi MA, Fonte P, Makila EM, Salonen JJ, Hirvonen JT, Granja PL, Santos HA, Sarmento B: The impact of nanoparticles on the mucosal translocation and transport of GLP-1 across the intestinal epithelium. *Biomaterials* 2014, 35:9199-9207.
- (30) Loo Y, Grigsby CL, Yamanaka YJ, Chellappan MK, Jiang X, Mao HQ, Leong KW: Comparative study of nanoparticle-mediated transfection in different GI epithelium co-culture models. *J Control Release* 2012, 160:48-56.
- (31) Bhattacharjee S, de Haan LH, Evers NM, Jiang X, Marcelis AT, Zuillhof H, Rietjens IM, Alink GM: Role of surface charge and oxidative stress in cytotoxicity of organic monolayer-coated silicon nanoparticles towards macrophage NR8383 cells. *Particle and fibre toxicology* 2010, 7:25.
- (32) Ruizendaal L, Bhattacharjee S, Pournazari K, Rosso-Vasic M, de Haan LHJ, Alink GM, Marcelis ATM, Zuillhof H: Synthesis and cytotoxicity of silicon nanoparticles with covalently attached organic monolayers. *Nanotoxicology* 2009, 3:339-347.
- (33) Bohmert L, Girod M, Hansen U, Maul R, Knappe P, Niemann B, Weidner SM, Thunemann AF, Lampen A: Analytically monitored digestion of silver nanoparticles and their toxicity on human intestinal cells. *Nanotoxicology* 2014, 8:631-642.
- (34) Gerloff K, Pereira DI, Faria N, Boots AW, Kolling J, Forster I, Albrecht C, Powell JJ, Schins RP: Influence of simulated gastrointestinal conditions on particle-induced cytotoxicity and interleukin-8 regulation in differentiated and undifferentiated Caco-2 cells. *Nanotoxicology* 2013, 7:353-366.
- (35) Cho WS, Thielbeer F, Duffin R, Johansson EMV, Megson IL, MacNee W, Bradley M, Donaldson K: Surface functionalization affects the zeta potential, coronal stability and membranolytic activity of polymeric nanoparticles. *Nanotoxicology* 2014, 8:202-211.
- (36) Lesniak A, Fenaroli F, Monopoli MP, Aberg C, Dawson KA, Salvati A: Effects of the presence or absence of a protein corona on silica nanoparticle uptake and impact on cells. *ACS Nano* 2012, 6:5845-5857.
- (37) Walkey CD, Chan WC: Understanding and controlling the interaction of nanomaterials with proteins in a physiological environment. *Chem Soc Rev* 2012, 41:2780-2799.
- (38) Baier G, Costa C, Zeller A, Baumann D, Sayer C, Araujo PHH, Mailander V, Musyanovych A, Landfester K: BSA Adsorption on Differently Charged Polystyrene Nanoparticles using Isothermal Titration Calorimetry and the Influence on Cellular Uptake. *Macromolecular Bioscience* 2011, 11:628-638.
- (39) Ehrenberg MS, Friedman AE, Finkelstein JN, Oberdorster G, McGrath JL: The influence of protein adsorption on nanoparticle association with cultured endothelial cells. *Biomaterials* 2009, 30:603-610.
- (40) Tedja R, Lim M, Amal R, Marquis C: Effects of serum adsorption on cellular uptake profile and consequent impact of titanium dioxide nanoparticles on human lung cell lines. *ACS nano* 2012, 6:4083-4093.
- (41) Aggarwal P, Hall JB, McLeland CB, Dobrovolskaia MA, McNeil SE: Nanoparticle interaction with plasma proteins as it relates to particle biodistribution, biocompatibility and therapeutic efficacy. *Advanced Drug Delivery Reviews* 2009, 61:428-437.

- (42) Monopoli MP, Walczyk D, Campbell A, Elia G, Lynch I, Bombelli FB, Dawson KA: Physical-chemical aspects of protein corona: relevance to in vitro and in vivo biological impacts of nanoparticles. *J Am Chem Soc* 2011, 133:2525-2534.
- (43) Lundqvist M, Stigler J, Cedervall T, Berggard T, Flanagan MB, Lynch I, Elia G, Dawson K: The Evolution of the Protein Corona around Nanoparticles: A Test Study. *Acs Nano* 2011, 5:7503-7509.
- (44) Luykx DM, Peters RJ, van Ruth SM, Bouwmeester H: A review of analytical methods for the identification and characterization of nano delivery systems in food. *J Agric Food Chem* 2008, 56:8231-8247.

5

Bioavailability and biodistribution of differently charged polystyrene nanoparticles upon oral exposure in rats

Agata P. Walczak
Peter J.M. Hendriksen
Ruud A. Woutersen
Meike van der Zande
Anna K. Undas
Richard Helsdingen
Johannes H.J. van den Berg
Ivonne M.C.M. Rietjens
Hans Bouwmeester

Submitted for publication to Journal of Nanoparticle Research

ABSTRACT

The likelihood of oral exposure to nanoparticles (NPs) is increasing and it is necessary to evaluate the oral bioavailability of NPs. *In vitro* approaches could help reducing animal studies. Previously, we assessed the translocation of 50 nm polystyrene NPs of different charges (neutral, positive, and negative) using a Caco-2/HT29-MTX *in vitro* intestinal translocation model. The present study aimed to validate this model by an *in vivo* study. For this, Fischer rats were orally exposed to a single dose of the same types of polystyrene NPs and uptake in organs was determined. One type of negatively charged NP was taken up more than the other NPs, with the highest amounts in kidney (37.4 µg/g tissue), heart (52.8 µg/g tissue), stomach wall (98.3 µg/g tissue), and small intestinal wall (94.4 µg/g tissue). This partly confirms our *in vitro* findings, where the same NPs translocated to the highest extent as well. However, the relative order of uptake for the other NPs differed from the *in vitro* findings. The estimated bioavailability ranged from 0.2% to 1.7% *in vivo*, which was much lower than that *in vitro* (1.6% to 12.3%). In conclusion, our results show that the uptake of the NPs, as predicted from our *in vitro* Caco-2/HT29-MTX model, overestimates the translocation across the rat intestine *in vivo*. Therefore, the integrated *in vitro* model cannot be used for a direct prediction of the bioavailability of orally administered NPs. However, the model can be used for prioritizing NPs before further *in vivo* testing for risk assessment.

INTRODUCTION

The number and range of consumer products containing nanoparticles (NPs) is constantly growing, examples range from e.g. lipsticks, toothpaste, food additives, health supplements, juice clarifiers to food packaging materials (Chaudhry et al. 2008; PEN 2013, Bouwmeester et al., 2014). Therefore, the likelihood of oral exposure to NPs is still increasing. Thus, there is a need to develop methods to assess the oral bioavailability of NPs. For scientific, ethical and economical reasons, *in vitro* models are desired.

To assess the performance of *in vitro* models, NPs need to be selected that differ in translocation efficiency. In several studies polystyrene NPs (PS-NPs) have been shown to translocate across *in vitro* intestinal barrier models (Walczak et al., 2014; Kulkarni and Feng 2013; Martinez-Argudo et al. 2007) and this translocation depended on NP characteristics like size, charge and surface chemistry. In addition, *in vivo* studies have demonstrated the bioavailability of PS-NPs after oral exposure as well (Jani et al., 1989; Jani et al., 1990; Hussain et al. 1997). However, no data is available from studies that used the same PS-NPs *in vitro* and *in vivo*. For these reasons we previously selected PS-NPs to perform *in vitro* gut translocation studies (Walczak et al., 2014). With the present study we aim to evaluate the validity of our *in vitro* model by comparison of previously obtained *in vitro* data with *in vivo* data. In order to do this we used the same range of PS-NPs that were previously used *in vitro* in an *in vivo* study.

In these previous *in vitro* studies we developed an integrated *in vitro* gastrointestinal digestion and *in vitro* intestinal epithelium model as a screening tool for assessing the translocation efficiency of orally administered PS-NPs. The translocation of these PS-NPs ranged from 1.6 to 12.3% (Walczak et al., in press). Furthermore, these results indicated that the translocation rate of the PS-NPs was affected by at least three factors: (i) the physicochemical properties of the PS-NPs (i.e. size and surface chemistry) (Walczak et al., 2014), (ii) the environmental conditions that the PS-NPs were exposed to (i.e. incubation in an *in vitro* gastrointestinal digestion model) (Walczak et al., in press), and (iii) the properties of the *in vitro* monolayer simulating the intestinal epithelium (i.e. presence of mucus) (Walczak et al., 2014). Effects of size, surface chemistry, and the properties of the *in vitro* monolayer on PS-NP translocation have also been reported by others (Hussain et al. 2001; Szentkuti 1997; des Rieux et al. 2005; Fazlollahi et al. 2011; Mahler et al. 2012).

In order to reduce the undesirable use of animals in the toxicological evaluation of NPs (Hartung et al., 2013), alternative *in vitro* intestinal translocation models need to be developed. However, before such *in vitro* models can be used in risk assessment of NPs, they need to be validated (Kandarova and Letasiova 2011; Worth and Balls 2004) using *in vivo* data (Genschow et al. 2002). As mentioned earlier, the aim of this study was to assess to which extent our *in vitro* model (combination of a gastrointestinal digestion model and an intestinal epithelium translocation model) predicts the translocation efficiency occurring *in vivo*. To that end, rats were orally exposed to a single dose of the same PS-NPs as used in previous *in vitro* studies (i.e. neutral, positive, and negative, the latter from two different suppliers with different surface modifications (Walczak et al., 2014)) and PS-NP bioavailability in organs was determined.

MATERIALS AND METHODS

Nanoparticles

Neutral, amine- and carboxyl-modified 50 nm PS-NPs (referred to as 50 (0), 50 (+), 50 (-M)) with a red fluorophore core (Ex/Em: 530/590) were purchased from Magsphere (Pasadena, CA, USA). Carboxyl-modified 50 nm PS-NPs (referred to as 50 (-P)) with a yellow-green fluorophore core (Ex/Em: 485/530) were purchased from Polysciences (Warrington, Pennsylvania, USA). PS-NPs were washed prior to administration by centrifugation for 5 h at 18 000 g, 15°C and re-suspension in deionised water, in order to remove preservatives and surfactants present in the suspension solution. The final mass concentration of all stock suspensions was 2.5 %.

NP characterization

The nanoparticles, as purchased, were characterized previously (Walczak et al., 2014) using Scanning Electron Microscopy (SEM), Dynamic Light Scattering (DLS), and zeta-potential measurements. To confirm the size of the PS-NPs as administered to animals (i.e. following washing and re-suspension in deionised water), hydrodynamic sizes were again determined using DLS. The measurements were performed as previously described (Walczak et al. 2012). Suspensions of 100 µg/ml were analysed in triplicate and the results are presented as the mean ± SD.

Stability of the fluorescent dye in PS-NPs during exposure

No detectable leakage of the fluorescent dye from the used PS-NPs was shown upon incubation under simulated gastric digestion conditions. For this, PS-NPs were incubated in simulated gastric juice for 2 hrs at 37°C, after which the suspensions were brought to neutral pH and suspensions at 250 µg/ml were centrifuged (30 min, 3 000 g, 20°C) in filter tubes (Amicon Ultra-4 3kDa Ultracel-PL memb 24/Pk; Millipore BV, Netherlands). The filtrates were then analysed for fluorescence.

Animal experiment

Five weeks old male Fischer 344 rats with a body weight of 107 ± 8 g (upon arrival) were obtained from Harlan (Horst, The Netherlands). Upon arrival, rats were left to acclimatise for three weeks in groups of two under standard conditions of humidity (55-65%), temperature (22 ± 3 °C), and light (12 h light/ 12 h dark cycles), with *ad libitum* access to feed pellets (Abdiets, Woerden, The Netherlands) and tap water. After three weeks, 25 rats were divided into five groups ($n=5$) for the experiment, based on their weight to have a similar weight distribution in each group (201 ± 13 g). Before treatment, rats were fasted for 2 h. A single dose of 1 ml PS-NP suspension per 200 g bw was administered through oral gavage at a concentration of 25 mg/ml (resulting in a dose of 125 mg/kg bw). Rats in the control group received the same volume of vehicle solution (i.e. deionised water) only. After administration, rats were housed separately until the end of the experiment. All animal experiments were approved by the ethical committee on animal experimentation of Wageningen University & Research centre, The Netherlands.

Blood samples (around 100 μ l) were withdrawn from the tail vein at time points: 0, 0.5, 1, 2 and 4 h and collected in heparinized tubes. At $t=6$ h, rats were sacrificed under anaesthesia, blood was collected from the aorta, after which liver, kidneys, spleen, lungs, heart, testis, brain, stomach, small intestine and large intestine were collected. Food remainders and faecal contents were gently removed from the stomach, small- and large intestines with a spoon and the tissues were subsequently rinsed in PBS, to remove any unabsorbed PS-NPs. The organs were weighed and divided into two pieces for fluorescent and histopathological evaluation. The pieces meant for fluorescence measurements were preserved on ice, and the pieces meant for histopathology/microscopic observations were preserved in Bouin solution (testis) or in 10% neutral buffered formalin (all other organs).

Fluorescence measurements of blood and organs

Harvested tissue samples were digested using an aqueous enzyme solution containing 1g/l proteinase K (Sigma-Aldrich, St. Louis, MP, USA) in 50 mM NH_4HCO_3 buffer (to maintain a constant pH value of 7.4 during enzymatic digestion) and 5g/l SDS to improve activity of the enzyme (Loeschner et al., 2013). Organs were carefully weighed, cut in pieces and digested in digestion buffer at a weight ratio of 1:5. The samples were thoroughly vortexed and incubated at 37°C under continuous stirring on a magnetic stirrer for 4 h. This resulted in slightly turbid but homogenous suspensions. Fluorescence of the samples was measured using a SpectraMax M2 microplate reader (Molecular Devices, Berkshire, UK) at excitation/emission wavelengths of 530/590 nm and 470/520 nm, for red and yellow-green PS-NPs, respectively. The PS-NP concentration was determined based on previously prepared standard calibration curves in each organ separately, obtained by spiking blank organ homogenates (prepared as described above) with serial dilutions of PS-NPs ranging from 0 to 20 μ g/ml. The PS-NP bioavailability was estimated by summing up the amounts of NPs measured in all tested organs except for the brain, stomach wall and small- and large intestinal walls. For this, the amounts of NPs per gram tissue were multiplied by the weights of the organs.

Histopathology

Samples for histopathology, fixed in 10% formalin or Bouin solution, were dehydrated in a series of ethanol and embedded in paraffin. Approximately 5 μ m thick sections were cut, mounted on glass slides and stained with hematoxylin and eosin (H&E). The sections were observed under an optical microscope (Zeiss, Cambridge, UK) at different magnifications.

Fluorescence imaging

Intact livers, kidneys, spleens, lungs, testes, small intestinal wall and large intestinal wall were scanned for fluorescence with a fluorescence imager (Cellavista V3.1, SynenTec Bio Services GmbH, Münster, Germany) using illumination at wavelengths Ex/Em= 470nm/520nm or 530nm/590nm, for yellow-green (-P) PS-NPs and red (0, +, -M) PS-NPs, respectively.

Statistics

Data were analysed with SPSS (IBM, Version 21) and the charts were generated with Prism software (v5.02; GraphPad Software, Inc., La Jolla, USA). A one-way analysis of variance ANOVA test and post-hoc Tukey test were used to determine significant differences between the groups. T-test was used to compare the estimated bioavailability between the groups.

RESULTS

NP characterization

The PS-NPs with different surface modifications were characterized in water using SEM and zeta-potential measurements as reported previously (Walczak et al., 2014). Briefly, all types of 50 nm PS-NPs had similar size distributions (as measured with SEM in stock suspensions) with an average size of 31.6 - 35.0 nm, except for the 50 nm (+) PS-NPs, which had a larger average size of 50.6 nm (Table 1). The zeta-potential measurements in stock suspensions of the 50 nm (+) and 50 nm (-) PS-NPs in water confirmed their positive and negative charges (Table 1). The two types of negatively charged 50 nm PS-NPs (-M and -P) had the same zeta-potential (i.e. -27.7 and -27.8mV), while the zeta-potential of the positively charged PS-NPs was 26.6 mV. The neutral PS-NPs had a negative charge of -26.0 mV in water. The size of PS-NPs re-suspended in deionised water, as administered to animals, was measured with DLS. The PS-NPs were monodispersed and their hydrodynamic diameters ranged from 50.0 ± 0 nm to 54.3 ± 0.1 nm (Table 1).

Fluorescence measurements of blood and organs

Fluorescence of the collected blood and organs was determined. The concentration of the 50 nm (-P) PS-NPs was high enough for detection in the kidney and small- and large intestinal walls at the appropriate wavelength using fluorescent microscopy, and the concentrations of the 50 nm (0), (+), and (-M) PS-NPs were high enough for detection in the small- and large intestinal walls only (Fig. 1 a, b, c). The fluorescence intensity could not be quantified reliably using whole organs. Therefore, fluorescence intensity was quantified using organ

Table 1. Physicochemical characterization of 50 nm PS-NPs

PS-NPs	SEM (nm) ^a	DLS (nm) ^b	Zeta-potential (mV) ^c
50 nm (0)	33.4 ± 12.7	50.0 ± 0.0	-26.0 ± 16.2
50 nm (+)	50.6 ± 9.3	50.3 ± 0.4	26.6 ± 13.9
50 nm (-M)	35.0 ± 15.3	52.7 ± 2.4	-27.7 ± 19.3
50 nm (-P)	31.6 ± 13.6	54.3 ± 0.1	-27.8 ± 17.4

^aDiameters [nm] of PS-NPs in water, as measured with SEM in stock suspensions ($n=80-380$). ^bHydrodynamic diameters [nm] of PS-NPs in water, as determined by DLS at $t=0$ h, after re-suspending the PS-NPs in deionised water. ^cZeta-potential [mV] of PS-NPs in water, as determined by a zeta-sizer in stock suspensions at $t=0$ h. Abbreviations: (0): neutral PS-NPs, (+): positively charged PS-NPs, (-M) and (-P): negatively charged PS-NPs from Magsphere and Polysciences, respectively. Data in ^a and ^c from Walczak et al., 2014.

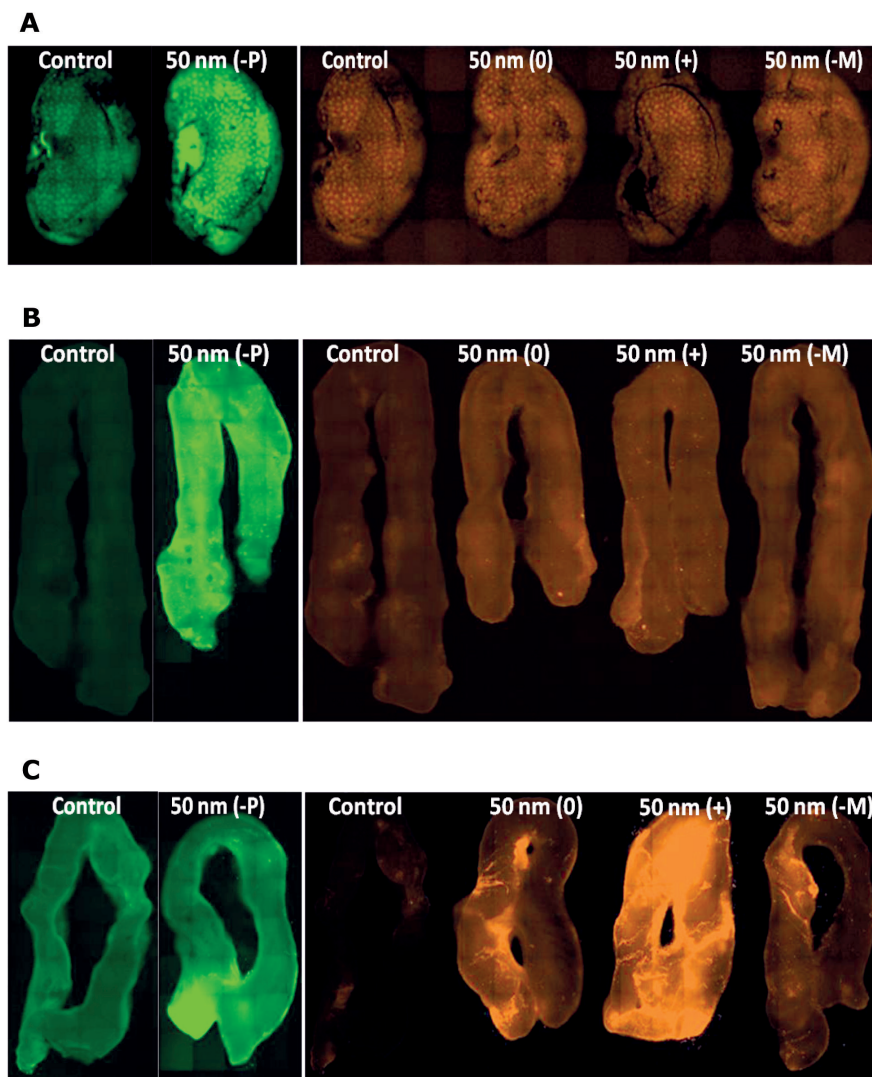
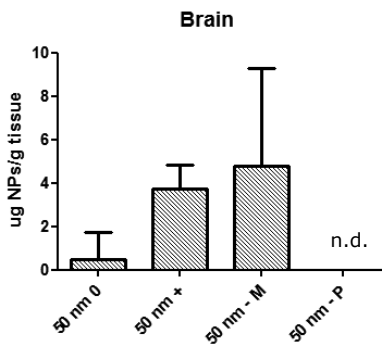
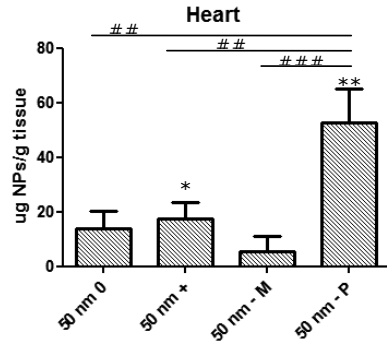
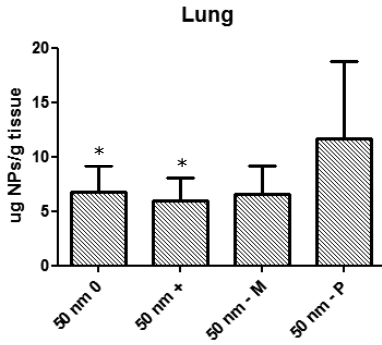
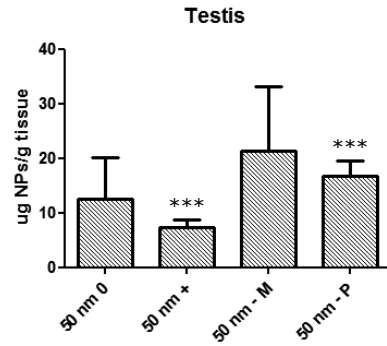
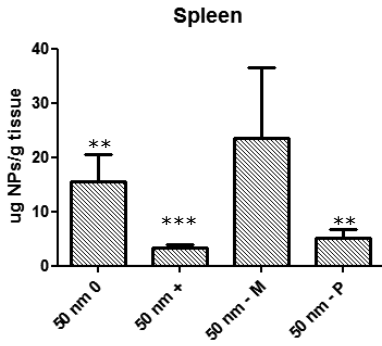
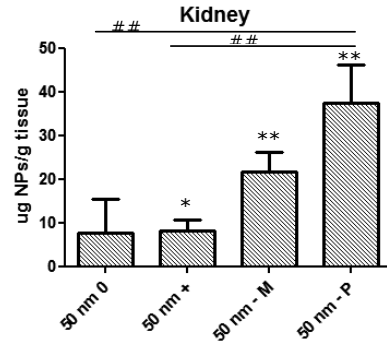
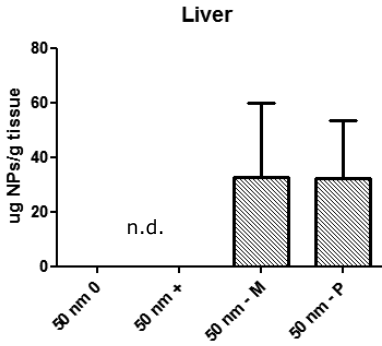
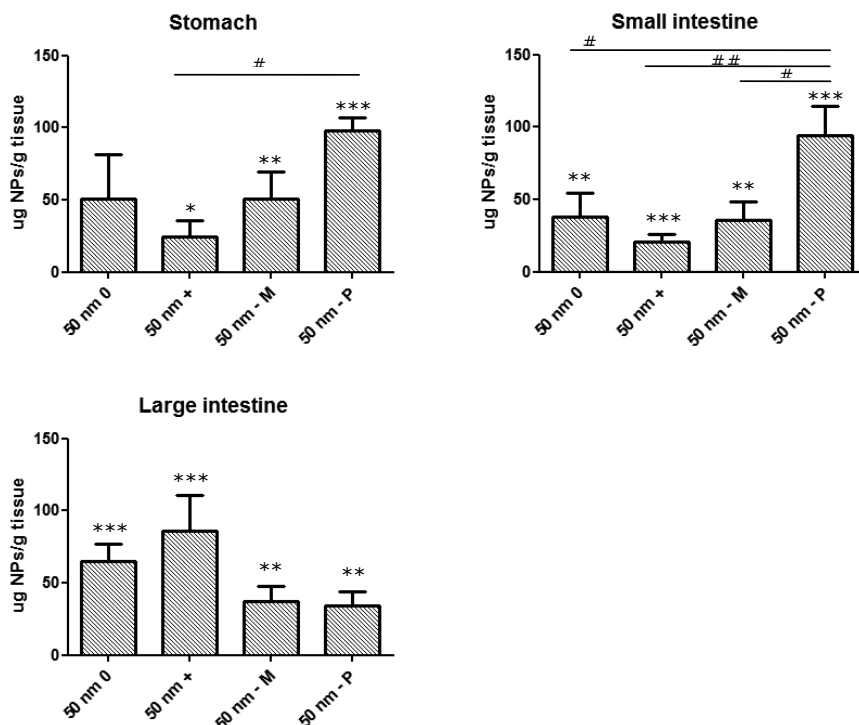


Figure 1. Whole organ fluorescence following a single oral administration of 125 mg/kg bw PS-NPs. Pictures of kidney (A), small (B) and large intestinal wall (C) at $t=6h$ showing fluorescence under the illumination with wavelengths $Ex/Em= 470nm/520nm$ or $530nm/590nm$, for yellow-green (-P) PS-NPs and red (0, +, -M) PS-NPs, respectively. Control organs were collected from animals treated with only water. Abbreviations: (0): neutral PS-NPs, (+): positively charged PS-NPs, (-M) and (-P): negatively charged PS-NPs from Magsphere and Polysciences, respectively.

homogenates and PS-NP organ concentrations were determined based on standard calibration curves made in each organ. The PS-NP concentrations in the different organs are shown in Figure 2. Each of the four types of PS-NPs induced a significant increase of fluorescence in at least one of the tested organs, indicating passage of these PS-NPs through





◀ Figure 2. Organ distribution of 50 nm PS-NPs after 6 h from a single oral exposure (125 mg/kg bw), expressed as µg PS-NPs/ g tissue, detected in organs from exposed animals. Abbreviations: n.d.: not detectable, 0: neutral PS-NPs, +: positively charged PS-NPs, -M and -P: negatively charged PS-NPs from Magsphere and Polysciences, respectively. Error bars show the standard error of mean ($n=5$). Significant difference between the blank and exposed organs is illustrated as: * ($p<0.1$), ** ($p<0.05$) and *** ($p<0.01$). Significant difference between different types of PS-NPs is illustrated as: # ($p<0.1$), ## ($p<0.05$) and ### ($p<0.01$).

Table 2. Comparison of results from *in vitro* and *in vivo* experiments measuring intestinal translocation in Caco-2/HT29-MTX cells and systemic uptake in rats, respectively.

PS-NPs	In vitro translocation (% of administered dose)*	In vivo estimated bioavailability (% of administered dose)
50 nm (0)	9.1 ± 0.8 %	0.3 ± 0.1 %
50 nm (+)	4.8 ± 0.7 %	0.2 ± 0.0 %
50 nm (-M)	1.6 ± 0.2 %	1.5 ± 0.9 %
50 nm (-P)	12.3 ± 1.1 %	1.7 ± 0.7 %

*Data from (Walczak et al., in press). Abbreviations: (0): neutral PS-NPs, (+): positively charged PS-NPs, (-M) and (-P): negatively charged PS-NPs from Magsphere and Polysciences, respectively.

the intestinal wall. In animals exposed to 50 nm (-P) PS-NPs, the concentration of these PS-NPs was significantly increased in kidney ($p<0.05$), spleen ($p<0.05$), testis ($p<0.01$), heart ($p<0.05$), stomach wall ($p<0.000$), small intestinal wall ($p<0.01$) and large intestinal wall ($p<0.05$). In animals exposed to 50 nm (+) PS-NPs, the concentration of these PS-NPs was significantly increased in kidney ($p<0.1$), spleen ($p<0.01$), testis ($p<0.01$), lung ($p<0.1$), heart ($p<0.1$), stomach wall ($p<0.1$), small intestinal wall ($p<0.01$) and large intestinal wall ($p<0.01$). The concentrations of 50 nm (0) and (-M) PS-NPs in the organs were considerably lower than those of 50 nm (-P) and (+) PS-NPs, and they reached significance only in few organs. In the animals exposed to 50 nm (0) PS-NPs, the concentration of these PS-NPs was significantly increased in spleen ($p<0.05$), lung ($p<0.1$), small intestinal wall ($p<0.05$) and large intestinal wall ($p<0.01$). The concentration of 50 nm (-M) PS-NPs was significantly increased in kidney ($p<0.05$), stomach wall ($p<0.05$), small intestinal wall ($p<0.05$) and large intestinal wall ($p<0.05$). No PS-NPs were detected in blood samples from any time point.

In some organs, the PS-NP concentration was significantly different between the different types of PS-NPs, depending on their surface modifications. In kidney, the concentration of 50 nm (-P) PS-NPs was significantly higher than that of the 50 nm (+) ($p<0.05$) and 50 nm (0) PS-NPs ($p<0.05$). Also in heart, the concentration of 50 nm (-P) PS-NPs was significantly higher than that of 50 nm (+) ($p<0.05$), 50 nm (0) ($p<0.05$) and 50 nm (-M) PS-NPs ($p<0.01$). In the stomach wall, the concentration of 50 nm (-P) PS-NPs was significantly higher than that of 50 nm (+) ($p<0.1$), and in the small intestinal wall the concentration of 50 nm (-P) PS-NPs was significantly higher than that of 50 nm (+) ($p<0.05$), 50 nm (0) ($p<0.1$) and 50 nm (-M) PS-NPs ($p<0.1$).

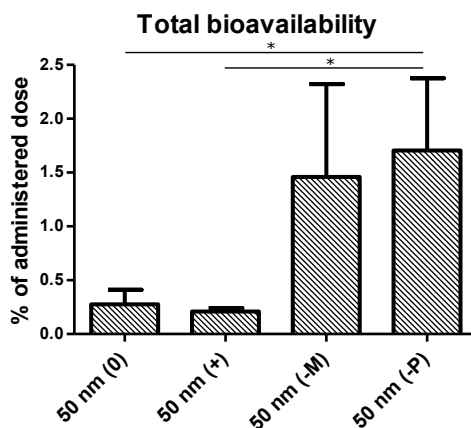


Figure 3. Estimated bioavailability of 50 nm PS-NPs, expressed as a percentage of the administered dose (125 mg/kg bw), calculated by summing up the amounts of PS-NPs detected in all analysed organs, except the stomach- and intestinal walls, and brain. Abbreviations: (0): neutral PS-NPs, (+): positively charged PS-NPs, (-M) and (-P): negatively charged PS-NPs from Magsphere and Polysciences, respectively. Error bars show the standard error of mean ($n=5$). *: Significant difference ($p<0.1$).

The overall bioavailability of PS-NPs was estimated by summing up the amounts of PS-NPs in all measured organs, except the stomach wall and intestinal walls, as PS-NPs present in these organs were most likely the result of direct absorption rather than from uptake from the blood, and except the brain, due to the selectivity of the blood-brain barrier. As shown in Figure 3, the resulting amount of PS-NPs as a percentage of the administered dose was as low as 0.3 % and 0.2 % for 50 nm (0) and (+) PS-NPs, respectively, while the (-M) and (-P) PS-NPs reached bioavailable levels of 1.5 % and 1.7 %, respectively. The estimated bioavailability of 50 nm (-P) PS-NPs was significantly ($p < 0.1$) higher than that of 50 nm (0) and 50 nm (+) PS-NPs.

Microscopic observations of tissue slides did not reveal any histopathological changes.

DISCUSSION

In the present study we evaluated the biodistribution of differently charged PS-NPs in rats after a single oral administration. Our results show the bioavailability and biodistribution of PS-NPs from the gastrointestinal tract to different organs within 6 hours. The highest amounts of PS-NPs were measured in the stomach- and intestinal walls. PS-NPs were detected also in lung, testis, spleen, kidney and heart, meaning that the PS-NPs were systemically available. However, the overall estimated bioavailability was low, ranging from 0.2% to 1.7% of the administered dose. All types of PS-NPs used in our study had the same size, yet the organ uptake and distribution pattern was different. This shows that surface charge and chemistry of PS-NPs affected their bioavailability to the organs, as reported before for PS-NPs (Hillery and Florence 1996; Hussain et al. 1997; Jani et al. 1989) and other types of NPs (El-Shabouri 2002; Xiao et al. 2011).

Irrespective of surface charge, all types of PS-NPs were measured in significant amounts in the small- and large intestinal walls, as shown by fluorescence measurements and organ imaging. The intestinal wall has been shown before to be the main site of biodistribution for PS-NPs after oral administration (Hussain et al. 1997; Jani et al. 1992). High levels of PS-NPs measured in intestinal walls in our study could be related with the uptake of PS-NPs in lymphoid tissue associated with these organs, as shown before (Florence et al. 1995; Hillery et al. 1994; Seifert et al. 1996). Also testis, spleen, kidney and heart had considerably high concentrations of PS-NPs, irrespective of the type of administered PS-NPs. These organs, and additionally also liver, have been shown before to be the main organs where PS-NPs (Hussain et al. 1997; Jani et al. 1990) and other types of NPs (Baek et al. 2012; Cho et al. 2013; van der Zande et al. 2012) were distributed after being taken up into systemic circulation after an oral exposure. In addition, oral exposure of mice to zinc oxide NPs has been shown to induce histopathological changes in the testis (Talebi et al. 2013). Strikingly, the liver showed no significant increase in fluorescence above background levels, for any of the used NP types. This could be related to the size of the PS-NP. It has been shown that while liposome NPs smaller than 70 nm accumulated in liver, liposome NPs larger than 200 nm accumulated in spleen (Liu et al. 1992). The PS-NPs used in the present study could possibly agglomerate during the passage through the gastrointestinal tract and as a result

Table 3. Overview of oral studies performed with PS-NPs in rats.

NP type	Detection method	Experimental conditions	Dose	Size	Uptake (% of the administered dose)	Ref.
Carboxylated polystyrene nanospheres linked with rhodamine	Fluorescence microscopy observations	Female Sprague-Dawley rats; gavage	1.25 mg/kg bw, daily for 10 days	100 nm, 1 µm	Uptake only semiquantitatively quantified: very low uptake in the stomach wall, small intestinal wall and mesentery node; low uptake in the Peyer's patch, colon, and liver; no NPs in kidney, lungs, heart and spleen	(Jani et al. 1989)
Non-ionized polystyrene microspheres linked with fluorescein				100 nm, 500 nm, 1 µm, 3µm	low uptake in the spleen, stomach wall and small intestinal wall; moderate uptake in liver and colon; high uptake in the Peyer's patch and mesentery node; no NPs in kidney, lungs and heart	
Non-ionized polystyrene microspheres linked with fluorescein	Presence of polystyrene was analysed by gel permeation chromatography; measurement of radioactivity of tissues	Female Sprague-Dawley rats; gavage	1.25 mg/kg bw, daily for 10 days	50 nm	- total uptake: 33.7% -without stomach, small- and large intestinal walls: 6.6% (*) -liver: 3.3% -spleen: 0.9% -kidney: 0.2% -stomach wall: 1.1% -small intestinal wall: 12% -large intestinal wall: 14% -no NPs in lungs and heart	(Jani et al. 1990)
				100nm	- total uptake: 26% -without stomach, small- and large intestinal walls: 5.9% (*) -liver: 3.8% -spleen: 0.7% -stomach wall: 0.7% -small intestinal wall: 3.4% -large intestinal wall: 16% -no NPs in kidney, lungs and heart	

Table 3. Overview of oral studies performed with PS-NPs in rats. (Continued)

NP type	Detection method	Experimental conditions	Dose	Size	Uptake (% of the administered dose)	Ref.
				300 nm	- total uptake: 9.5% -without stomach, small- and large intestinal walls: 2.7% (*) -liver: 1.4% -spleen: 0.2% -stomach wall: 0.5% -small intestinal wall: 2% -large intestinal wall: 4.3% -no NPs in kidney, lungs and heart	
				500 nm	-total uptake: 13.7 % -without stomach, small- and large intestinal walls: 1.9% (*)	
				1 µm	-total uptake: 4.6 % -without stomach, small- and large intestinal walls: 0.8% (*)	
Non-ionized polystyrene microspheres linked with fluorescein	Fluorescence microscopy observations	Female Sprague-Dawley rats; gavage	12.5 mg/kg, 6 hours	50 nm	Uptake only semiquantitatively quantified: significant uptake in the Peyer's patches and mesentery nodes; no NPs in liver and spleen	(Jani et al. 1992)
				500 nm	low uptake in the Peyer's patches; evident uptake in mesentery nodes; no NPs in liver and spleen	
				1 µm	low uptake in the Peyer's patches; no NPs in mesentery nodes, liver and spleen	
Carboxylated polystyrene NPs coupled with lectin	Fluorescence microscopy observations; gel permeation chromatography	Female Wistar rats; gavage	12.5 mg/kg, daily for 5 days	500 nm	Total estimated uptake: 37.6% (*) -without stomach, small- and large intestinal walls: 23% -liver: 2.6% -spleen: 1.2% -heart: 0.3% -kidney: 0.7% -intestinal wall: 12.8%	(Hussain et al. 1997)

Table 3. Overview of oral studies performed with PS-NPs in rats. (Continued)

NP type	Detection method	Experimental conditions	Dose	Size	Uptake (% of the administered dose)	Ref.
- with N-acetylchito-tetraose					-spleen: 0.42%	
Non-ionized polystyrene NPs with covalently linked fluorescein, coated with 407 poloxamer	Fluorescence microscopy observations; gel permeation chromatography	Female Sprague-Dawley rats; gavage	14 mg/kg, daily for 5 days	60 nm	Uptake across the GI tract: 3%; -lymphoid large intestine: 2.0% -non-lymphoid large intestine: 1%	(Hillery and Florence 1996)
- coated with 188 poloxamer					Uptake across the GI tract: 1.5%; -lymphoid large intestine: 1.5%	
Non-ionized polystyrene NPs with covalently linked fluorescein	Fluorescence microscopy observations; gel permeation chromatography	Female Sprague-Dawley rats; oral gavage	14 mg/kg, daily for 5 days	60 nm	Uptake across the GI tract: 10%; -lymphoid small intestine: 3.4% -non-lymphoid small intestine: 2.3% -lymphoid large intestine: 3.0% -non-lymphoid large intestine: 2.2%	(Hillery et al. 1994)
Polystyrene NPs FITC-labelled	Fluorescence microscopy observations	Male Wistar rats: -young (5 wk); intraduodenally administered, single dose -middle age (5 months) -old (9 months)	3.7x10 ⁸ in 1 ml, 6 hours	1 µm	Measured in lymph fluid: -2x10 ⁻⁶ % (*) -2x10 ⁻⁵ % (*) -1.4x10 ⁻⁵ % (*)	(Seifert et al. 1996)

(*) : calculated from the numbers given in the manuscript

become larger than 70 nm. Also another study performed with 50 nm PS-NPs has shown the absence of the NPs in liver after 6 h from a single oral exposure (Jani et al. 1992). Neither were PS-NPs detected in blood at any time point, even with the intervals of half an hour, possibly due to a rapid transport of PS-NPs from the blood circulation to the organs, like shown before (Geraets et al. 2014).

Several *in vivo* oral studies have been performed before with different types of PS-NPs. Table 3 summarizes oral studies performed in rats with differently sized and coated PS-NPs. The results from these studies highlight the dependence of uptake and accumulation of PS-NPs on several factors, including the size, surface charge and type of coating material (Araujo et al. 1999; Hillery et al. 1994; Hillyer and Albrecht 2001; Hussain and Florence 1998; Hussain et al. 1997; Jani et al. 1989). In general, smaller PS-NPs were taken up to a higher extent than the larger ones (Jani et al. 1990), the non-ionized more than the carboxylated ones (Jani et al. 1989) and 407 poloxamer-coated more than 188 poloxamer-coated across the GI tract (Hillery and Florence 1996; Hussain et al. 1997).

The estimated oral bioavailability that we report here (i.e. 0.2 - 1.7%) is lower than in a previous oral study using 50 nm PS-NPs, where 6.6% estimated total uptake was reported (Jani et al. 1990) (Table 3). Also the amounts of PS-NPs associated with intestinal tissues that we detected (ranging between 0.38 and 0.74% depending on the type of PS-NPs, calculated as a sum of the small- and large intestinal walls, data not shown) were lower than the ones reported by others for 60 nm PS-NPs, which varied between 1.5 and 10%, depending on the type of PS-NPs used ((Hillery and Florence 1996; Hillery et al. 1994). The difference between data from the present study and those of other *in vivo* studies might be due to the use of different exposure conditions, as we exposed the rats for 6 h while in the previous studies rats were exposed for 5 or 10 days. Furthermore, the bioavailability values given here were estimated from the amounts of PS-NPs that were measured in a selection of organs, and therefore can be underestimated. The differences in the described amounts of NPs that pass the intestinal walls could be further caused by differences in tissue sampling methods and methods of quantifying the concentration of PS-NPs in tissues, and by large interindividual differences as shown before after intraduodenal administration of PS-NPs, where the numbers of particles subsequently found in lymph ducts varied considerably between the different animals (Seifert et al. 1996). However, the amount of 50 nm (-P) PS-NPs that was detected in kidney (0.3%) was similar to the 0.2% reported by others for 50 nm PS-NPs (Jani et al. 1990). Comparison of our results from 50 nm (-P) PS-NP to 300 nm PS-NPs in another study shows that the amount of the 50 nm (-P) PS-NPs that we detected in the liver (1.3%), spleen (0.07%), and stomach wall (0.54%) was similar to the 1.4%, 0.2% and 0.5% reported for the liver, spleen and stomach wall of 300 nm PS-NP treated animals respectively (Jani et al. 1990). Furthermore, the amount of PS-NPs we detected in the heart (0.17%) was largely similar to the 0.3% detected for 500 nm PS-NPs (Hussain et al. 1997)). However, our bioavailability values are lower than the extrapolated 23% that was reported for much larger 500 nm PS-NPs (Hussain et al. 1997). Even larger PS-NPs of 1 μm had a lower uptake than what we report here (2×10^{-6} of 1 μm PS-NPs detected in lymph fluid (Seifert et al. 1996)).

Comparison of the bioavailability values ranging between 0.2% and 1.7% that we report here, with the translocation values of the same 50 nm PS-NPs in our integrated *in vitro* digestion and *in vitro* intestinal model, which ranged from 1.6% to 12.3% (Walczak et al., in press), shows lower uptake values in the *in vivo* model. (Table 2). Therefore, our integrated *in vitro* model appears to overestimate the translocation through the rat intestinal wall. Also the relative order of translocation *in vitro* (Walczak et al. 2014; Walczak et al., in press) differed from the order of uptake of PS-NPs *in vivo*. However, the 50 nm (-P) PS-NPs, which translocated to the largest extent *in vitro*, were also taken up to the largest extent in the present *in vivo* study, as shown in organs where the PS-NPs concentrations were highest (i.e. in kidney and heart).

CONCLUSIONS

In conclusion, our results show that the predicted uptake of PS-NPs from our integrated *in vitro* model appears to overestimate the actual uptake occurring in the rat *in vivo*. Therefore, the *in vitro* model cannot be used for a direct prediction of bioavailability of orally administered PS-NPs in a rat model. However, our model can be used for screening and prioritizing NPs before further *in vivo* testing for risk assessment. Similar to *in vitro* results, the surface charge and surface chemistry affected the uptake and biodistribution of 50 nm PS-NPs after oral exposure in rats. The negatively charged PS-NPs were present in almost all organs to a much higher extent than the neutral and positively charged PS-NPs, which is in line with the *in vitro* translocation data of these PS-NPs.

ACKNOWLEDGEMENTS

The authors would like to thank Geert Stoop for generating photos of fluorescence in the organs. This project was funded by ZonMw (grant no. 40-40100-94-9016) to APW, the Dutch Ministry of Economic Affairs (PJM, RH and HB). This work is supported by NanoNextNL (MZ), a micro- and nanotechnology consortium of the Government of The Netherlands and 130 partners.

REFERENCES

- (1) Araujo L, Lobenberg R, Kreuter J (1999) Influence of the surfactant concentration on the body distribution of nanoparticles *Journal of drug targeting* 6:373-385.
- (2) Baek M et al. (2012) Pharmacokinetics, tissue distribution, and excretion of zinc oxide nanoparticles *International journal of nanomedicine* 7:3081-3097.
- (3) Bouwmeester H, Brandhoff P, Marvin HJP, Weigel S, Peters RJB. 2014. State of the safety assessment and current use of nanomaterials in food and food production. *Trends in Food Science & Technology* xx:1-11. <http://dx.doi.org/10.1016/j.tifs.2014.08.009>.
- (4) Chaudhry Q et al. (2008) Applications and implications of nanotechnologies for the food sector *Food Addit Contam Part A Chem Anal Control Expo Risk Assess* 25:241-258.
- (5) Cho WS, Kang BC, Lee JK, Jeong J, Che JH, Seok SH (2013) Comparative absorption, distribution, and excretion of titanium

- dioxide and zinc oxide nanoparticles after repeated oral administration Part Fibre Toxicol 10:9.
- (6) des Rieux A, Ragnarsson EGE, Gullberg E, Preat V, Schneider YJ, Artursson P (2005) Transport of nanoparticles across an in vitro model of the human intestinal follicle associated epithelium Eur J Pharm Sci 25:455-465.
 - (7) El-Shabouri MH (2002) Positively charged nanoparticles for improving the oral bioavailability of cyclosporin-A International journal of pharmaceutics 249:101-108.
 - (8) Fazlollahi F et al. (2011) Polystyrene nanoparticle trafficking across MDCK-II Nanomedicine : nanotechnology, biology, and medicine 7:588-594.
 - (9) Florence AT, Hillery AM, Hussain N, Jani PU (1995) Nanoparticles as Carriers for Oral Peptide Absorption - Studies on Particle Uptake and Fate J Control Release 36:39-46.
 - (10) Genschow E et al. (2002) The ECVAM international validation study on in vitro embryotoxicity tests: results of the definitive phase and evaluation of prediction models. European Centre for the Validation of Alternative Methods Alternatives to laboratory animals : ATLA 30:151-176.
 - (11) Geraets L, Oomen AG, Krystek P, Jacobsen NR, Wallin H, Laurentie M, Verharen HW, Brandon EFA, de Jong WH. 2014. Tissue distribution and elimination after oral and intravenous administration of different titanium dioxide nanoparticles in rats. Particle and Fibre Toxicology 11:30.
 - (12) Hartung T, Luechtefeld T, Maertens A, Kleensang A. 2013. Integrated testing strategies for safety assessments. Altex 30:3-18.
 - (13) Hillery AM, Florence AT (1996) The effect of adsorbed poloxamer 188 and 407 surfactants on the intestinal uptake of 60-nm polystyrene particles after oral administration in the rat International journal of pharmaceutics 132:123-130.
 - (14) Hillery AM, Jani PU, Florence AT (1994) Comparative, quantitative study of lymphoid and non-lymphoid uptake of 60 nm polystyrene particles Journal of drug targeting 2:151-156.
 - (15) Hillyer JF, Albrecht RM (2001) Gastrointestinal persorption and tissue distribution of differently sized colloidal gold nanoparticles J Pharm Sci 90:1927-1936.
 - (16) Hussain N, Florence AT (1998) Utilizing bacterial mechanisms of epithelial cell entry: Invasin-induced oral uptake of latex nanoparticles Pharmaceutical research 15:153-156.
 - (17) Hussain N, Jaitley V, Florence AT (2001) Recent advances in the understanding of uptake of microparticulates across the gastrointestinal lymphatics Adv Drug Deliver Rev 50:107-142.
 - (18) Hussain N, Jani PU, Florence AT (1997) Enhanced oral uptake of tomato lectin-conjugated nanoparticles in the rat Pharmaceutical research 14:613-618.
 - (19) Jani P, Halbert GW, Langridge J, Florence AT (1989) The uptake and translocation of latex nanospheres and microspheres after oral administration to rats The Journal of pharmacy and pharmacology 41:809-812.
 - (20) Jani P, Halbert GW, Langridge J, Florence AT (1990) Nanoparticle uptake by the rat gastrointestinal mucosa: quantitation and particle size dependency The Journal of pharmacy and pharmacology 42:821-826.
 - (21) Jani P, McCarthy DE, Florence AT. 1992. Nanosphere and microsphere uptake via Peyer's patches: observation of the rate of uptake in the rat after a single oral dose. International Journal of Pharmaceutics 86:239-246.
 - (22) Kandarova H, Letasiova S (2011) Alternative methods in toxicology: pre-validated and validated methods Interdisciplinary toxicology 4:107-113.
 - (23) Kulkarni SA, Feng SS (2013) Effects of Particle Size and Surface Modification on Cellular Uptake and Biodistribution of Polymeric Nanoparticles for Drug Delivery Pharmaceutical research 30:2512-2522.
 - (24) Liu D, Mori A, Huang L. 1992. Role of liposome size and RES blockade in controlling biodistribution and tumor uptake of GM1-containing liposomes. Biochim Biophys Acta. 1104(1):95-101.
 - (25) Loeschner K, Navratilova J, Kobler C, Molhave K, Wagner S, von der Kammer F, Larsen EH. 2013. Detection and characterization of silver nanoparticles in chicken meat by asymmetric flow field flow fractionation with detection by conventional

- or single particle ICP-MS. *Anal Bioanal Chem* 405:8185-8195.
- (26) Mahler GJ, Esch MB, Tako E, Southard TL, Archer SD, Glahn RP, Shuler ML (2012) Oral exposure to polystyrene nanoparticles affects iron absorption *Nat Nanotechnol* 7:264-271.
- (27) Martinez-Argudo I, Sands C, Jepson MA (2007) Translocation of enteropathogenic *Escherichia coli* across an in vitro M cell model is regulated by its type III secretion system *Cell Microbiol* 9:1538-1546.
- (28) PEN. 2013. The project on emerging nanotechnologies. 28 October 2013 edition. <http://www.nanotechproject.org/news/archive/9242/>.
- (29) Seifert J, Haraszti B, Sass W (1996) The influence of age and particle number on absorption of polystyrene particles from the rat gut *Journal of anatomy* 189 (Pt 3):483-486.
- (30) Szentkuti L (1997) Light microscopical observations on luminally administered dyes, dextrans, nanospheres and microspheres in the pre-epithelial mucus gel layer of the rat distal colon *J Control Release* 46:233-242.
- (31) Talebi AR, Khorsandi L, Moridian M (2013) The effect of zinc oxide nanoparticles on mouse spermatogenesis *Journal of assisted reproduction and genetics* 30:1203-1209.
- (32) van der Zande M et al. (2012) Distribution, elimination, and toxicity of silver nanoparticles and silver ions in rats after 28-day oral exposure *ACS Nano* 6:7427-7442.
- (33) Walczak AP et al. (2012) Behaviour of silver nanoparticles and silver ions in an in vitro human gastrointestinal digestion model *Nanotoxicology* 7(7):1198-1210.
- (34) Walczak AP, Kramer E, Hendriksen PJ, Tromp P, Helsper JP, van der Zande M, Rietjens IM, Bouwmeester H. 2014. Translocation of differently sized and charged polystyrene nanoparticles in in vitro intestinal cell models of increasing complexity. *Nanotoxicology* 5:1-9.
- (35) Worth AP, Balls M (2004) The principles of validation and the ECVAM validation process *Alternatives to laboratory animals : ATLA* 32 Suppl 1B:623-629.
- (36) Xiao K et al. (2011) The effect of surface charge on in vivo biodistribution of PEG-oligocholic acid based micellar nanoparticles *Biomaterials* 32:3435-3446.

6

General discussion and future perspectives

GENERAL DISCUSSION

After some decades of development, the interest in nanotechnology continues to attract much attention. A special domain within nanotechnology is the synthesis and use of nanoparticles (NPs). NPs are commonly defined as particles having a size smaller than 100 nm. Due to their small size, NPs gain unique physical and chemical properties that differ from their bulk counterparts. Because of these properties, NPs find applications in many types of industry, including electronics, clothing, textiles, health care, medicine, cosmetics and food. A great variety of food and food-related products containing NPs are currently being produced. Silver, silica and titanium dioxide are the NPs that are used most commonly in the food sector. These products are used for food processing and packaging, but also as storage life sensors, food additives, and juice clarifiers (Wijnhoven et al. 2010; Chaudhry et al. 2008; Weir et al. 2012; Nanoparticle Products Inventory, PEN). Due to these types of application of NPs, there is a high likelihood of oral exposure of consumers to NPs, both intentionally and unintentionally.

There are many specific benefits of using NPs in products. However, due to the same unique characteristic, NPs also give rise to safety concerns for human health (Oberdorster et al. 2005; Drake & Hazelwood 2005; Navarro et al. 2008; Sung et al. 2009). Several *in vivo* studies with oral administration of different types of NPs showed that oral consumption of NPs results in systemic uptake, toxic effects and bioaccumulation of NPs in various organs (Jani et al. 1990; Hussain et al. 1997; Hillery and Florence 1996; Hillery et al. 1994; Seifert et al. 1996; van der Zande et al. 2012, van der Zande et al. 2014; Kim et al. 2008; Kim et al. 2010). Given the number of products containing NPs that are already on the market, a risk assessment of NPs is urgently needed. Only a few risk assessment studies for NPs have been published in the scientific literature (Dekkers et al. 2013; van Kesteren et al. 2014; Wijnhoven et al. 2009). The current risk assessment of NPs (and chemicals) relies mainly on *in vivo* studies (EFSA and Committee, 2011). However, given the great number of different NPs and their variability (ageing) to test, immense amounts of animals would be needed for such an approach. For several reasons, scientific, ethical and economical, efficient alternative approaches need to be developed. Lately the development of *in vitro* methods for prediction of toxicity and bioavailability of NPs gets much attention (Hartung et al. 2013). At the start of this project, there were some *in vitro* models simulating gastrointestinal digestion and intestinal exposure, but they had not been used for NP testing. Several studies have shown an adverse effect of NPs on human intestinal cells (Abbott Chalew and Schwab 2013; Kang et al. 2013; Wang et al. 2008) and demonstrated translocation of NPs through the intestinal epithelium (Kulkarni and Feng 2013; Martinez-Argudo et al. 2007; Hussain et al. 2001; Szentkuti 1997; des Rieux et al. 2005; Fazlollahi et al. 2011; Mahler et al. 2012; Oh et al. 2011; Elbakry et al. 2012; Varela et al. 2012; Schubbe et al. 2012). However, no *in vitro* approach has been taken to link different elements of oral exposure in one exposure scenario and predict the NP bioavailability in the human body after oral exposure. Therefore, the aim of the present thesis was to develop an integrated *in vitro* approach to evaluate the uptake of NPs in the human body following ingestion for the prediction of their oral

bioavailability in the human body. To this end, an *in vitro* gastrointestinal digestion model was used, to test the fate of NPs upon digestion in the human digestion tract. Further, *in vitro* intestinal epithelial models were used to evaluate the potential translocation of NPs across the intestinal barrier to predict their potential systemic absorption. Next, the *in vitro* gastrointestinal digestion model was combined with the intestinal barrier model in order to assess the translocation of digested NPs across the intestinal model. Lastly, an *in vivo* experiment was performed to pre-validate the integrated *in vitro* model.

In the present thesis, two types of NPs were used: silver NPs (AgNPs) and polystyrene NPs (PS-NPs). AgNPs were selected due to their common application in food and food-related products, and PS-NPs were selected because they are excellent model NPs, suitable for model development studies, due to their commercial availability with a wide variety of physicochemical properties like charge and fluorescent labelling.

In order to study the fate of NPs in the human body after ingestion, the first step is to assess what happens with NPs during passage through the human gastrointestinal tract. Chapter 2 of this thesis describes the effect of digestion on the behaviour and physicochemical properties of AgNPs. AgNPs of 60 nm were studied together with silver ions (in the form of AgNO_3) as a control. Samples were digested in an *in vitro* human digestion model composed of oral, gastric and intestinal digestion phases, and digestion was carried out in two variants: with and without digestive enzymes and proteins. Samples after each step of the digestion (saliva, gastric and intestinal) were analysed with several analytical techniques (SP-ICPMS, DLS and scanning electron microscopy with energy dispersive X-ray analysis (SEM-EDX)). In the absence of proteins, the number of AgNPs dropped significantly after gastric digestion and stayed at the same level after intestinal digestion. This reduction in number of AgNPs was accompanied with a decrease of their size. In the presence of proteins, after gastric digestion the number of AgNPs dropped significantly and SEM-EDX revealed that reduction in number of particles was caused by their clustering and that these clusters were composed of AgNPs and chlorine. This effect of gastric digestion on AgNPs was demonstrated later in other studies as well (Mwilu et al. 2013; Rogers et al. 2012). It was also shown that these agglomerates were coated with insoluble silver chloride formed from re-precipitated Ag^+ ions, prior released from NP surface (Mwilu et al. 2013). In salt solutions of increased chloride concentrations AgNPs aggregated with AgCl bridging in between (Chambers et al. 2014). After the gastric incubation, samples were incubated in the intestinal juice. Upon this incubation, the NP clusters disintegrated back into the free 60 nm AgNPs, same amounts of NPs were measured compared to the mouth phase. This suggests that AgNPs as used in this study, digested under physiologically relevant conditions, can reach the intestinal wall in their initial size and elemental composition. The phenomenon of cluster formation and disintegration was also observed for silica NPs (Peters et al. 2012).

Strikingly, after intestinal digestion in the presence of physiological enzymes Ag^+ ions formed 20-30 nm silver salt particles that were composed of silver, sulphur and chlorine. In another *in vitro* study silver chloride agglomerates were formed as a result of gastric digestion of pure Ag^+ ions (Mwilu et al. 2013). Interestingly, an oral feeding study using rats revealed silver salt particles (containing sulphur and selenium) in the intestinal wall following

exposure to AgNPs and Ag⁺ ions (Loeschner et al. 2011). The authors suggested that these complex silver particles were derived from Ag⁺ ions, which was confirmed by another study (van der Zande et al. 2012). The fact that Ag⁺ ions transformed during digestion into silver salts has a great importance for toxicity assessment of ingestion of Ag⁺ ions. The conclusion from this study was that the gastrointestinal digestion can impact AgNPs in both size and composition, therefore NPs tested for *in vitro* intestinal translocation should be digested prior to exposure.

In order to reach the systemic circulation, NPs need to pass the gut wall. Therefore, in order to assess the potential bioavailability of nanoparticles (NPs), a proper model for intestinal translocation is essential. Currently, several *in vitro* models of human intestinal epithelium exist, using cells grown on a semi-permeable membrane, separating apical and basolateral chambers (Lefebvre et al. 2014). An increasing number of studies report the use of models with different degrees of complexity for testing NPs. The simplest and most commonly used is a mono-culture of Caco-2 cells. More complex models also incorporate mucus producing cells and M cells grown in co-cultures with Caco-2 cells (Mahler et al. 2012; des Rieux et al. 2005; Bouwmeester et al. 2011b). All these models have not been compared with each other in one study to evaluate their applicability for NP testing. Therefore, in Chapter 3, we compared the translocation of NPs in a mono-culture (Caco-2 cells), a co-culture with mucus secreting HT29-MTX cells and a tri-culture with M-cells. For this study on the definition of an adequate *in vitro* model, it was best to choose NPs that fulfilled several criteria. PS-NPs were selected because they: 1) have been already shown to translocate across *in vitro* intestinal models (Kulkarni and Feng 2013; Martinez-Argudo et al. 2007), 2) appeared to translocate differently depending on NP characteristics like size, charge and surface chemistry (Mahler et al. 2012; Bhattacharjee et al. 2013b), and 3) have been demonstrated to be bioavailable in *in vivo* studies after oral exposure (Jani et al. 1989; Jani et al. 1990; Hussain et al. 1997). To test if size or charge of NPs influence the translocation in the models, differently sized (50 and 100 nm) and charged (neutral, positively and negatively) polystyrene NPs were used. Our findings clearly show that ingested PS-NPs, depending on their size and physicochemical properties, translocate across intestinal barrier *in vitro*. Not only NP size and charge were shown to strongly affect the translocation of NPs. Additionally, surface chemistry was also shown to be important, as the two types of negatively charged NPs (with the same size and zeta potential) with different surface modifications had an over 30-fold difference in translocation. Clearly, the chemical composition at the surface seems more important than the zeta potential. Compared with the Caco-2 mono-culture, presence of mucus significantly reduced the translocation of neutral 50 nm NPs in the co-culture. In the tri-culture, incorporation of M-cells shifted the translocation rate for these NPs closer to this in the mono-culture model. In another study, a similar reduction of translocation in the co-culture, comparing to the mono- and tri-culture, was reported for plain 50 nm PS-NPs (Schimpel et al. 2014). The relative pattern of NP translocation in all three used intestinal models was similar, however the absolute amounts of translocated NPs differed per model with no coherence that one specific model had more efficient translocation than others. Therefore, for comparing the

relative translocation of different NPs, using one intestinal model would be sufficient. However, when absolute translocation values are needed, it should be kept in mind that depending on the chosen model, the outcomes will differ. It was concluded from this study that *in vivo* experiments were needed in order to assess which of the three models is most closely reflecting the *in vivo* translocation.

In Chapter 4, an integrated *in vitro* oral model was developed by integrating the previously described digestive and intestinal models. The combination of *in vitro* gastrointestinal digestion with *in vitro* intestinal translocation was expected to give a prediction of bioavailability of orally administered NPs, which was the aim of this thesis. The PS-NPs, as used in the previous study, were first digested and in this form applied on the intestinal cell model. Because in the previous study mucus was shown to play a crucial role in influencing the translocation of PS-NPs and because it has the advantage of reducing chyme toxicity to cells, a co-culture of intestinal Caco-2 and HT29-MTX cells was selected for this study. *In vitro* digestion significantly increased the translocation of all, except the neutral, PS-NPs. Upon *in vitro* digestion, translocation was 4-fold higher for positively charged NPs and 80- and 1.7-fold higher for two types of negatively charged NPs. The effect of digestion on the protein corona of NPs was also studied, as it was expected that the enzymes of digestive juices affect the proteins adsorbed onto the NPs. It was shown that digestion affected both the amount and composition of the protein corona. The amount of protein after digestion was significantly reduced in the corona of three out of four types of NPs: 4.8-fold for neutral, 3.5-fold for positively charged and 1.8-fold for one type of negatively charged PS-NPs. The digestion changed the composition of the protein corona by decreasing the amount of higher molecular weight proteins and shifting the protein content of the corona to low molecular weight proteins. From the results obtained in Chapter 2 it was already known that digestion changes the physicochemical properties of NPs, and this study demonstrated that digestion influences the protein corona of NPs and further impacts the interactions with cells, leading to different translocation rates. This study clearly illustrated that gastrointestinal digestion affects *in vitro* translocation behaviour of different types of PS-NPs. In case of our non-degradable PS-NPs the digestion increased the intestinal translocation, while the opposite has been shown by others for degradable chitosan NPs (Lee et al. 2011). These findings stress the importance of including *in vitro* digestion in future *in vitro* intestinal translocation screening studies for risk assessment of orally taken NPs.

After developing the integrated *in vitro* digestion-translocation model and measuring the NP translocation in this model, it was necessary to validate the findings by an *in vivo* study (Kandarova and Letasiova 2011; Worth and Balls 2004). For this, we orally exposed Fischer rats to a single dose of the same PS-NPs as used in the *in vitro* studies and uptake in organs was determined. The estimated bioavailability *in vivo* ranged from 0.2% to 1.7% (depending on the type of NP), which was much lower than that *in vitro* (1.6% to 12.3%). One type of negatively charged NPs which translocated to the largest extent *in vitro*, were also taken up to the largest extent in the *in vivo* study, as shown in organs where the PS-NPs concentrations were highest (i.e. in kidney and heart). However, the relative order of uptake

for the other NPs differed from the *in vitro* findings. In conclusion, our results show that the translocation of the NPs, as predicted from our *in vitro* Caco-2/HT29-MTX model, overestimates the translocation across the rat intestine *in vivo*. Therefore, the integrated *in vitro* model cannot be directly used for a quantitative prediction of the bioavailability of orally administered NPs. However, the model can be used for screening and prioritizing NPs before further *in vivo* testing for risk assessment.

FUTURE PERSPECTIVES AND CONCLUSIONS

After obtaining the results summarised and discussed above, it is also of interest to consider what aspects are of importance and need special attention to further develop the concepts of the present thesis and add to the development of adequate *in vitro* models for testing of NPs. Some of these aspects are discussed in some more detail in the next sections.

1. Characterization of NPs

Characterization of NPs is a basic need in any experiment, still too often research studies are not accompanied by proper characterization data. It has been argued before that in any experiment with NPs, at least their pristine physicochemical properties should be characterized. The minimal set of these properties encompasses size, shape, core composition, surface charge, composition of capping functional groups, etc (Oberdorster et al. 2005; Bouwmeester et al. 2009; Bouwmeester et al. 2011a). While nowadays a lot of attention is focused on the minimal set of characterization of pristine NPs (shape, size, charge), there are more important parameters. Studies show the importance of also other surface properties, like hydrophobicity (shown to influence the cell membrane binding of NPs (Li et al. 2008)), and charge density (shown to affect the protein adsorption on NPs (Gessner et al. 2002)). It has been shown that steric shielding of the charge and steric interaction of chemical groups on the surface of NPs, as well as molecular weight and density of the coating (Gref et al. 2000) can affect the protein corona of NPs (Jedlovsky-Hajdu et al. 2012) and their biological responses (Bhattacharjee et al. 2013a; Bhattacharjee et al. 2013c; Yoncheva et al. 2005). Characterization of these parameters is often lacking. This is mainly due to technical limitations, because for measuring hydrophobicity or exact composition of functional groups on NPs routine analytical instrumentation is not available. As concluded from this thesis, more efforts should now be devoted to relate the chemical surface properties of NPs with the same surface charge but different surface modification to their different biological behaviour.

Perhaps, characterization of the pristine material is not the most important aspect of characterization of NPs. The physicochemical properties of NPs- due to their unique properties resulting from their small size- are extremely dynamic and matrix-dependent. Thus, introduction of NPs in any medium (e.g. cell culture medium, fluids of a high ionic strength, of low pH or containing proteins, food) affects their properties to a high extent. Therefore, not only the properties of pristine NPs should be characterized, but also- and perhaps more importantly- the properties of NPs as present in medium, as this is the

form in which they actually come in contact with biological systems (Walczyk et al. 2010). The outcomes of this thesis show clearly that incubation of NPs in media (e.g. chyme) can change their biological activity. In order to understand the relationship between the physicochemical properties of NPs and their biological activity the exposure-relevant characterization should be performed.

1a. Detection and characterization of NPs in complex matrices

Characterization of NPs in a matrix is even more challenging than characterization of the pristine NPs. There are clear analytical limitations here and the availability of techniques suitable for characterizing NPs in media depends on the complexity of these media (Loeschner et al. 2011; Peters et al. 2014a). While in cell culture media NPs can be measured relatively easily, this is more difficult in complex media, e.g. in chyme or even separate digestive juices. The nowadays routinely used DLS, zeta-sizer or electron microscopy techniques are difficult to apply in these media due to disturbance of proteins and other organic matter. The work in this thesis shows that characterization of NPs in digestive juices is only possible in certain combinations of NPs and techniques. Therefore, it is clear that the methods for detection and characterization of NPs in complex matrices still need to be improved. The outcomes of this thesis clearly show that without sufficient data on the physicochemical properties of NPs in the relevant (complex) media, it is difficult to fully understand the observed biological effects. For example, it would be helpful to know the exact size and zeta-potential of PS-NPs as they come out of the digestion model, so in the form in which they are applied on cells, however these measurements were not possible. Characterizing these digested NPs with available techniques was only possible after extensive sample clean-up preparations (like centrifugation, washing, re-suspending in water or other simple medium or filtration), which however can be expected to influence the physicochemical properties of NPs in a new way. Therefore, there is a need of analytical methods that require less destructive or transformative sampling techniques (Szakal et al. 2014), of which some examples are presented hereafter.

1b. Detection and characterization of NPs in animal tissues

Detection and reliable quantification of NPs in tissues from animal studies (e.g. after oral exposure) is even more challenging, mainly because of the typically low amounts of NPs in these tissues. Clearly, different detection techniques have to be used for NPs with different chemical properties (i.e. metal or organic).

For NPs like polystyrene (used in Chapter 5) SP-ICPMS is not suitable, as it cannot distinguish ionized polystyrene from the other organic material in the samples. Not too many alternatives are available: polystyrene cannot be observed with electron microscopy techniques in matrices as complex as tissue samples. Fluorescent PS-NPs can be used, but detection of fluorescent PS-NPs in tissues can be done only above certain threshold, because of the autofluorescence of the tissues, giving a background signal. A recommendation in this case, in order to further improve the sensitivity, would be to use fluorescence probes in sensitive wavelengths, outside the spectrum encountered in tissues and (especially) blood.

For metal and metal oxide NPs different and very sensitive techniques are available. For example SP-ICPMS as used in Chapter 2 of this thesis, which is a relatively new technique and was being developed at the start of this thesis. It allows measurement of NPs even in very complex matrices by using plasma destruction (Peters et al. 2014a). SP-ICPMS allows measurement of the size and number of NPs in biological samples, even at extremely low concentrations. Additionally, it has a very good performance regarding trueness, repeatability, and reproducibility (Peters et al. 2014b). However, for SP-ICPMS improvement is needed to enable the detection and quantification of small-sized (< 20 nm) NPs (Peters et al. 2014c). Field Flow Fractionation coupled to SP-ICPMS is a promising approach and, alternatively, by using exchanging columns (like IES) the background signal can be removed to improve the small size NP detection (Hadioui et al. 2014). Also problematic is the characterization of metal NPs that are prone to dissolution. For risk assessment it is crucial to be able to differentiate between the NPs and their ionic forms, and this still cannot be reliably done with SP-ICPMS. Several studies have shown accumulation of silver in organs of orally exposed animals (van der Zande et al. 2012), where it was not possible to assess whether these were AgNPs or silver containing salt particles formed from Ag^+ ions. This problem arises from using ICPMS or AAS, which cannot indicate the form of silver in samples. On the other hand, it is possible to visualize the AgNPs in tissue samples with TEM and perform their elemental analysis with TEM-EDX. This technique, however, lacks a high resolution, and therefore in practice it is often only applicable for studying agglomerates, but not single NPs.

2. Regulations, safety assessment

Another aspect that needs further attention is the safety assessment and regulation of NPs. While we are nowadays likely exposed to a great number and diversity of products containing NPs, investigations on the possible toxic effects of these NPs are lagging behind. In addition, no accurate data on the potential current level of oral exposure are available and only a few case studies can be found in literature (i.e. Weir et al. 2012 and Peters et al. 2014c on TiO_2 , and Dekkers et al. 2011 on silica). So, even after years of research on nanotoxicology not much is known about the potential risks of nanomaterials (Dekkers et al. 2013; Szakal et al. 2014). For safety evaluation of NPs, two aspects should be taken into consideration: exposure assessment and hazard assessment. For both, adequate and reliable detection and characterization data of the NPs in products are necessary (see section on characterization). The products containing nanomaterials should be properly labelled in order to inform consumers of the presence of nanomaterials in food. Currently, the regulation about labelling products containing nanomaterials (Article 18(3) of Regulation (EU) No 1169/2011) says that “*all ingredients present in the form of engineered nanomaterials must be clearly indicated in the list of ingredients and the names of such ingredients must be followed by the word ‘nano’ in brackets*” (European Commission, 2011a). However, currently use of this regulation is problematic due to the lack of a clear definition of what should be regarded as nanomaterial. Currently, there are two definitions used in EU. (Engineered) NM in food products (European Commission, 2011a) are defined as “*any intentionally produced*

material that has one or more dimensions of the order of 100 nm or less or that is composed of discrete functional parts, either internally or at the surface, many of which have one or more dimensions of the order of 100 nm or less, including structures, agglomerates or aggregates, which may have a size above the order of 100 nm but retain properties that are characteristic of the nanoscale". Meanwhile, the EU Definition Recommendation (2011/696/EU), which is broadly applicable across different regulatory sectors, defines NMs regardless of their origin and thereby includes also natural and incidental NM (European Commission, 2011b). The main difference between these two is that one defines NPs as "any intentionally produced material", while the other defines them regardless of their origin, so includes both the natural and incidental NM. This obviously creates problems with interpretation. Therefore, the starting point should be clarifying the definition and based on this identifying products which should be subject to regulation. Subsequently, the next step should be to define priorities within this large number of NP types and products containing them. To this end, the use of adequate *in vitro* models seems essential. This could be the point for the further application of our integrated *in vitro* model. The products labelled as "nano" would be an interesting target for application in our model to reveal the fate of the NPs from these products in the digestion model and their subsequent translocation rate and help to set priorities for subsequent *in vivo* testing.

3. Alternative models for animal studies in hazard identification of NPs

As mentioned in the previous chapters of this thesis, for the hazard identification of NPs (like any other chemicals), the classical approach relies heavily on animal studies (EFSA and Committee, 2011). For several reasons, scientific, ethical and economical, efficient alternative approaches need to be developed. Lately, the development of *in vitro* methods for prediction of toxicity and bioavailability of NPs gets much attention (Hartung et al. 2013). Except for reducing the animal studies, *in vitro* methods for testing NPs have many more advantages. *In vitro* approaches provide possibilities for faster and more high-throughput testing. They also allow to obtain more mechanistic insight of the tested processes. Reliable *in vitro* models to assess the potential bioavailability of NPs can be used in a tiered safety assessment approach (EFSA and Committee, 2011). To approximate human conditions, it is necessary to mimic the complexity of human gut, with its physiology and anatomy. Currently such alternative methods are being developed and one of such attempts is presented in this thesis (chapter 2, 3, and 4). Using integrated models with elements of human origin (e.g. human cells, digestion models based on human parameters) can give eventually a closer insight in effects of exposure of humans than using inbred young rats. The integrated *in vitro* model presented in this thesis is a step in the direction of this development. The model can serve for screening and prioritizing NPs for further animal studies and in this way it can help refining and reducing the animal studies. However, the values for NP translocation obtained in the model gave an overestimation of the bioavailability obtained *in vivo*. A similar overestimation of NP translocation compared to *in vivo* results has been recently demonstrated in another study using a model of Caco-2 and THP-1 cells grown in a 3-D matrix (Huang et al. 2014). While with the results of this thesis we get closer to developing an integrated *in vitro* model for

predicting *in vivo* fate and bioavailability of NPs, there are still some points for improvement. They are listed and described in detail below.

3a. Inclusion of extracellular matrix

A change to our model could be including extracellular matrix (e.g. collagen) lining on the insert membrane in the cell models, which might make the *in vitro* model and exposure more realistic. Collagen matrix has been used in studies with Caco-2 cells seeded in inserts (Maznah 1999; Leonard et al. 2010; Esch et al. 2014). Human cells can be grown on collagen hydrogel scaffolds, which are made to replicate the shape and size of human small intestinal villi. These 3-D hydrogel scaffolds seem to mimic *in vivo* cellular differentiation and absorption better than conventional culture systems (Yu et al. 2012). Instead of collagen, also more permeable synthetic membranes can be utilized for *in vitro* cell models (Giovino et al. 2013). Yet another alternative for collagen is using a Matrigel solution to create a 3-D matrix where cells can be grown (Huang et al. 2014).

Our model did not include a collagen layer because in the control experiments it was shown to limit the free passage of NPs through the pores of inserts. Keeping in mind that the *in vitro* model in the current form overestimated the *in vivo* absorption, a factor limiting translocation, like collagen, could shift the results towards more *in vivo*-like values. In addition, inclusion of an extracellular matrix would render the *in vitro* model more similar to the *in vivo* anatomy, where a connective tissue layer is present under the epithelial cells and certainly might limit the absorption of NPs from the intestinal lumen.

3b. Inclusion of other cell types

Macrophages present in the human intestinal mucosa play a crucial role in taking up NPs (Lomer et al. 2001; Lomer et al. 2002). Including macrophages in our co-culture model of Caco-2 and HT29-MTX cells could possibly make the *in vitro* translocation more similar to the *in vivo* bioavailability. THP-1 cells grown to mimic macrophages have been already co-cultured with Caco-2 cells (Satsu et al. 2006; Huang et al. 2014). Especially interesting is the model where macrophages are grown in a collagen matrix layer on the insert membrane, on top of which Caco-2 cells are cultured (Leonard et al. 2010). In such a model, macrophages could potentially take up the NPs as they translocate across the collagen layer, limiting their translocation to the basolateral compartment.

3c. Exposure condition improvement

A limitation of experiments performed with intestinal cells *in vitro* is the fact that standard cell culture media do not contain gastrointestinal lumen factors. These lumen factors may be relevant for the intestinal cells grown *in vitro* to express their full physiological potential and could be included in media (Patel et al. 2006). An additional reason to include the gastrointestinal lumen factors is that these factors likely affect the physicochemical properties of NPs, of which the importance has been shown in this thesis. It would be interesting to study the protein corona of NPs formed during incubation in physiologically relevant media. In line with this, an interesting point to study could be exposure of cells to NPs in the absence of serum (not present in the intestinal lumen *in vivo*), which has been done before, also in Caco-2 cells (Nowak et al. 2014).

3d. Kinetic modelling to extrapolate the outcomes of *in vitro* translocation to *in vivo* bioavailability

Using an *in vitro* approach, translocation kinetics can be studied in a fast and high-throughput manner. In many experiments relatively long exposure durations are used, which not necessarily correspond to *in vivo* exposure situation. The actual contact of NPs with the rat small intestinal wall would last approximately only 1 or 2 h (Durmus-Altun et al. 2011). An exposure to NPs in our model shorter than 24 h would likely lead to a lower translocation level, as shown by Schimpel et al. in different intestinal cell models (2014). Kinetic studies *in vitro* with more time points could be used for kinetic modelling to extrapolate the translocation to earlier time points, especially in cases where detection limits would not allow detection of translocated NPs at earlier time points. In addition, kinetic modeling of the data can be used to study the consequences of the *in vitro* kinetics (i.e. linear, Michaelis Menten) for the *in vivo* situation. In this modeling the obtained *in vitro* translocation information can be extrapolated to the *in vivo* situation. For these *in silico* approaches using physiologically based pharmacokinetic modeling (PBPK) modeling and physiologically based toxico-kinetics programs can be used. While these models are readily available for conventional chemicals, less has been done for NPs. One of the few attempts is on AgNPs and Ag⁺ ions (Bachler et al. 2013). In case of our integrated *in vitro* model (i.e. combining the digestion and translocation), it is possible to collect NPs at each step of the digestion and translocation and assess the physicochemical changes in NPs. This can be used for more advanced nano (quantitative) structure bioavailability relationship studies.

3e. Gut-on-a-Chip technologies

Current advances in bioengineering and microchip development can further improve intestinal *in vitro* models as developed in this thesis. Moving from static conditions to dynamic conditions, with i.e. flow on both the apical and basolateral side of a cell model could be very important. When growing cells on flexible membranes that can mimic physiological peristaltic motions, the shear forces resulting from the flow have been shown to induce Caco-2 cells differentiation into a polarized columnar epithelium that spontaneously grows into folds resembling the structure of intestinal villi (Kim et al. 2012). Additionally, these structures have been demonstrated to be covered with mucus (Kim and Ingber 2013). This does not happen with Caco-2 cells grown in static conditions in transwell systems. It allows studying the translocation efficiency of NPs in fully formed human small intestine. At the same time, this is a highly controlled microfluidic environment, which allows more detailed, accurate and real-time analysis of toxicity, uptake and translocation (Vergeres et al. 2012). In such fluidics systems, the basolateral flow can be used linking the GI system to another cell model, e.g. endothelial or hepatocyte culture (Huh et al. 2013).

OVERALL CONCLUSION

Overall, the present thesis presents the development of an integrated *in vitro* strategy for studying the fate and bioavailability of NPs after ingestion. The developed integrated *in vitro* model combines an *in vitro* gastrointestinal digestion model with an *in vitro* intestinal

model. The translocation of the NPs, as predicted from the integrated *in vitro* model, overestimated the translocation across the rat intestine *in vivo*. Therefore, the integrated *in vitro* model cannot be directly used for a quantitative prediction of the bioavailability of orally administered NPs. However, the model can be used for screening and prioritizing NPs before further *in vivo* testing for risk assessment.

REFERENCES

- (1) Abbott Chalew TE, Schwab KJ. 2013. Toxicity of commercially available engineered nanoparticles to Caco-2 and SW480 human intestinal epithelial cells. *Cell biology and toxicology* 29:101-16.
- (2) Bachler G, von Goetz N, Hungerbuhler K. 2013. A physiologically based pharmacokinetic model for ionic silver and silver nanoparticles. *International journal of nanomedicine* 8:3365-3382.
- (3) Bhattacharjee S, Ershov D, Gucht J, Alink GM, Rietjens IM, Zuilhof H, Marcelis AT. 2013a. Surface charge-specific cytotoxicity and cellular uptake of tri-block copolymer nanoparticles. *Nanotoxicology* 7:71-84.
- (4) Bhattacharjee S, van Opstal EJ, Alink GM, Marcelis ATM, Zuilhof H, Rietjens IMCM. 2013b. Surface charge-specific interactions between polymer nanoparticles and ABC transporters in Caco-2 cells. *J Nanopart Res* 15.
- (5) Bhattacharjee S, Rietjens IMCM, Singh MP, Atkins TM, Purkait TK, Xu Z, Regli S, Shukaliak A, Clark RJ, Mitchell BS, Alink GM, Marcelis ATM, Fink MJ, Veinot JGC, Kauzlarich SM, Zuilhof A. 2013c. Cytotoxicity of surface-functionalized silicon and germanium nanoparticles: the dominant role of surface charges. *Nanoscale* 5:4870-83.
- (6) Bouwmeester H, Dekkers S, Noordam MY, Hagens WI, Bulder AS, de Heer C, ten Voorde SECG, Wijnhoven SWP, Marvin HJP, Sips AJAM. 2009. Review of health safety aspects of nanotechnologies in food production. *Regul Toxicol Pharm* 53:52-62.
- (7) Bouwmeester H, Lynch I, Marvin HJ, Dawson KA, Berges M, Braguer D, Byrne HJ, Casey A, Chambers G, Cliff MJ, Elia G, Fernandes TF, Fjellsbo LB, Hatto P, Juillerat L, Klein C, Kreyling WG, Nickel C, Riediker M, Stone V. 2011a. Minimal analytical characterization of engineered nanomaterials needed for hazard assessment in biological matrices. *Nanotoxicology* 5:1-11.
- (8) Bouwmeester H, Poortman J, Peters RJ, Wijma E, Kramer E, Makama S, Puspitaninganindita K, Marvin HJ, Peijnenburg AA, Hendriksen PJ. 2011b. Characterization of translocation of silver nanoparticles and effects on whole-genome gene expression using an *in vitro* intestinal epithelium coculture model. *ACS Nano* 5:4091-103.
- (9) Chambers BA, Afrooz AR, Bae S, Aich N, Katz L, Saleh NB, Kirisits MJ. 2014. Effects of chloride and ionic strength on physical morphology, dissolution, and bacterial toxicity of silver nanoparticles. *Environ Sci Technol* 48:761-9.
- (10) Chaudhry Q, Scotter M, Blackburn J, Ross B, Boxall A, Castle L, Aitken R, Watkins R. 2008. Applications and implications of nanotechnologies for the food sector. *Food Addit Contam Part A Chem Anal Control Expo Risk Assess* 25:241-258.
- (11) Dekkers S, Bouwmeester H, Bos PMJ, Peters RJB, Rietveld AG, Oomen AG. 2013. Knowledge gaps in risk assessment of nanosilica in food: evaluation of the dissolution and toxicity of different forms of silica. *Nanotoxicology* 7:367-377.
- (12) Dekkers S, Krystek P, Peters RJ, Lankveld DP, Bokkers BG, van Hoeven-Arentzen PH, Bouwmeester H, Oomen AG. 2011. Presence and risks of nanosilica in food products. *Nanotoxicology* 5:393-405.
- (13) des Rieux A, Ragnarsson EGE, Gullberg E, Preat V, Schneider YJ, Artursson P. 2005. Transport of nanoparticles across an *in vitro* model of the human intestinal follicle associated epithelium. *Eur J Pharm Sci* 25:455-465.
- (14) Drake PL, Hazelwood KJ. 2005. Exposure-related health effects of silver and silver

- compounds: a review. *Ann Occup Hyg* 49:575-585.
- (15) Durmus-Altun G, Vatansever U, Arzu VS, Altaner S, Dirlik B. 2011. Scintigraphic evaluation of small intestinal transit in the streptozotocin induced diabetic rats. *Hippokratia* 15:262-264.
 - (16) EFSA and Committee ES. 2011. Guidance on the risk assessment of the application of nanoscience and nanotechnologies in the food and feed chain. *EFSA J* 9:36.
 - (17) Elbakry A, Wurster EC, Zaky A, Liebl R, Schindler E, Bauer-Kreisel P, Blunk T, Rachel R, Goepferich A, Breunig M. 2012. Layer-by-layer coated gold nanoparticles: size-dependent delivery of DNA into cells. *Small* 8:3847-56.
 - (18) Esch MB, Mahler GJ, Stokol T, Shuler ML. 2014. Body-on-a-chip simulation with gastrointestinal tract and liver tissues suggests that ingested nanoparticles have the potential to cause liver injury. *Lab on a chip* 14:3081-92.
 - (19) European Commission. 2011a. "REGULATION (EU) No 1169/2011 OF THE EUROPEAN PARLIAMENT AND OF THE COUNCIL of 25 October 2011 on the provision of food information to consumers," Official Journal of the European Union p. L 304/18.
 - (20) European Commission. 2011b. Official Journal of the European Union L275; European Commission Recommendation of 18 October 2011 on the definition of nanomaterial.
 - (21) Fazlollahi F, Angelow S, Yacobi NR, Marchelletta R, Yu AS, Hamm-Alvarez SE, Borok Z, Kim KJ, Crandall ED. 2011. Polystyrene nanoparticle trafficking across MDCK-II. *Nanomedicine: nanotechnology, biology, and medicine* 7:588-94.
 - (22) Gessner A, Lieske A, Paulke B, Muller R. 2002. Influence of surface charge density on protein adsorption on polymeric nanoparticles: analysis by two-dimensional electrophoresis. *European journal of pharmaceuticals and biopharmaceutics : official journal of Arbeitsgemeinschaft fur Pharmazeutische Verfahrenstechnik e.V* 54:165-70.
 - (23) Giovino C, Ayensu I, Tetteh J, Boateng JS. 2013. An integrated buccal delivery system combining chitosan films impregnated with peptide loaded PEG-b-PLA nanoparticles. *Colloids and surfaces. B, Biointerfaces* 112:9-15.
 - (24) Gref R, Luck M, Quellec P, Marchand M, Dellacherie E, Harnisch S, Blunk T, Muller RH. 2000. 'Stealth' corona-core nanoparticles surface modified by polyethylene glycol (PEG): influences of the corona (PEG chain length and surface density) and of the core composition on phagocytic uptake and plasma protein adsorption. *Colloids and surfaces. B, Biointerfaces* 18:301-313.
 - (25) Hadioui M, Peyrot C, Wilkinson KJ. 2014. Improvements to Single Particle ICPMS by the Online Coupling of Ion Exchange Resins. *Anal Chem* 86:4668-4674.
 - (26) Hartung T, Luechtefeld T, Maertens A, Kleensang A. 2013. Integrated testing strategies for safety assessments. *Altex* 30:3-18.
 - (27) Hillery AM, Florence AT. 1996. The effect of adsorbed poloxamer 188 and 407 surfactants on the intestinal uptake of 60-nm polystyrene particles after oral administration in the rat. *International journal of pharmaceutics* 132:123-130.
 - (28) Hillery AM, Jani PU, Florence AT. 1994. Comparative, quantitative study of lymphoid and non-lymphoid uptake of 60 nm polystyrene particles. *Journal of drug targeting* 2:151-6.
 - (29) Huang Z, Wang ZZ, Long SS, Jiang HY, Chen JN, Zhang JF, Dong L. 2014. A 3-D Artificial Colon Tissue Mimic for the Evaluation of Nanoparticle-Based Drug Delivery System. *Molecular pharmaceutics* 11:2051-2061.
 - (30) Huh D, Kim HJ, Fraser JP, Shea DE, Khan M, Bahinski A, Hamilton GA, Ingber DE. 2013. Microfabrication of human organs-on-chips. *Nat Protoc* 8:2135-2157.
 - (31) Hussain N, Jaitley V, Florence AT. 2001. Recent advances in the understanding of uptake of microparticulates across the gastrointestinal lymphatics. *Adv Drug Deliver Rev* 50:107-142.
 - (32) Hussain N, Jani PU, Florence AT. 1997. Enhanced oral uptake of tomato lectin-conjugated nanoparticles in the rat. *Pharmaceutical research* 14:613-618.
 - (33) Jani P, Halbert GW, Langridge J, Florence AT. 1989. The uptake and translocation of latex nanospheres and microspheres after

- oral administration to rats. *The Journal of pharmacy and pharmacology* 41:809-12.
- (34) Jani P, Halbert GW, Langridge J, Florence AT. 1990. Nanoparticle uptake by the rat gastrointestinal mucosa: quantitation and particle size dependency. *The Journal of pharmacy and pharmacology* 42:821-6.
- (35) Jedlovsky-Hajdu A, Bombelli FB, Monopoli MP, Tombacz E, Dawson KA. 2012. Surface coatings shape the protein corona of SPIONs with relevance to their application in vivo. *Langmuir* 28:14983-91.
- (36) Kandarova H, Letasiova S. 2011. Alternative methods in toxicology: pre-validated and validated methods. *Interdisciplinary toxicology* 4:107-13.
- (37) Kang T, Guan R, Chen X, Song Y, Jiang H, Zhao J. 2013. In vitro toxicity of different-sized ZnO nanoparticles in Caco-2 cells. *Nanoscale research letters* 8:496.
- (38) Kim HJ, Huh D, Hamilton G, Ingber DE. 2012. Human gut-on-a-chip inhabited by microbial flora that experiences intestinal peristalsis-like motions and flow. *Lab on a chip* 12:2165-2174.
- (39) Kim HJ, Ingber DE. 2013. Gut-on-a-Chip microenvironment induces human intestinal cells to undergo villus differentiation. *Integr Biol-Uk* 5:1130-1140.
- (40) Kim YS, Kim JS, Cho HS, Rha DS, Kim JM, Park JD, Choi BS, Lim R, Chang HK, Chung YH, Kwon IH, Jeong J, Han BS, Yu IJ. 2008. Twenty-eight-day oral toxicity, genotoxicity, and gender-related tissue distribution of silver nanoparticles in Sprague-Dawley rats. *Inhal Toxicol* 20:575-583.
- (41) Kim YS, Song MY, Park JD, Song KS, Ryu HR, Chung YH, Chang HK, Lee JH, Oh KH, Kelman BJ, Hwang IK, Yu IJ. 2010. Subchronic oral toxicity of silver nanoparticles. *Part Fibre Toxicol* 7:20.
- (42) Kulkarni SA, Feng SS. 2013. Effects of Particle Size and Surface Modification on Cellular Uptake and Biodistribution of Polymeric Nanoparticles for Drug Delivery. *Pharmaceutical research* 30:2512-2522.
- (43) Lee J, Ko S, Kim H, Kwon H. 2011. Integrity and Cell-monolayer Permeability of Chitosan Nanoparticles in Simulated Gastrointestinal Fluids. *Food Sci Biotechnol* 20:1033-1042.
- (44) Lefebvre DE, Venema K, Gombau L, Valerio LG, Jr., Raju J, Bondy GS, Bouwmeester H, Singh RP, Clippinger AJ, Collnot EM, Mehta R, Stone V. 2014. Utility of models of the gastrointestinal tract for assessment of the digestion and absorption of engineered nanomaterials released from food matrices. *Nanotoxicology*:1-20.
- (45) Leonard F, Collnot EM, Lehr CM. 2010. A three-dimensional coculture of enterocytes, monocytes and dendritic cells to model inflamed intestinal mucosa in vitro. *Molecular pharmaceutics* 7:2103-19.
- (46) Li Y, Chen X, Gu N. 2008. Computational Investigation of Interaction between Nanoparticles and Membranes: Hydrophobic/Hydrophilic Effect. *Journal of Physical Chemistry B* 112:16647-16653.
- (47) Loeschner K, Hadrup N, Qvortrup K, Larsen A, Gao X, Vogel U, Mortensen A, Lam HR, Larsen EH. 2011. Distribution of silver in rats following 28 days of repeated oral exposure to silver nanoparticles or silver acetate. *Part Fibre Toxicol* 8:18.
- (48) Lomer MC, Harvey RS, Evans SM, Thompson RP, Powell JJ. 2001. Efficacy and tolerability of a low microparticle diet in a double blind, randomized, pilot study in Crohn's disease. *European journal of gastroenterology & hepatology* 13:101-6.
- (49) Lomer MC, Thompson RP, Powell JJ. 2002. Fine and ultrafine particles of the diet: influence on the mucosal immune response and association with Crohn's disease. *The Proceedings of the Nutrition Society* 61:123-30.
- (50) Mahler GJ, Esch MB, Tako E, Southard TL, Archer SD, Glahn RP, Shuler ML. 2012. Oral exposure to polystyrene nanoparticles affects iron absorption. *Nat Nanotechnol* 7:264-71.
- (51) Martinez-Argudo I, Sands C, Jepson MA. 2007. Translocation of enteropathogenic *Escherichia coli* across an in vitro M cell model is regulated by its type III secretion system. *Cell Microbiol* 9:1538-1546.
- (52) Maznah I, Jr. 1999. The use of Caco-2 cells as an in vitro method to study bioavailability of iron. *Malaysian journal of nutrition* 5:31-45.
- (53) Mwilu SK, El Badawy AM, Bradham K, Nelson C, Thomas D, Scheckel KG, Tolaymat T, Ma L, Rogers KR. 2013. Changes in silver nanoparticles exposed to human synthetic stomach fluid: effects of particle size and surface chemistry. *The Science of the total environment* 447:90-8.

- (54) Navarro E, Piccapietra F, Wagner B, Marconi F, Kaegi R, Odzak N, Sigg L, Behra R. 2008. Toxicity of silver nanoparticles to *Chlamydomonas reinhardtii*. *Environ Sci Technol* 42:8959-8964.
- (55) Nowak JS, Mehn D, Nativo P, Garcia CP, Gioria S, Ojea-Jimenez I, Gilliland D, Rossi F. 2014. Silica nanoparticle uptake induces survival mechanism in A549 cells by the activation of autophagy but not apoptosis. *Toxicol Lett* 224:84-92.
- (56) Oberdorster G, Maynard A, Donaldson K, Castranova V, Fitzpatrick J, Ausman K, Carter J, Karn B, Kreyling W, Lai D, Olin S, Monteiro-Riviere N, Warheit D, Yang H. 2005. Principles for characterizing the potential human health effects from exposure to nanomaterials: elements of a screening strategy. *Part Fibre Toxicol* 2:8.
- (57) Oh E, Delehanty JB, Sapsford KE, Susumu K, Goswami R, Blanco-Canosa JB, Dawson PE, Granek J, Shoff M, Zhang Q, Goering PL, Huston A, Medintz IL. 2011. Cellular uptake and fate of PEGylated gold nanoparticles is dependent on both cell-penetration peptides and particle size. *ACS Nano* 5:6434-48.
- (58) Patel N, Forbes B, Eskola S, Murray J. 2006. Use of simulated intestinal fluids with Caco-2 cells in rat ileum. *Drug development and industrial pharmacy* 32:151-161.
- (59) PEN. 2013. The project on emerging nanotechnologies. 28 October 2013 edition. <http://www.nanotechproject.org/news/archive/9242/>.
- (60) Peters R, Kramer E, Oomen AG, Herrera Rivera ZE, Oegema G, Tromp PC, Fokkink R, Rietveld A, Marvin HJ, Weigel S, Peijnenburg AA, Bouwmeester H. 2012. Presence of Nano-Sized Silica during In Vitro Digestion of Foods Containing Silica as a Food Additive. *ACS Nano* 6(3):2441-51.
- (61) Peters RJB, Rivera ZH, Bouwmeester H, Weigel S, Marvin HJP. 2014a. Advanced analytical techniques for the measurement of nanomaterials in complex samples: a comparison. *Qual Assur Saf Crop* 6:281-290.
- (62) Peters RJB, Rivera ZH, van Bommel G, Marvin HJP, Weigel S, Bouwmeester H. 2014b. Development and validation of single particle ICP-MS for sizing and quantitative determination of nano-silver in chicken meat. *Anal Bioanal Chem* 406:3875-3885.
- (63) Peters RJB, van Bommel G, Herrera Rivera Z, Helsper HPG, Marvin HJP, Weigel S, Tromp PC, Oomen AG, Rietveld AG, Bouwmeester H. 2014c. Characterization of titanium dioxide nanoparticles in food products: analytical methods to define nanoparticles. *J. Agric. Food Chem.* 62:6285-6293.
- (64) Rogers KR, Bradham K, Tolaymat T, Thomas DJ, Hartmann T, Ma L, Williams A. 2012. Alterations in physical state of silver nanoparticles exposed to synthetic human stomach fluid. *The Science of the total environment* 420:334-339.
- (65) Satsu H, Ishimoto Y, Nakano T, Mochizuki T, Iwanaga T, Shimizu M. 2006. Induction by activated macrophage-like THP-1 cells of apoptotic and necrotic cell death in intestinal epithelial Caco-2 monolayers via tumor necrosis factor-alpha. *Experimental cell research* 312:3909-19.
- (66) Schimpel C, Teubl B, Absenger M, Meindl C, Frohlich E, Leitinger G, Zimmer A, Roblegg E. 2014. Development of an Advanced Intestinal in Vitro Triple Culture Permeability Model To Study Transport of Nanoparticles. *Molecular pharmaceutics* 11:808-818.
- (67) Schubbe S, Schumann C, Cavalius C, Koch M, Muller T, Kraegeloh A. 2012. Size-Dependent Localization and Quantitative Evaluation of the Intracellular Migration of Silica Nanoparticles in Caco-2 Cells. *Chem Mater* 24:914-923.
- (68) Seifert J, Haraszti B, Sass W. 1996. The influence of age and particle number on absorption of polystyrene particles from the rat gut. *Journal of anatomy* 189 (Pt 3):483-6.
- (69) Sung JH, Ji JH, Park JD, Yoon JU, Kim DS, Jeon KS, Song MY, Jeong J, Han BS, Han JH, Chung YH, Chang HK, Lee JH, Cho MH, Kelman BJ, Yu IJ. 2009. Subchronic inhalation toxicity of silver nanoparticles. *Toxicol Sci* 108:452-461.
- (70) Szakal C, Roberts SM, Westerhoff P, Bartholomaeus A, Buck N, Illuminato I, Canady R, Rogers M. 2014. Measurement of Nanomaterials in Foods: Integrative Consideration of Challenges and Future Prospects. *ACS Nano* 8:3128-3135.
- (71) Szentkuti L. 1997. Light microscopical observations on lumenally administered dyes, dextrans, nanospheres and microspheres in the pre-epithelial mucus gel

- layer of the rat distal colon. *J Control Release* 46:233-242.
- (72) van der Zande M, Vandebriel RJ, Groot MJ, Kramer E, Herrera Rivera ZE, Rasmussen K, Ossenkoppelle JS, Tromp P, Gremmer ER, Peters RJ, Hendriksen PJ, Marvin HJ, Hoogenboom RL, Peijnenburg AA, Bouwmeester H. 2014. Sub-chronic toxicity study in rats orally exposed to nanostructured silica. *Part Fibre Toxicol* 11:8.
- (73) van der Zande M, Vandebriel RJ, Van Doren E, Kramer E, Herrera Rivera Z, Serrano-Rojero CS, Gremmer ER, Mast J, Peters RJ, Hollman PC, Hendriksen PJ, Marvin HJ, Peijnenburg AA, Bouwmeester H. 2012. Distribution, elimination, and toxicity of silver nanoparticles and silver ions in rats after 28-day oral exposure. *ACS Nano* 6:7427-42.
- (74) van Kesteren PC, Cubadda F, Bouwmeester H, van Eijkeren JC, Dekkers S, de Jong WH, Oomen AG. 2014. Novel insights into the risk assessment of the nanomaterial synthetic amorphous silica, additive E551, in food. *Nanotoxicology*:1-10.
- (75) Varela JA, Bexiga MG, Aberg C, Simpson JC, Dawson KA. 2012. Quantifying size-dependent interactions between fluorescently labeled polystyrene nanoparticles and mammalian cells. *Journal of nanobiotechnology* 10:39.
- (76) Vergeres G, Bogicevic B, Buri C, Carrara S, Chollet M, Corbino-Giunta L, Egger L, Gille D, Kopf-Bolanz K, Laederach K, Portmann R, Ramadan Q, Ramsden J, Schwander F, Silacci P, Walther B, Gijs M. 2012. The NutriChip project - translating technology into nutritional knowledge. *Brit J Nutr* 108:762-768.
- (77) Walczyk D, Bombelli FB, Monopoli MP, Lynch I, Dawson KA. 2010. What the Cell “Sees” in Bionanoscience. *J Am Chem Soc* 132:5761-5768.
- (78) Wang L, Nagesha DK, Selvarasah S, Dokmeci MR, Carrier RL. 2008. Toxicity of CdSe Nanoparticles in Caco-2 Cell Cultures. *Journal of nanobiotechnology* 6:11.
- (79) Weir A, Westerhoff P, Fabricius L, Hristovski K, von Goetz N. 2012. Titanium dioxide nanoparticles in food and personal care products. *Environ. Sci. Technol.* 46:2242-2250.
- (80) Wijnhoven SWP, Dekkers S, Kooi M, Jongeneel WP, de Jong WH. 2010. Nanomaterials in consumer products; update of products on the European market in 2010. RIVM Report 340370003/2010.
- (81) Wijnhoven SWP, Peijnenburg WJGM, Herberts CA, Hagens WI, Oomen AG, Heugens EHW, Roszek B, Bisschops J, Gosens I, van de Meent D, Dekkers S, de Jong WH, van Zijverden M, Sips AJAM, Geertsma RE. 2009. Nano-silver - a review of available data and knowledge gaps in human and environmental risk assessment. *Nanotoxicology* 3:109-138.
- (82) Worth AP, Balls M. 2004. The principles of validation and the ECVAM validation process. *Alternatives to laboratory animals : ATLA* 32 Suppl 1B:623-9.
- (83) Yoncheva K, Gomez S, Campanero MA, Gamazo C, Irache JM. 2005. Bioadhesive properties of pegylated nanoparticles. *Expert opinion on drug delivery* 2:205-18.
- (84) Yu J, Peng S, Luo D, March JC. 2012. In vitro 3D human small intestinal villous model for drug permeability determination. *Biotechnology and bioengineering* 109:2173-8.

7

Summary

SUMMARY

Nanotechnology developed in the past decades and resulted in many innovative products. A branch of nanotechnology focuses on the manufacturing and use of nanoparticles (NPs). Currently, we find many products containing NPs on the market (Wijnhoven et al. 2010; Chaudhry et al. 2008; Woodrow Wilson institute). Because many of these products are food or food-related products (Bouwmeester et al. 2014), human oral exposure to NPs is very likely. Before entering the EU market, a risk assessment of NPs applied in these products is required. Many of the products are also available via internet. At the moment, the risk assessment of chemicals and NPs relies heavily on animal studies. For scientific, ethical and economical reasons, there is a demand to refine, reduce and replace animal testing by developing *in vitro* alternatives for hazard characterization. *In vitro* methods are ideally incorporated in a tiered testing approach and for oral exposure the focus is on the effect of passing the gastrointestinal tract on the physicochemical properties of the NPs and on the subsequent passage of the gut wall. This can be followed by *in vitro* effect screening, if indications of systemic bioavailability is obtained. Thus, the aim of the present thesis was to develop an integrated *in vitro* approach based on *in vitro* models (i.e. *in vitro* digestion model and *in vitro* gut epithelium model) to evaluate the uptake of NPs following ingestion for the prediction of their oral bioavailability in the human body.

Chapter 1 of the thesis gives an introduction to the topic, highlights the importance of careful characterization of NPs tested in the various assays and presents existing *in vitro* models of gastrointestinal digestion and human intestinal epithelium used for toxicity testing of NPs. Some of these *in vitro* models were selected and evaluated for testing NPs in the next (experimental) chapters.

In order to study the fate of NPs after ingestion, the first step was to study the suitability of an *in vitro* digestion model to assess what happens with NPs during the passage through the human gastrointestinal tract. For this, in **chapter 2** of this thesis the effects of the digestion on the fate and physicochemical properties of 60 nm silver nanoparticles (AgNPs) and Ag⁺ ions were studied. Samples were incubated in a static *in vitro* human digestion model composed of subsequent oral, gastric and intestinal digestion phases. It was demonstrated that gastrointestinal digestion impacted AgNPs and Ag⁺ ions in such a way that they changed during gastrointestinal digestion. As measured with (single particle) inductively coupled plasma-mass spectroscopy (SP-ICPMS), AgNPs agglomerated to a high extent during gastric passage, a process facilitated by chlorine interparticle bridges as shown by scanning electron microscopy with energy dispersive X-ray (SEM-EDX) analysis. These clusters were shown to break down during subsequent intestinal incubation, releasing the original AgNPs from the clusters. Strikingly, the NPs retained their original size in the intestinal juice. Thus, it was concluded that orally ingested 60 nm AgNPs, digested under physiologically relevant conditions, ultimately can reach the intestinal wall in their initial size and composition. Interestingly, the results of this study also revealed that intestinal digestion of Ag⁺ ions resulted in formation of 20-30 nm particles composed of silver, sulphur and chlorine. Therefore, we concluded also that ingestion of Ag⁺ ions ultimately leads to intestinal exposure to NPs, albeit with a complex chemical composition.

In order to reach the systemic circulation, NPs need to pass the gut wall. Therefore, in order to assess the potential bioavailability of NPs, measuring their intestinal translocation is essential. Given the aim to select and validate *in vitro* alternative testing strategies, selection of an *in vitro* model was undertaken in Chapter 3 of the thesis. **Chapter 3** presents a comparison of three cell culture models: a mono-culture (Caco-2 cells), a co-culture with mucus secreting HT29-MTX cells, and a tri-culture with M-cells. Differently sized (50 and 100 nm) and charged (neutral, positively and negatively) polystyrene nanoparticles (PS-NPs) were used to challenge these models. PS-NPs were shown to translocate across the *in vitro* intestinal barriers, depending on their physicochemical properties. Size and charge were shown to strongly affect the translocation of NPs, but also surface chemistry was shown to be important, because the two types of negatively charged NPs with different surface modifications had an over 30-fold difference in translocation. This result indicates that the chemical composition at the surface of the NPs is more important than the zeta potential. The relative pattern of NP translocation in all three used intestinal models was similar, but the absolute amounts of translocated NPs differed per model. Therefore, we concluded that for comparing the relative translocation of different NPs, using one intestinal model would be sufficient. Preferably, a model with mucus should be chosen, as mucus creates more realistic exposure conditions, also protecting cells from toxic effect of chyme. However, for screening studies in a tiered risk assessment approach, when absolute translocation values are needed, it should be kept in mind that depending on the chosen model, the outcomes will differ.

In chapter 2 *in vitro* digestion was shown to influence the physicochemical properties of AgNPs. To test if this would affect the translocation efficiency of PS-NPs, we integrated the *in vitro* digestion model with the *in vitro* intestinal co-culture model to test the translocation of digested PS-NPs. In **chapter 4** the translocation results from this integrated *in vitro* model are presented. It demonstrates that *in vitro* digestion of differently charged 50 nm PS-NPs influenced both their translocation behaviour and their protein corona. Translocation of all digested PS-NPs was clearly increased compared to the translocation of their pristine equivalent PS-NPs and was ranging from 1.6% to 12.3%, depending on NP type. One type of negatively charged NP was the NP translocating to the highest extent. The protein corona was affected in both the amount of proteins and their composition. Digested PS-NPs contained less protein in their corona than their equivalent pristine PS-NPs. The composition of the protein corona of PS-NPs was changed, which resulted in a shift from larger proteins (present in coronas of pristine NPs) towards low molecular weight proteins. This study clearly illustrated that gastrointestinal digestion affects *in vitro* translocation behaviour of different types of PS-NPs. These findings stress the importance of including the *in vitro* digestion in future *in vitro* intestinal translocation screening studies for risk assessment of orally taken NPs.

To assess the utility of the developed integrated *in vitro* model for assessing the bioavailability, it required validation by an *in vivo* study. **Chapter 5** presents the estimated bioavailability resulting from an oral exposure of rats to a single dose of the same PS-NPs as tested in the integrated *in vitro* model. Similar to the *in vitro* results, the surface charge

and surface chemistry affected the uptake and biodistribution of PS-NPs in rats after oral exposure. Also in line with the *in vitro* results it appeared that one type of negatively charged NP was taken up to a larger extent than the other NPs. The highest amounts of NPs were detected in kidney, heart, stomach wall, and small intestinal wall. This partly confirmed our *in vitro* findings, where the same NPs translocated to the highest extent among all tested NPs. However, the relative order of uptake for the other NPs differed from the *in vitro* findings. The estimated bioavailability ranged from 0.2% to 1.7% *in vivo*, which was much lower than that *in vitro* (1.6% to 12.3%). These results show that the predicted uptake of PS-NPs from our integrated *in vitro* model appears to overestimate the actual uptake occurring in the rat *in vivo*. In conclusion, the integrated *in vitro* model cannot be directly used for a quantitative prediction of the bioavailability of orally administered NPs. However, the integrated *in vitro* model can be used for prioritizing NPs, based on their translocation rate, for further *in vivo* testing for risk assessment.

Chapter 6 presents a discussion on the *in vitro* and *in vivo* findings of the present thesis and some future perspectives for research on issues raised in this thesis.

Overall, the present thesis presents the development of an integrated *in vitro* strategy for studying the fate and bioavailability of NPs after ingestion. The developed integrated *in vitro* model combines an *in vitro* gastrointestinal digestion model with an *in vitro* intestinal model. The translocation of the NPs, as predicted from the integrated *in vitro* model, overestimated the translocation across the rat intestine *in vivo*. Therefore, the integrated *in vitro* model cannot be directly used for a quantitative prediction of the bioavailability of orally administered NPs. However, the model can be used for screening and prioritizing NPs before further *in vivo* testing for risk assessment.

8

Samenvatting

SAMENVATTING

In de afgelopen decennia heeft de nanotechnologie zich verder ontwikkeld en dat heeft geresulteerd in veel innovatieve producten. Een van de branches van de nanotechnologie richt zich op het fabriceren en het gebruik van nanodeeltjes (NPs). Tegenwoordig zijn er veel producten in de handel die NPs bevatten (Wijnhoven et al. 2010; Chaudry et al. 2008; Woodrow Wilson institute). Omdat veel van deze producten voedingsmiddelen of voedselgerelateerd zijn (Bouwmeester et al. 2014), is orale blootstelling van mensen aan NPs waarschijnlijk. Voordat dergelijke producten in de EU op de markt mogen verschijnen, is een risicobeoordeling vereist van NPs die in deze producten zijn verwerkt. Veel van deze producten zijn echter beschikbaar via internet. De risicobeoordeling van chemicaliën en NPs is momenteel vooral gebaseerd op dierstudies. Er zijn wetenschappelijke, ethische en economische redenen die vragen om dierproeven te verfijnen, te reduceren en te vervangen door *in vitro* alternatieven. *In vitro* methodes zijn idealiter opgenomen in een trapsgewijze testbenadering en voor orale blootstelling ligt de nadruk in eerste instantie op het effect van de fysisch-chemische eigenschappen van de NPs en de invloed daarvan op het passeren van het gastro-intestinale kanaal en daaropvolgend de darmwand. Als aanwijzingen van systemische biobeschikbaarheid verkregen zijn, kan dit worden gevolgd door een *in vitro* effectscreening. Het doel van dit proefschrift was om een geïntegreerde *in vitro* benadering te ontwikkelen die is gebaseerd op *in vitro* modellen (bijv. het *in vitro* verteringsmodel en het *in vitro* darmwandepitheel-model) om zo de opname van NPs in het menselijk lichaam via orale biobeschikbaarheid te voorspellen.

Hoofdstuk 1 van dit proefschrift geeft een inleiding op het onderwerp, belicht het belang van zorgvuldige karakterisering van NPs die zijn getest in verschillende assays en presenteert bestaande *in vitro* modellen voor gastro-intestinale vertering en voor humaan darmwand epitheel die zijn gebruikt voor het testen van de biobeschikbaarheid van NPs. Enkele van deze *in vitro*-modellen zijn in de volgende (experimentele) hoofdstukken geselecteerd en geëvalueerd voor het testen van NPs.

Om het lot van NPs na orale opname te bestuderen, was de eerste stap het bestuderen van de geschiktheid van een *in vitro* model om te bepalen wat met NPs gebeurt gedurende de passage door het humaan maag-darm kanaal. Daarom werden in **hoofdstuk 2** van dit proefschrift de effecten van de condities in het maag-darm kanaal bestudeerd op enkele fysisch-chemische eigenschappen van 60 nm zilvernano-deeltjes (AgNPs) en Ag⁺ ionen. Monsters werden geïncubeerd in een statisch *in vitro* humaan spijsverteringsmodel dat was samengesteld uit orale, maag en dunne darm verteringsfasen. De gastro-intestinale spijsvertering bleek de eigenschappen van zowel AgNPs en Ag⁺ ionen te beïnvloeden. Gemeten met ('*Single particle*') inductief-gekoppelde plasma-massaspectroscopie (SP-ICPMS) bleken AgNPs zich om te vormen tot clusters van deeltjes met een grote omvang tijdens de passage door de maag. In deze clusters werden de AgNPs bijeen gehouden door chloor bevattende interpartikel bruggen, zoals was te zien tijdens de elektronen-microscopische scanning met energie dispergerende X-straling (SEM-EDX) analyse. Dit chloor was afkomstig van de verteringsfasen in de maag. Deze clusters verdwenen tijdens de opvolgende dunne darm incubatie, waarbij de originele AgNPs uit de clusters

vrijkwamen. Wat opviel was dat de NPs hun oorspronkelijke afmeting behielden in het darmvocht. Dit leidde tot de conclusie dat oraal ingenomen 60 nm AgNPs die werden verteerd onder fysiologisch relevante condities, uiteindelijk de darmwand kunnen bereiken in hun initiële afmeting en samenstelling. Een andere interessante bevinding van deze studie is dat incubatie van Ag^+ ionen onder gesimuleerde maag-darm condities resulteerde in de vorming van 20-30 nm partikels samengesteld uit zilver, zwavel en chloor. Daaruit concludeerden wij dat opname van Ag^+ ionen uiteindelijk leidt tot intestinale blootstelling aan NPs, zij het met een complexe chemische samenstelling.

Om de systemische circulatie te bereiken moeten de NPs de darmwand passeren. Om de potentiële biobeschikbaarheid van NPs te beoordelen is het meten van hun intestinale translocatie essentieel. Vanwege het doel *in vitro* alternatieve proefstrategieën te selecteren en valideren werd in hoofdstuk 3 van het proefschrift de selectie van een *in vitro* model uitgewerkt. **Hoofdstuk 3** laat een vergelijking zien van drie celkweekmodellen: een monocultuur (Caco-2 cellen), een co-cultuur met mucus afscheidende HT29-MTX cellen en een tri-cultuur met M-cellen. Verschillende maten (50 en 100 nm) en verschillend geladen (neutraal, positief en negatief) polystyrene nanodeeltjes (PS-NPs) werden gebruikt om deze modellen te testen. PS-NPs bleken, afhankelijk van hun fysisch-chemische eigenschappen, de *in vitro* intestinale barrières te passeren. Grootte en oppervlaktelading (de zogenaamde zeta potentiaal) bleken de translocatie van NPs sterk te beïnvloeden, maar ook oppervlaktechemie van de NPs bleek van belang te zijn. Dit laatste kwam naar voren uit de vergelijking van de twee typen van negatief geladen NPs met verschillende oppervlaktekarakteristieken die een meer dan 30-voudig verschil in translocatie hadden. Dit resultaat toont aan dat de chemische samenstelling aan de oppervlakte van NPs belangrijker is dan de zeta-potentiaal. Het relatieve patroon van NP translocatie in alle drie gebruikte intestinale modellen was gelijk, maar de absolute aantallen van getransloceerde NPs verschilden per model. Daaruit concludeerden we dat, om de relatieve translocatie van verschillende NPs te vergelijken, één intestinaal model voldoende zou zijn. Bij voorkeur zou een model met mucus gekozen moeten worden omdat mucus meer realistische blootstellingscondities creëert, en ook cellen beschermt tegen het toxisch effect van chyme. Echter voor het screenen van studies in een trapsgewijze risicoschattingsbenadering, wanneer absolute translocatiewaarden nodig zijn, moet eraan gedacht worden dat de uitkomsten zullen verschillen, afhankelijk van het gekozen model.

In hoofdstuk 2 bleek de *in vitro* spijsvertering de fysisch-chemische eigenschappen van AgNPs te beïnvloeden. Om te testen of dit de translocatie-efficiëntie van PS-NPs zou beïnvloeden, integreerden we in **hoofdstuk 4** het *in vitro* spijsverteringsmodel uit hoofdstuk 2 met het *in vitro* intestinale co-cultuurmodel beschreven in hoofdstuk 3 om de translocatie van verteerde PS-NPs te testen. In hoofdstuk 4 worden de translocatieresultaten van dit geïntegreerde *in vitro* model gepresenteerd. De resultaten tonen aan dat *in vitro* spijsvertering van verschillend geladen 50 nm PS-NPs zowel hun translocatiegedrag als hun eiwitcorona beïnvloedde. Translocatie van alle verteerde PS-NPs was duidelijk toegenomen vergeleken met de translocatie van hun ongerepte equivalent PS-NPs en varieerde van 1.6% tot 12.3%, afhankelijk van PS-NP-type. Eén van de twee typen van negatief geladen

NPs vertoende de hoogste translocatie. De eiwitcorona om de PS-NPs werd zowel qua eiwithoeveelheid als qua eiwitsamenstelling beïnvloed. Verteerde PS-NPs bevatten minder eiwit in hun corona dan hun equivalent ongerepte PS-NPs. Na de vertering bevatte de eiwitcorona van PS-NPs vooral kleinere laag-moleculaire eiwitten. Deze studie liet duidelijk zien dat de condities in de maag-darm kanaal het *in vitro* translocatiegedrag van verschillende types PS-NPs beïnvloedt. Deze bevindingen benadrukken het belang om in de toekomst *in vitro* spijsvertering mee te nemen in *in vitro* intestinale translocatiescreening-studies voor risicobeoordeling van oraal ingenomen NPs.

Om de bruikbaarheid van het ontwikkelde geïntegreerde *in vitro* model voor het beoordelen van de biobeschikbaarheid te bepalen, is validatie door middel van een *in vivo* studie noodzakelijk. **Hoofdstuk 5** presenteert de geschatte biobeschikbaarheid zoals gemeten na een orale blootstelling van ratten aan een enkele dosis van dezelfde PS-NPs als die getest werden in het geïntegreerde *in vitro* model. Net als bij de *in vitro* resultaten, beïnvloedden de oppervlaktelading en de oppervlaktechemie de opname en biodistributie van PS-NPs in ratten na orale blootstelling. Evenals bij de *in vitro* resultaten bleek dat één type van negatief geladen PS-NPs in een grotere hoeveelheid werd opgenomen dan de andere PS-NPs. De grootste hoeveelheden van NPs werden gevonden in nier, hart, maagwand en dunnedarmwand. Dit bevestigde ten dele onze *in vitro* resultaten, waar dezelfde negatief geladen PS-NPs het meest de *in vitro* darmwand passeerden. De relatieve volgorde van opname van de andere PS-NPs verschilde echter van de *in vitro* resultaten. De geschatte biobeschikbaarheid varieerde van 0.2% tot 1.7% *in vivo* en dat is veel lager dan *in vitro* (1.6% tot 12.3%). Deze resultaten laten zien dat de voorspelde opname van PS-NPs uit ons geïntegreerde *in vitro* model de feitelijke opname die in de rat *in vivo* voorkomt, overschat. Concluderend betekent dit dat het geïntegreerde *in vitro* model niet zonder meer kan worden gebruikt voor een kwantitatieve voorspelling van de biobeschikbaarheid van oraal toegediende NPs. Het geïntegreerde *in vitro* model kan echter wel worden gebruikt om NPs te prioriteren, gebaseerd op hun translocatiegraad, voor verdere *in vivo* proeven voor risicoschatting.

Hoofdstuk 6 presenteert een discussie over de *in vitro* en *in vivo* resultaten van het huidige proefschrift en enkele toekomstperspectieven voor onderzoek naar onderwerpen die in dit proefschrift zijn onderzocht.

Dit proefschrift presenteert de ontwikkeling van een geïntegreerde *in vitro* strategie voor het bestuderen van lot en biobeschikbaarheid van NPs na orale inname. Het ontwikkelde geïntegreerde *in vitro* model combineert een *in vitro* gastro-intestinaal verteringsmodel met een *in vitro* intestinaal model. De translocatie van de NPs, zoals voorspeld door het geïntegreerde *in vitro* model, overschatte de translocatie in de ratten darm *in vivo*. Daarom kan het geïntegreerde *in vitro* model niet zonder meer worden gebruikt voor een kwantitatieve voorspelling van biobeschikbaarheid van oraal toegediende NPs. Het model kan echter wel worden gebruikt voor screening en prioritering van NPs, voorafgaand aan verder *in vivo* onderzoek voor risicoschatting.

A

Acknowledgements

Curriculum Vitae

List of publications

Overview of completed training activities

ACKNOWLEDGEMENTS

I would like to express here my gratitude and appreciation to many people who supported and encouraged me for the last years, so that I can be who I am and where I am now. Without all of you, the outcomes of my work would definitely not be as many and as nice, and this book would not exist.

First of all, I want to thank my promotor Ivonne Rietjens. For these 4 years I experienced your dedicated supervision, support, encouragement and guidance on how to be a good scientist, efficient and determined. I appreciate your sharpness, intelligence and so many discussions we had and stimulating suggestions you gave. Thank you very much for your patience for me, especially in the last moments of the creation of this book. I cannot express how amazed I was, receiving from you a few corrections (about some small typo's!) to the final version of this book ... on a day when you were flying overseas. This is a pure efficiency! Thank you very much!

I would like to express my extreme gratitude to my supervisor Hans Bouwmeester. It was a pleasure to work with you and have you as my supervisor. I appreciate your knowledge, sharpness and intelligence and I learnt a lot from you (I hope!). You were always there with a tricky question like "And why not like this?", testing my scientific reasoning and ability to defend my opinion and decision. What I also appreciate a lot is your friendly character that I always experienced. By this I mean that we can joke together, sometimes letting some humor into serious discussions. But I mean also the fact that you always supported me. I could always just drop by your office and ask a small question (that often led to a very long discussion), and you were always there to help me with my questions, problems, dilemmas and doubts.

I want to extend my gratitude and appreciation to my supervisor Peter Hendriksen. It was nice to have you in meetings and discussions, where you always gave a critical (constructive!) look to the situation, plan, decisions and results. What others would overlook, you always "fished out" and it definitely led to the increase of the quality of our work. I appreciate your knowledge and perseverance. Thank you for all the patience and support you gave me for all these years.

I want to thank all the colleagues at RIKLT that I worked with and that helped me design studies, do the experiments and interpret the data: special thanks goes to Evelien (for your valuable input in the discussions, helping me a lot in the lab, nice company during experiments and taking over some cell-culture responsibilities during Christmas!), Meike (for help with small and big things, important input in the discussions and (especially) in in-depth correcting my manuscripts and improving their graphical appearance), Ruud Peters (for patiently discussing with me the possibilities and limitations of sp-ICPMS), Zahira and Elly (for measuring my endless samples), Hans Helsper (for your help in characterizing NPs), Anna Undas (for the help in getting the organ samples digested and analyzed as thoroughly as possible), Ad, Lonneke, Ewa, Richard and Geert (for the help in the in vivo experiment), Marcia and Valentinha (for nice chatting and lunches together), Si, Nathana (for the help with my first gels) and of course my dear friend Carlinita (after

you left RIKILT, it was never the same again... thank you very very much for your sincere support and help in the moment when I needed it the most!) and Sabrina (for your hard work and nice results).

I would like to thank all my PhD colleagues at Toxicology, for both the scientific and personal interactions. In the beginning, when I started my PhD, because I stayed always at RIKILT, I never actually met you. And then we went to that PhD trip, I had a chance to get to know you and then it all started. All this coming to Toxicology to discuss some scientific topic with one, and ending up talking with all. Coming to measure some samples and ending up... dancing salsa, while the samples were being measured. It is always nice to come to Toxicology, see nice and happy people and a friendly atmosphere in every corner. Talking about salsa dancing, I would like to thank Jonathan for sharing not only common interests but also a very nice friendship. It was a sad day when you moved from RIKILT to Toxicology, but fortunately from time to time I saw an announcement of your arrival and a coffee proposal to light up my day! ;) And of course in the rest of the cases I would come to Tox and bother you. Even though you are always busy with thousand things, still you would stop and listen to my thousand stories! Unbelievable! Thanks also for being my paranymph. Thanks also to Reiko for being my paranymph, helping me prepare THIS day. I appreciate a lot your friendship. A friendship that started during that PhD trip- I guess after sharing same room for the whole trip, we didn't have a choice ;) Thanks for all the coffees, lunches and dinners that we always had with serious talking and sharing personal things. Now, from the perspective of time, I see that the business I once did with you, trading something for something, has had a beneficial impact on me! Samantha! Thank you for all the nano-wisdom we shared, discussions about DLS, zeta-potential and analyzing protein corona. I'm glad we had all those coffees, lunches and (Turkish) dinners together, full of talking silly and serious. And of course about our fabulous trip to Turkey one could write a book! Amanda, I think we discovered how to sharpen appetite for scientific knowledge with a proper use of hamam and künefe. Talking further about food, thank you, Nacho, for bringing me once a special sausage from Spain... and letting it rotten in your fridge. But except for this, thanks for all the hard work, your devotion, patience, precision and attention to detail during your work as my student! Working together was super nice and it led to obtaining many good results and creating a friendship often challenged with some "Na!" and "Do you see this one?".

Many thanks to staff and colleagues at Toxicology: Ruud Woutersen (for your help, advice and input in my in vivo experiment and always nice discussions), Irene and Gre (your help in all the administrative work is highly appreciated), Hans (big thanks for participating in my in vivo experiment and showing a lot of expertise), Wasma, Barae (a member of the Aquarius team), Myrthe, Karsten, Rungnapa (for Thai recipes and perfect sense of direction), Sourav (for scientific and other very entertaining conversations), Merel (ahhh this earth-shaking laughter, whether we spoke about struggles with nano), Sunday (for sharing the nano- knowledge) and Myrto (Fish Girl, our team will stay the best forever!).

Big thanks to Remco Fokink! Your willingness to help with practical issues and to find an explanation to the outcomes was really amazing. I also appreciate the fruitful collaboration with Peter Tromp and his work, nice data reports and help.

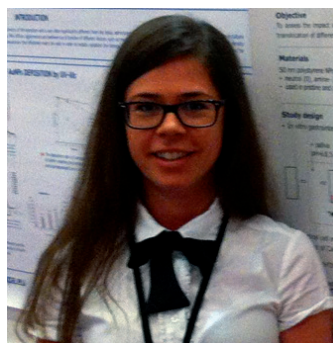
Big thanks to all my friends who supported me and participated in my relaxation times: Demonia (for coming once to my birthday party with your new friend ;) and for- since then- being my friend always and forever, for support, advice, sharing all the stuff, craziness, beating records on skype and all the drama stories!), Remko (for being my father and best friend in one person, not many people know me as well as you do, for alllll the moments during these... 8 years now?!), Anuška (for the great friendship, sharing everything, figuring out together “why???”), endless support and advices, flowerish words of appreciation ;), parties and craziness), Aditka (for being my sincere and honest friend, all the crazy parties, all the Saturdays together, teaching me Spanish and fat-cow stories!), Seba (you know... for everything!!), Nadya (for teaching me how to deal with an introvert ;) and all the gossiping), Kamielka (babo! for our friendship that stretches back all the way back to... wspólne zaopatrywanie się w sklepiku, a po szkole: podwójne zapiekanki!, and since I left- for always waiting for me), Jelonka (for your sincere friendship, advices and support!), Franci Krosta (for all the crazy moments always, holidays together and gossiping in Italian), Pushi machu (yes, youuu! thank you for those wonderful three weeks back then), Dani (for being my dedicated dancing partner), dear Polish friends Marcin, Ilo, Nacio, Koza, Agata and Michal (for all the things we ever did and experienced, support in “down” moments and, Michal, all the times you let me play your console) and of course Oleslaw (for sharing with me a friendship enhanced with a note of culinary fantasy, for many gastronomic events, dinners at McDonald’s, for coming for my zupy studenckie :P and for feeding me with his pulpety od mamy, but seriously for a greatest friendship, support, care and always an encouraging word!), Percy (for the nice distraction, also in my cave-woman periods), my “holiday friends” Sarah, Leah, Alejandra and Anne, and also Mr. Divulgativo-Papamianto.

I would like to mention here two persons who were the first to welcome me in the Netherlands. Jan van der Wolf and Patricia van der Zouwen, I have always been very grateful that I could work with both of you. Because of your friendliness, warmth and- I had a feeling- parental care about me, my stay at PRI I count as one of the happiest periods of my life and it definitely influenced my further life choices.

Dziękuję całej rodzinie, która zawsze mnie wspiera i trzyma kciuki przed ważnymi wydarzeniami życiowymi, naukowymi i przełomami w karierze. Na koniec zostawiam specjalne podziękowania dla moich kochanych rodziców, którzy zawsze mnie wspierali, wspierają i będą wspierać zawsze, otaczają opieką i pomocą kiedykolwiek tego potrzebuję i wierzą we mnie, czegokolwiek bym się w życiu nie podjęła. Bardzo to doceniam i mam nadzieję, że zawsze będziecie ze mnie dumni! I also thank my beloved sister Zuzia. The small sister, but also the best friend! Thanks for checking the references and popularizing my PhD research in Polish schools and among teenagers ;) Thank you for the support and all the things that will stay forever just between us in the name of sisterhood ;)

CURRICULUM VITAE

Agata Paulina Walczak was born on 1st of February 1984 in Toruń, Poland. After her secondary education in Toruń, in 2003 she started her undergraduate study in Medical Biotechnology at the Intercollegiate Faculty of Biotechnology at the University of Gdansk and Medical University of Gdansk in Poland. During her bachelor studies, she was an active member of a students' scientific association at the Department of Physiology of Medical University of Gdansk. After receiving her BSc degree in 2006, she moved to the Netherlands. She worked for 9 months at Plant Research International in Wageningen as a junior researcher on a project involving the control of seed-borne plant pathogenic microorganisms. Then she continued with a master study in Medical Biotechnology at Wageningen University. During her master, Agata conducted a thesis in the Laboratory of Nematology of Wageningen University and afterwards she spent a 4 month internship at the Flanders Institute for Biotechnology in Ghent, Belgium. She completed her master studies in 2010. From May 2010 until May 2014 she worked as a PhD student on the project presented in this thesis, which was a collaboration between the Division of Toxicology of Wageningen University and RIKILT Wageningen UR. This project was conducted under the supervision of Prof. dr. ir. Ivonne M.C.M. Rietjens, Dr. ir. Hans Bouwmeester and Dr. Peter J.M. Hendriksen. During her PhD study, Agata followed several courses from the Postgraduate Education in Toxicology program.



LIST OF PUBLICATIONS

Walczak, A.P., Fokkink, R., Peters, R., Tromp, P., Herrera Rivera, Z.E., Rietjens, I.M.C.M., Hendriksen, P.J.M., Bouwmeester, H. (2012) Behaviour of silver nanoparticles and silver ions in an in vitro human gastrointestinal digestion model. *Nanotoxicology* 7:1198-1210.

Walczak, A.P., Kramer, E., Hendriksen, P.J.M., Tromp, P., Helsper, J.P.F.G., van der Zande, M., Rietjens, I.M.C.M., Bouwmeester, H. (2014) Translocation of differently sized and charged polystyrene nanoparticles in in vitro intestinal cell models of increasing complexity. *Nanotoxicology* 5:1-9.

Walczak, A.P., Kramer, E., Hendriksen, P.J.M., Helsdingen, R., van der Zande, M., Rietjens, I.M.C.M., Bouwmeester, H. (2014) In vitro gastrointestinal digestion increases the translocation of polystyrene nanoparticles in an in vitro intestinal co-culture model. *Nanotoxicology*, in press.

Walczak, A.P., Hendriksen, P.J.M., Woutersen, R.A., van der Zande, M., Undas, A.K., Helsdingen, R., van den Berg, J.H.J., Rietjens, I.M.C.M., Bouwmeester H. Bioavailability and biodistribution of differently charged polystyrene nanoparticles upon oral exposure in rats. *Submitted for publication to Journal of Nanoparticle Research*.

Kloet, S.K., Walczak, A.P., Louisse, J., van den Berg, J.H.J., Bouwmeester, H., Tromp, P., Fokkink, R.G., Rietjens, I.M.C.M. Transport of positively and negatively charged polystyrene nanoparticles in an in vitro placental model. *In preparation for submission*.

OVERVIEW OF COMPLETED TRAINING ACTIVITIES

Discipline specific activities

Reproductive toxicology, Postgraduate Education in Toxicology (PET), 2014
Cell toxicology, PET, 2013
Organ toxicology, PET, 2013
Food toxicology and food safety, PET, 2013
Laboratory animal science, PET, 2013
Pathobiology, PET, 2013
Medical and forensic toxicology, PET, 2012
Molecular toxicology, PET, 2012

Meetings

7th International Nanotoxicology Congress, Antalya, Turkey, 2014 (Poster)
NanoNextNL meeting, Wageningen, The Netherlands, 2013 (Oral presentation)
NanoNextNL RATA meeting, Bilthoven, The Netherlands, 2012 (Poster)
NanoImpactNet-QNano Conference, Dublin, Ireland, 2012 (Oral presentation)
NanoImpactNet Training School, Dublin, Ireland, 2010

General courses

Techniques for writing and presenting scientific papers, Wageningen Graduate Schools, 2011
Information literacy including EndNote introduction, Wageningen Graduate Schools, 2011
Basic statistics, WU, 2012
Career assessment, Wageningen Graduate Schools, 2014

Optional activities

Preparation of PhD research proposal, 2010
Scientific presentations at Toxicology, 2010-2014
Cluster meetings RIKILT, 2010-2014
General toxicology, WU, 2012
PhD trip Toxicology to Switzerland and Italy, 2011

The studies described in this thesis were conducted within a collaborative project of Wageningen University and RIKILT Wageningen UR. The research was financially supported by ZonMw (The Netherlands Organisation for Health Research and Development), grant number: 40-40100-94-9016.

Financial support from Wageningen University and RIKILT Wageningen UR for printing this thesis is gratefully acknowledged.

Layout and printing: Off Page, Amsterdam, The Netherlands.

Cover design: Agata Walczak and Toni.

Agata Paulina Walczak, 2015